

1 **Large but decreasing effect of ozone on the European carbon**

2 **sink**

3 Rebecca J Oliver<sup>1</sup>, Lina M Mercado<sup>1,2</sup>, Stephen Sitch<sup>2</sup>, David Simpson<sup>3,4</sup>, Belinda E Medlyn<sup>5</sup>,

4 Yan-Shih Lin<sup>5</sup>, Gerd A Folberth<sup>6</sup>

5

6 <sup>1</sup> Centre for Ecology and Hydrology, Benson Lane, Wallingford, OX10 8BB, UK

7 <sup>2</sup> College of Life and Environmental Sciences, University of Exeter, EX4 4RJ, Exeter, UK

8 <sup>3</sup> EMEP MSC-W Norwegian Meteorological Institute, PB 43, NO-0313, Oslo, Norway

9 <sup>4</sup> Dept. Space, Earth & Environment, Chalmers University of Technology, Gothenburg, SE-41296 Sweden

10 <sup>5</sup> Hawkesbury Institute for the Environment, Western Sydney University, Locked Bag 1797, Penrith NSW 2751

11 Australia

12 <sup>6</sup> Met Office Hadley Centre, Exeter, UK.

13 *Correspondence to:* Rebecca Oliver (rfu@ceh.ac.uk)

14

15

16

17

18

19

20

21

22

23

24

25

26 **Abstract**

27

28 The capacity of the terrestrial biosphere to sequester carbon and mitigate climate change is governed by the ability  
29 of vegetation to remove emissions of CO<sub>2</sub> through photosynthesis. Tropospheric O<sub>3</sub>, a globally abundant and  
30 potent greenhouse gas, is, however, known to damage plants, causing reductions in primary productivity, yet the  
31 impact of this gas on European vegetation and the land carbon sink is largely unknown. Despite emission control  
32 policies across Europe, background concentrations of tropospheric O<sub>3</sub> have risen significantly over the last  
33 decades due to hemispheric-scale increases in O<sub>3</sub> and its precursors. Therefore, plants are exposed to increasing  
34 background concentrations, at levels currently causing chronic damage. We use the JULES land-surface model  
35 recalibrated for O<sub>3</sub> impacts on European vegetation, with an improved stomatal conductance parameterization, to  
36 quantify the impact of tropospheric O<sub>3</sub>, and its interaction with CO<sub>2</sub>, on gross primary productivity (GPP) and  
37 land carbon storage across Europe. A factorial set of model experiments showed that tropospheric O<sub>3</sub> can  
38 ~~significantly~~ suppress terrestrial carbon uptake across Europe over the period 1901 to 2050. ~~By 2050, simulated~~  
39 ~~GPP was reduced by 4 to 9% due to plant ozone damage and land carbon storage by 3 to 7%.~~ ~~However, the~~  
40 ~~combined physiological effects of elevated future CO<sub>2</sub> (acting to reduce stomatal opening) and reductions in O<sub>3</sub>~~  
41 ~~concentrations resulted in reduced O<sub>3</sub> damage in the future, contrary to predictions from earlier studies. This~~  
42 ~~alleviation of O<sub>3</sub> damage by CO<sub>2</sub> induced stomatal closure was around 1 to 2% for low and high sensitivity~~  
43 ~~respectively (on both land carbon and GPP). Reduced land carbon storage resulted from diminished soil carbon~~  
44 ~~stocks consistent with the reduction in GPP. Regional variations are identified with larger impacts shown for~~  
45 ~~temperate Europe (GPP reduced by 10 to 20%) compared to boreal regions (GPP reduced by 2 to 8%). These~~  
46 ~~results highlight that O<sub>3</sub> damage needs to be considered when predicting GPP and land carbon, and that the effects~~  
47 ~~of O<sub>3</sub> on plant physiology need to be considered in regional -add to the uncertainty of future trends in the land~~  
48 ~~carbon cycle assessments. sink, and, as such, this should be incorporated into carbon cycle assessments.~~

49

50

51

52

53

54

55

56

57

58

Commented [ORJ1]: RC1 1):

RC1 2):

59 **1 Introduction**

60  
61 The terrestrial biosphere absorbs around 30% of anthropogenic CO<sub>2</sub> emissions and acts to mitigate climate change  
62 (Le Quéré et al., 2015). Early estimates of the European carbon balance suggest a terrestrial carbon sink of between  
63 135 to 205 TgC yr<sup>-1</sup> (Janssens et al., 2003). Schulze et al. (2009) determined a larger carbon sink of 274 TgC yr<sup>-1</sup>,  
64 and more recent estimates suggest a European terrestrial sink of between 146 to 184 TgC yr<sup>-1</sup> (Luyssaert et al.,  
65 2012). The carbon sink capacity of land ecosystems is dominated by the ability of vegetation to sequester carbon  
66 through photosynthesis and release it back to the atmosphere through respiration. Therefore, any change in the  
67 balance of these fluxes will alter ecosystem source-sink behaviour.

68  
69 In recent decades much attention has focussed on the effects of rising atmospheric CO<sub>2</sub> on vegetation productivity  
70 (Ceulemans and Mousseau, 1994;Norby et al., 2005;Norby et al., 1999;Saxe et al., 1998). The Norby et al. (2005)  
71 synthesis of Free Air CO<sub>2</sub> Enrichment (FACE) experiments suggests a median stimulation (23 ± 2%) of forest  
72 NPP in response to a doubling of CO<sub>2</sub>. Similar average increases (20%) were observed for C<sub>3</sub> crops, although this  
73 translated into smaller gains in biomass (17%) and crop yields (13%) (Long et al., 2006). ~~The long-term effects~~  
74 ~~of CO<sub>2</sub> fertilization on plant growth and carbon storage are nevertheless uncertain (!!! INVALID CITATION !!!)~~  
75 Little attention, however, has been given to tropospheric ozone (O<sub>3</sub>), a globally abundant ~~and-increasing~~ air  
76 pollutant recognised as one of the most damaging pollutants for forests (Karlsson et al., 2007;Royal-Society,  
77 2008;Simpson et al., 2014b). Tropospheric O<sub>3</sub> is a secondary air pollutant formed by photochemical reactions  
78 involving carbon monoxide (CO), volatile organic compounds (VOCs), methane (CH<sub>4</sub>) and nitrogen oxides (NO<sub>x</sub>)  
79 from both man-made and natural sources, as well as downward transport from the stratosphere ~~and lightning~~  
80 ~~which is a source of NO<sub>x</sub>~~. The phytotoxic effects of O<sub>3</sub> exposure are shown to decrease vegetation productivity  
81 and biomass, with consequences for terrestrial carbon sequestration (Felzer et al., 2004;Loya et al., 2003;Mills et  
82 al., 2011b;Sitch et al., 2007). Few studies, however, consider the simultaneous effects of exposure to both gases,  
83 and few Earth-system models (ESMs) currently explicitly consider the role of tropospheric O<sub>3</sub> in terrestrial carbon  
84 dynamics (IPCC, 2013), both of which are key to understanding the carbon sequestration potential of the land-  
85 surface, and future carbon dynamics regionally and globally.

86  
87 Due to increased anthropogenic precursor emissions over the industrial period, background concentrations of  
88 ground-level O<sub>3</sub> have risen (Vingarzan, 2004) (Parrish et al., 2012). ~~O<sub>3</sub> levels at the start of the 20<sup>th</sup> century are~~  
89 ~~estimated to be around 10 ppb for the site Montsouris Observatory near Paris, data for Arkona on the Baltic coast~~  
90 ~~increased from ca. 15 ppb in the 1950s to 20-27 ppb by the early 1980s, and the Irish coast site Mace Head shows~~  
91 ~~around 40 ppb by the year 2000 (Logan et al., 2012;Parrish et al., 2012). Present day annual average background~~  
92 ~~O<sub>3</sub> concentrations reported in the review of (Vingarzan, 2004) show O<sub>3</sub> concentrations range between~~  
93 ~~approximately 20 and 45ppb, with the greatest increase occurring since the 1950s. Trends vary from site to site~~  
94 ~~though, even on a decadal basis (Logan et al., 2012;Simpson et al., 2014b), depending, for example, on~~  
95 ~~local/regional trends in precursor (especially NO<sub>x</sub>) emissions, elevation, and exposure to long-range transport.~~  
96 ~~Nevertheless, there is some indication that background O<sub>3</sub> levels over the mid-latitudes of the Northern~~  
97 ~~Hemisphere have continued to rise at a rate of approximately 0.5–2% per year, although not uniform (Vingarzan,~~  
98 ~~2004). As a result of controls on precursor emissions in Europe and North America, peak O<sub>3</sub> concentrations in~~

Commented [ORJ2]: RC2 minor comment 2.

Commented [ORJ3]: RC2 minor comment 3.

Commented [ORJ4]: RC1 5)

99 these regions have decreased or stabilised over recent decades (Cooper et al., 2014; Logan et al., 2012; Parrish et  
100 al., 2012; Simpson et al., 2014b). Nevertheless, climate change may increase the frequency of weather events  
101 conducive to peak O<sub>3</sub> incidents in the future (e.g. summer droughts and heat-waves; e.g., (Sicard et al., 2013), and  
102 may increase biogenic emissions of the O<sub>3</sub>-precursors isoprene and NO<sub>x</sub>, although such impacts are subject to  
103 great uncertainty (Simpson et al., 2014b; Young et al., 2013; Young et al., 2009). ~~Furthermore, intercontinental~~  
104 ~~transport of air pollution- from regions such as Asia that currently have poor emission controls are thought to~~  
105 ~~contribute substantially to rising means background O<sub>3</sub> concentrations- have risen significantly- over the last~~  
106 ~~decades (Cooper et al., 2010; Verstraeten et al., 2015).~~ Northern Hemisphere background concentrations of O<sub>3</sub> are  
107 now close to established levels for impacts on human health and the terrestrial environment (Royal-Society, 2008).  
108 Therefore, although peak O<sub>3</sub> concentrations are in decline across Europe, plants are exposed to increasing  
109 background levels, at levels currently causing chronic damage (Mills et al., 2011b). Intercontinental transport  
110 means future O<sub>3</sub> concentrations in Europe are dependent on how O<sub>3</sub> precursor emissions evolve globally,  
111 ~~including regions such as Asia that currently have poor emission controls (Cooper et al., 2010; Verstraeten et al.,~~  
112 ~~2015).~~

Commented [ORJ5]: RC2 minor comment 4.

Field Code Changed

113  
114 Elevated O<sub>3</sub> concentrations impact agricultural yields and nutritional quality of major crops (Ainsworth et al.,  
115 2012; Avnery et al., 2011), with consequences for global food security (Tai et al., 2014). As well as being a  
116 significant air pollutant, O<sub>3</sub> is a potent greenhouse gas (Royal-Society, 2008). High levels of O<sub>3</sub> are damaging to  
117 ecosystem health and reduce the global land carbon sink (Armeth et al., 2010; Sitch et al., 2007). Reduced uptake  
118 of carbon by plant photosynthesis due to O<sub>3</sub> damage allows more CO<sub>2</sub> to remain in the atmosphere. ~~This effect of~~  
119 ~~O<sub>3</sub> on plant physiology represents an additional climate warming to the direct radiative forcing of O<sub>3</sub> (Collins et~~  
120 ~~al., 2010; Sitch et al., 2007), the magnitude of which, however, remains highly uncertain (IPCC, 2013).~~

Commented [ORJ6]: RC2 minor comment 5.

Commented [ORJ7]: RC2 minor comment 6.

121  
122 Dry deposition of O<sub>3</sub> to terrestrial surfaces, primarily uptake by stomata on plant foliage and deposition on external  
123 surfaces of vegetation, is a ~~largesignificant~~ sink for ground level O<sub>3</sub> (Fowler et al., 2009; Fowler et al., 2001). On  
124 entry to sub-stomatal spaces, O<sub>3</sub> reacts with other molecules to form reactive oxygen species (ROS). Plants can  
125 tolerate a certain level of O<sub>3</sub> depending on their capacity to scavenge and detoxify the ROS (Ainsworth et al.,  
126 2012). Above this critical level, long-term chronic O<sub>3</sub> exposure reduces plant photosynthesis and biomass  
127 accumulation (Ainsworth, 2008; Ainsworth et al., 2012; Matyssek et al., 2010a; Wittig et al., 2007; Wittig et al.,  
128 2009), either directly through effects on photosynthetic machinery such as reduced Rubisco content (Ainsworth  
129 et al., 2012; Wittig et al., 2009) and/or indirectly by reduced stomatal conductance (g<sub>s</sub>) (Kitao et al., 2009; Wittig  
130 et al., 2007), alters carbon allocation to different pools (Grantz et al., 2006; Wittig et al., 2009), accelerates leaf  
131 senescence (Ainsworth, 2008; Nunn et al., 2005; Wittig et al., 2009) and changes plant susceptibility to biotic stress  
132 factors (Karnosky et al., 2002; Percy et al., 2002).

Commented [ORJ8]: RC2 minor comment 7.

133  
134 ~~The response of plants to O<sub>3</sub> is very wide ranging as reported in the literature from different field studies. We~~  
135 ~~compare results from the present study to values found in literature. The Wittig et al. (2007) meta-analysis of~~  
136 ~~temperate and boreal tree species showed future concentrations of O<sub>3</sub> predicted for 2050 significantly reduced leaf~~  
137 ~~level light saturated net photosynthetic uptake (-19%, range: -3% to -28%) and g<sub>s</sub> (-10%, range: +5% to -23%) in~~  
138 ~~both broadleaf and needle leaf tree species. In the Feng et al. (2008) meta-analysis of wheat, projected O<sub>3</sub>~~

139 concentrations for the future reduced aboveground biomass (-18%), CI (-13% to -24%), photosynthetic rate (-  
140 20%) and  $g_s$  (-22%). One of few long-term field based O<sub>3</sub> exposure studies (AspenFACE) showed that after 11  
141 years of exposing mature trees to elevated O<sub>3</sub> concentrations, O<sub>3</sub> decreased ecosystem carbon content (-9%), and  
142 decreased NPP (-10%), although the O<sub>3</sub> effect decreased through time (Talhelm et al., 2014). Zak et al. (2011)  
143 showed this was partly due to a shift in community structure as O<sub>3</sub>-tolerant species, competitively inferior in low  
144 O<sub>3</sub> environments, out competed O<sub>3</sub>-sensitive species. Zak et al. (2011) GPP was reduced (-12% to -19%) at two  
145 Mediterranean ecosystems exposed to elevated O<sub>3</sub> (dominated by either *Pinus* species or *Citrus* species)-studied  
146 by Fares et al. (2013). Biomass of mature beech trees was reduced (-44%) after 8 years of exposure to elevated  
147 O<sub>3</sub> (Matyssek et al., 2010a). After 5 years of O<sub>3</sub> exposure in a semi-natural grassland, annual biomass production  
148 was reduced (-23%), and in a Mediterranean annual pasture O<sub>3</sub> exposure significantly reduced total aboveground  
149 biomass (up to -25%) (Calvete-Sogo et al., 2014). However, these were empirical studies at individual sites, and  
150 these focus on O<sub>3</sub> effects on plant physiology and productivity, but do not quantify the impact on the land carbon  
151 sink. Modelling studies are needed to scale site observations to the regional and global scales. Models generally  
152 suggest that plant productivity and carbon sequestration will decrease with O<sub>3</sub> pollution, though the magnitudes  
153 vary. For example, based on a limited dataset to parameterise plant O<sub>3</sub> damage for a global set of plant functional  
154 types, Sitch et al. (2007) predicted a decline in global GPP of 14 to 23% by 2100. A second study by Lombardozzi  
155 et al. (2015) similarly predicted a 10.8% decrease of global GPP. Here we take a regional approach and take  
156 advantage of new measurements specifically for European vegetation and conduct a dedicated analysis for the  
157 European region. Results from the present study suggest projected O<sub>3</sub> concentrations for 2050 will reduce mean  
158 GPP for Europe (-4% to -9%), NPP (-6% to -11%), total carbon content (-3% to -7%) and  $g_s$  (-4% to -9%). Using  
159 GPP as a proxy for  $A_{gross}$  (these variables are not identical but they are related), our mean GPP and  $g_s$  estimates fall  
160 within the range given by the meta-analysis of Wittig et al. (2007). The remaining studies are not meta-analyses,  
161 so are site- and species-specific, our estimates appear to compare more conservatively with these, however these  
162 are a mean value for Europe and spatially our estimates show greater variability.

Commented [ORJ9]: RC1 3/4/6)

165 Understanding the response of plants to elevated tropospheric O<sub>3</sub> is challenged by the large variation in O<sub>3</sub>  
166 sensitivity both within and between species (Karnosky et al., 2007; Kubiske et al., 2007; Wittig et al., 2009).  
167 Additionally, other environmental stresses that affect stomatal behaviour will affect the rate of O<sub>3</sub> uptake and  
168 therefore the response to O<sub>3</sub> exposure, such as high temperature, drought and changing concentrations of  
169 atmospheric CO<sub>2</sub> (Mills et al., 2016; Fagnano et al., 2009; Kitao et al., 2009; Löw et al., 2006), such that the  
170 response of vegetation to O<sub>3</sub> is a balance between opposing drivers of stomatal behaviour. Increasing  
171 concentrations of atmospheric CO<sub>2</sub>, for example, are suggested to provide some protection against O<sub>3</sub> damage by  
172 causing stomata to close (Harmens et al., 2007; Wittig et al., 2007), however the long-term effects of CO<sub>2</sub>  
173 fertilisation. The long-term effects of CO<sub>2</sub> fertilization on plant growth and carbon storage remain are nevertheless  
174 uncertain (Baig et al., 2015; Ciais et al., 2013). Further, in some studies, stomata have been shown to respond  
175 sluggishly, losing their responsiveness to environmental stimuli with exposure to O<sub>3</sub> which can lead to higher O<sub>3</sub>  
176 uptake, increased water-loss and therefore greater vulnerability to environmental stresses such as drought (Mills  
177 et al., 2016; Mills et al., 2009; Paoletti and Grulke, 2010; Wilkinson and Davies, 2009). ....Mention uncertainties

Field Code Changed

178 around CO<sub>2</sub> fertilisation here, nutrient cycling and stomatal sluggishness here. Maybe introduce Medlyn model  
179 here

Commented [ORJ10]: RC2 6)

180  
181 ~~Given the critical role  $g_s$  plays in the uptake of both CO<sub>2</sub> and O<sub>3</sub>, we use an alternative~~ improved representation  
182 and parameterisation of  $g_s$  in JULES by implementing the Medlyn *et al.* (2011)  $g_s$  formulation. This model is  
183 ~~Based on the optimal theory of stomatal behaviour, it does not currently include a representation of sluggish~~  
184 ~~stomatal control, but it~~ Medlyn *et al.*, (2011) has the following advantages over the current JULES  $g_s$  formulation  
185 of Jacobs (1994): i) a single parameter ( $g_1$ ) which represents the marginal cost of water-use, compared to two  
186 parameters in Jacobs (1994) representing the the critical humidity deficit at the leaf surface ( $d_{crit}$ ) and the  $ci/ca$   
187 ratio at the leaf critical humidity deficit ( $f_l$ ) (Clark *et al.*, 2011); ii) ~~easier~~ to parameterise with leaf or canopy  
188 level observations of photosynthesis,  $g_s$  and humidity – all variables that are commonly measured, and (iii) values  
189 of  $g_1$  are available for many different plant functional types (PFTs) derived from a global data set of measured  
190 leaf-level measurements stomatal conductance, photosynthesis and vapour pressure deficit (VPD) (Lin *et al.*  
191 2015).

Commented [ORJ11]: RC2 3)

192  
193 ~~Here we~~ The main objective of this work is to assess the impact of historical and projected (1901 to 2050)  
194 changes in tropospheric O<sub>3</sub> and atmospheric CO<sub>2</sub> concentration ~~from 1901 to 2050 on the~~ predicted GPP and the  
195 European land-carbon sink for Europe. These are the two greenhouse gases that ~~directly~~ affect plant  
196 photosynthesis and  $g_s$ . We use a factorial suite of model experiments, using the Joint UK land environment  
197 simulator (JULES) (Best *et al.*, 2011; Clark *et al.*, 2011), the land-surface model of the UK Earth System Model  
198 (UKESM) (Collins *et al.*, 2011) to simulate plant O<sub>3</sub> uptake and damage, and to look at the interaction between  
199 O<sub>3</sub> and CO<sub>2</sub>. In this work, plant O<sub>3</sub> damage in JULES is developed further by introducing a term for dry  
200 deposition of O<sub>3</sub> to external plant surfaces, an important sink for tropospheric O<sub>3</sub> that was previously absent  
201 from the model. Further, the model is re-calibrated using the latest observations of vegetation sensitivity to O<sub>3</sub>,  
202 with the addition of a separate parameterisation for temperate/boreal regions versus the Mediterranean. The  
203 plant O<sub>3</sub> sensitivity of each PFT in JULES was re-calibrated for both a (high and low plant O<sub>3</sub> sensitivity to  
204 account for the large variation in O<sub>3</sub> sensitivity within and between species.) using the latest observations for  
205 European vegetation in order to capture a range of plant sensitivities to O<sub>3</sub>. (This includes separate sensitivities  
206 for Mediterranean regions, and for agricultural crops (wheat) versus natural grassland. We make a separate  
207 distinction for the Mediterranean region where possible because the work of Büker *et al.* (2015) showed that  
208 different O<sub>3</sub> dose-response relationships are needed to describe the O<sub>3</sub> sensitivity of dominant Mediterranean  
209 trees. We modify the representation of stomatal O<sub>3</sub> flux in JULES from Sitch *et al.*, (2007) by including a term  
210 for non-stomatal deposition of O<sub>3</sub> to leaf surfaces which is recognised as an important sink for ground-level  
211 O<sub>3</sub>. In addition, we introduce an alternative  $g_s$  scheme into JULES as described above. JULES is forced with  
212 spatially varying hourly O<sub>3</sub> concentrations from a high resolution atmospheric chemistry model for Europe,  
213 therefore our simulations account for diurnal variations in O<sub>3</sub> concentration and O<sub>3</sub> responses allowing for more  
214 accurate estimations of O<sub>3</sub> uptake by vegetation. ~~We do not attempt to make a full assessment of the carbon~~  
215 ~~cycle of Europe, instead we target O<sub>3</sub> damage, and its interaction with CO<sub>2</sub>, which is currently a missing~~  
216 ~~component in earlier carbon cycle assessments~~ (Le Quéré *et al.*, 2017; Sitch *et al.*, 2015). To this end, we  
217 prescribe changing O<sub>3</sub> and CO<sub>2</sub> concentrations from 1901 to 2050, but use a fixed pre-industrial climate. We

Commented [ORJ12]: RC2 minor comment 8.

218 acknowledge the use of a 'fixed' pre-industrial climate omits the additional uncertainty of the interaction  
219 between climate change and  $g_s$ , which will affect the rate of  $O_3$  uptake and therefore  $O_3$  concentrations. To  
220 understand the impact of these complex feedback mechanisms is an important area for future work, but in the  
221 current study our aim is to isolate the physiological response of plants to both  $O_3$  and  $CO_2$ , and determine the  
222 sensitivity of predicted GPP and the land carbon sink to this process, as the impact of  $O_3$  on European  
223 vegetation and the land carbon sink currently remains largely unknown.]

224 Given the critical role  $g_s$  plays in the uptake of both  $CO_2$  and  $O_3$ , we use an improved representation and  
225 parameterisation of  $g_s$  in JULES by implementing the Medlyn *et al.* (2011)  $g_s$  formulation. Based on the optimal  
226 theory of stomatal behaviour, Medlyn *et al.*, (2011) has the following advantages over the current JULES  $g_s$   
227 formulation: i) a single parameter ( $g_{s0}$ ) which represents the marginal cost of water use; ii) easy to parameterise  
228 with leaf or canopy level observations, and (iii) values of  $g_{s0}$  are available for different plant functional types  
229 (PFTs) derived from a global data set of measured leaf stomatal conductance, photosynthesis and vapour pressure  
230 deficit (VPD) (Lin *et al.*, 2015).

231  
232 We use a factorial suite of model experiments to investigate the temporal and spatial evolution of  $O_3$  impacts on  
233 European vegetation from 1901 to 2050. We do not attempt to make a full assessment of the carbon cycle of  
234 Europe, instead we target  $O_3$  damage which is currently a missing component in earlier carbon cycle assessments.  
235 Accounting for the well-known differences in plant sensitivity to  $O_3$  is complex, therefore, here we provide a  
236 sensitivity assessment by using two sets of simulations—a high and lower plant  $O_3$  sensitivity parameterisation,  
237 with  $O_3$  sensitivities that vary by PFT and region. We investigate the interaction between  $CO_2$  and  $O_3$ , the two  
238 greenhouse gases that directly affect plant photosynthesis, and indirectly  $g_s$ . Our aim is to quantify the impact of  
239 these two gases on GPP and land carbon storage across Europe. We go beyond the present day carbon budget and  
240 investigate the impact of state of art future scenarios up to year 2050.

## 241 242 2 Methods

### 243 244 2.1 Representation of $O_3$ effects in JULES

245  
246 JULES calculates the land-atmosphere exchanges of heat, energy, mass, momentum and carbon on a sub-daily  
247 time step, and includes a dynamic vegetation model (Best *et al.*, 2011; Clark *et al.*, 2011; Cox, 2001). [This work  
248 uses JULES version 3.3 (<http://www.jchmr.org>) at  $0.5^\circ \times 0.5^\circ$  spatial resolution and hourly model time step, the  
249 spatial domain is shown in Fig. S5.] JULES which has uses a multi-layer canopy radiation interception and  
250 photosynthesis scheme (10 layers in this instance) that accounts for direct and diffuse radiation, sun fleck  
251 penetration through the canopy, inhibition of leaf respiration in the light and change in photosynthetic capacity  
252 with depth into the canopy (Clark *et al.*, 2011; Mercado *et al.*, 2009). Soil water content also affects the rate of  
253 photosynthesis and  $g_s$ . It is modelled using a dimensionless soil water stress factor,  $\beta$ , which is related to the mean  
254 soil water concentration in the root zone, and the soil water contents at the critical and wilting point (Best *et al.*,  
255 2011).

256

Commented [ORJ13]: RC1 2)

Commented [ORJ14]: RC2 1)

Commented [ORJ15]: RC2 minor comment 9.

257 To simulate the effects of O<sub>3</sub> deposition on vegetation productivity and water use, JULES uses the flux-gradient  
 258 approach of Sitch *et al.*, (2007), modified to include non-stomatal deposition following Tuovinen *et al.* (2009).  
 259 JULES uses a coupled model of  $g_s$  and photosynthesis; because of the relationship between these two fluxes, the  
 260 direct effect of O<sub>3</sub> damage on photosynthetic rate also leads to a reduction in  $g_s$ . Changes in atmospheric CO<sub>2</sub>  
 261 concentration also affect photosynthetic rate and  $g_s$ , consequently the interaction between changing concentrations  
 262 of both gases is allowed for. Specifically, the potential net photosynthetic rate ( $A_p$ , mol CO<sub>2</sub> m<sup>-2</sup> s<sup>-1</sup>) is modified  
 263 by an 'O<sub>3</sub> uptake' factor ( $F$ , the fractional reduction in photosynthesis), so that the actual net photosynthesis ( $A_{net}$ ,  
 264 mol CO<sub>2</sub> m<sup>-2</sup> s<sup>-1</sup>) is given by equation 1 (Clark *et al.*, 2011, Sitch *et al.*, 2007).

$$265 \quad A_{net} = A_p F \quad (1)$$

267  
 268 The O<sub>3</sub> uptake factor ( $F$ ) is defined as:

$$269 \quad F = 1 - a * \max[F_{O_3} - F_{O_3crit}, 0.0] \quad (2)$$

270  
 271  
 272  $F_{O_3}$  is the instantaneous leaf uptake of O<sub>3</sub> (nmol m<sup>-2</sup> s<sup>-1</sup>),  $F_{O_3crit}$  is a PFT-specific threshold for O<sub>3</sub> damage (nmol  
 273 m<sup>-2</sup> PLA s<sup>-1</sup>, projected leaf area), and 'a' is a PFT-specific parameter representing the fractional reduction of  
 274 photosynthesis with O<sub>3</sub> uptake by leaves. Following Tuovinen *et al.* (2009), the flux of O<sub>3</sub> through stomata,  $F_{O_3}$ ,  
 275 is represented as follows:

$$276 \quad F_{O_3} = O_3 \left( \frac{g_b \left( \frac{g_l}{K_{O_3}} \right)}{g_b + \left( \frac{g_l}{K_{O_3}} \right) + g_{ext}} \right) \quad (3a)$$

277  
 278  
 279 O<sub>3</sub> is the molar concentration of O<sub>3</sub> at reference (canopy) level (nmol m<sup>-3</sup>),  $g_b$  is the leaf-scale boundary layer  
 280 conductance (m s<sup>-1</sup>, eq 3b),  $g_l$  is the leaf conductance for water (m s<sup>-1</sup>),  $K_{O_3}$  accounts for the different diffusivity of  
 281 ozone to water vapour is the ratio of leaf resistance for O<sub>3</sub> to leaf resistance for water vapour and takes a value of  
 282 1.51 after Massman (1998), and  $g_{ext}$  is the leaf-scale non-stomatal deposition to external plant surfaces (m s<sup>-1</sup>)  
 283 which takes a constant value of 0.0004 m s<sup>-1</sup> after Tuovinen *et al.* (2009). The leaf-level boundary layer  
 284 conductance ( $g_b$ ) is calculated as in Tuovinen *et al.* (2009)

$$285 \quad g_b = \alpha L d^{-1/2} U^{-1/2} \quad (3b)$$

286  
 287  
 288  $\alpha$  is a constant (0.0051 m s<sup>1/2</sup>),  $Ld$  is the cross-wind leaf dimension (m) and  $U$  is wind speed at canopy height (m  
 289 s<sup>-1</sup>). The rate of O<sub>3</sub> uptake is dependent on  $g_s$ , which is dependent on photosynthetic rate. Given  $g_s$  is a linear  
 290 function of photosynthetic rate in JULES (Clark *et al.*, 2011), from eq 1 it follows that:

$$291 \quad g_s = g_l F \quad (4)$$

292  
 293  
 294 The O<sub>3</sub> flux to stomata,  $F_{O_3}$ , is calculated at leaf level and then scaled to each canopy layer differentiating sunlit  
 295 and shaded leaf photosynthesis, and finally summed up to the canopy level. Because the photosynthetic capacity,

Commented [ORJ16]: RC2 minor comment 10.



296 photosynthesis and therefore  $g_s$  decline with depth into the canopy, this in turn affects  $O_3$  uptake, with the top leaf  
297 level contributing most to the total  $O_3$  flux and the lowest level contributing least.

298

## 299 **2.2 Calibration of $O_3$ uptake model for European vegetation**

300

301 Here we use the latest literature on  $O_3$  dose-response relationships derived from observed field data across Europe  
302 (CLRTAP, 2017) to determine the key PFT-specific  $O_3$  sensitivity parameters in JULES ( $a$  and  $F_{O_3crit}$ ). Each  
303 JULES PFT (broadleaf, needle leaf,  $C_3$  and  $C_4$  herbaceous, and shrub) was calibrated for a high and low plant  $O_3$   
304 sensitivity to account for uncertainty in variation of species sensitivity to  $O_3$ , using the approach of Sitch *et al.*,  
305 (2007). For the  $C_3$  herbaceous PFT – the dominant land cover type across Europe in this study (Fig. S1) - the  $O_3$   
306 sensitivity was calibrated against observations for wheat to give a representation of agricultural regions (high plant  
307  $O_3$  sensitivity), versus natural grassland (low plant  $O_3$  sensitivity), with a separate function for Mediterranean  
308 grasslands (low plant  $O_3$  sensitivity) (Table S1 and Figure S2). Broadleaf tree and shrub PFTs were calibrated  
309 against the birch/beech observed  $O_3$  dose-response functions for the high plant  $O_3$  sensitivity, with a separate  
310 function for Mediterranean broadleaf trees (deciduous oaks), needle leaf trees were calibrated against the function  
311 for Norway spruce, all data for dose-response functions were from CLRTAP (2017). The low plant  $O_3$  sensitivity  
312 functions for trees/shrubs were calibrated as being 20% less sensitive based on the difference in sensitivity  
313 between high and low sensitive tree species in the Karlsson *et al.* (2007) study. Due to limitations in data  
314 availability, the parameterisation for  $C_4$  herbaceous uses the observed dose-responses for  $C_3$  herbaceous, however  
315 the fractional cover of  $C_4$  herbs across Europe is low (Fig. S1), so this assumption affects a very small percentage  
316 of land cover.

317

318 To calibrate each JULES PFT for sensitivity to  $O_3$ , JULES was run, varying the value of parameter  $a$ , until model  
319 output of change in NPP with cumulative  $O_3$  exposure matched the observed  $O_3$  dose-response functions in  
320 CLRTAP (2017).

321 To calibrate the JULES  $O_3$  sensitivity (parameter ' $a$ ' in eq 2), JULES was run to be as directly comparable as  
322 possible to the dose-based  $O_3$  risk indicator used in CLRTAP (2017), using the  $O_3$  flux per projected leaf area to  
323 top canopy sunlit leaves. Hourly averaged  $F_{O_3}$  in excess of  $F_{O_3crit}$  were accumulated over a species specific  
324 accumulation period. Values of  $F_{O_3crit}$  came from the observations, the parameter ' $a$ ' was modified until the  
325 modelled change in response variable with cumulative uptake of  $O_3$  above the specified threshold matched the  
326 observations (see further method details in SI section S2).

327

## 328 **2.3 Representation of stomatal conductance**

329

330 In JULES,  $g_s$  ( $m s^{-1}$ ) is represented following the closure proposed by (Jacobs, 1994):

331

$$332 g_s = 1.6RT_l \frac{A_{net}\beta}{c_a - c_t} \quad (5)$$

333

334 In this parameterisation,  $c_t$  is unknown and where in the default JULES model is calculated as in equation 6,  
335 hereafter called JAC:

Commented [ORJ17]: RC2 3)

336

$$337 \quad c_i = (c_a - c_s) f_0 \left( 1 - \frac{dq}{dq_{crit}} \right) + c_s \quad (6)$$

338

339  $\beta$  is a soil moisture stress factor, the factor 1.6 accounts for  $g_s$  being the conductance for water vapour rather than  
 340  $\text{CO}_2$ ,  $R$  is the universal gas constant ( $\text{J K}^{-1} \text{mol}^{-1}$ ),  $T_l$  is the leaf surface temperature (K),  $c_a$  and  $c_i$  (both Pa) are the  
 341 leaf surface and internal  $\text{CO}_2$  partial pressures, respectively,  $c^*$  (Pa) is the  $\text{CO}_2$  photorespiration compensation  
 342 point,  $dq$  is the humidity deficit at the leaf surface ( $\text{kg kg}^{-1}$ ),  $dq_{crit}$  ( $\text{kg kg}^{-1}$ ) and  $f_0$  are PFT specific parameters  
 343 representing the critical humidity deficit at the leaf surface, and the leaf internal to atmospheric  $\text{CO}_2$  ratio ( $c_i/c_a$ )  
 344 at the leaf specific humidity deficit (Best *et al.* 2011), values are shown in Table S1.

345

346 In this work, we replace equation 6 with the closure described in Medlyn *et al.* (2011), using the key PFT  
 347 specific model parameter  $g_l$  ( $\text{kPa}^{0.5}$ ), and  $dq$  is expressed in kPa, shown in eq 7, hereafter called MED:

348

$$349 \quad c_i = c_a \left( \frac{g_l}{g_l + \sqrt{dq}} \right) \quad (7)$$

350

351 PFT specific values of the  $g_l$  parameter were derived for European vegetation from the data base of Lin *et al.*  
 352 (2015) and are shown in Table S1. The  $g_l$  parameter represents the sensitivity of the  $g_s$  to the assimilation rate,  
 353 i.e. plant water use efficiency, and it was derived as in Lin *et al.* (2015) by fitting the Medlyn *et al.*, (2011)  
 354 model to observations of  $g_s$ , photosynthesis, and VPD, with no  $g_0$  term (Lin *et al.*, 2015). The study of Hoshika *et al.*  
 355 (2013) show a significant difference in the  $g_l$  parameter (higher in elevated  $\text{O}_3$  compared to ambient) in  
 356 Siebold's beech in June of their experiment. However, this is only at the start of the growing season, further  
 357 measurements show no difference in this parameter between  $\text{O}_3$  treatments. found an effect of  $\text{O}_3$  on  $g_l$  for beech  
 358 trees (*Fagus sylvatica*) only at the start of the growing season (June), but not during the following months (August  
 359 and October). Quantifying an  $\text{O}_3$  effect directly on  $g_l$  would require a detailed meta-analysis of empirical data on  
 360 photosynthesis and  $g_s$  for different PFTs, which is currently lacking in the literature. As explained above, here we  
 361 take an empirical approach to modelling plant  $\text{O}_3$  damage, essentially by applying a reduction factor to the  
 362 simulated plant photosynthesis based on observations of whole plant losses of biomass with  $\text{O}_3$  exposure, for  
 363 which there is a lot more available data (e.g. CLRTAP, 2017). The impact of the  $g_s$  model formulation is shown  
 364 for two contrasting grid points (wet/dry) in central Europe (see SI section S3 for further details). We also carry  
 365 out site level evaluation of the two  $g_s$  models compared to FLUXNET observations (see SI section S4).

366

## 367 2.4 Model simulations for Europe

368

### 369 2.4.1 Forcing datasets

370

371 We used the WATCH meteorological forcing data set (Weedon *et al.*, 2010; Weedon *et al.*, 2011) at  $0.5^\circ \times 0.5^\circ$   
 372 spatial and three hour temporal resolution for our JULES simulations. JULES interpolates this down to an hourly  
 373 model time step. For this study, the climate was kept constant by recycling over the period 1901 to 1920, to allow  
 374 us to fully understand the impact  $\text{O}_3$ ,  $\text{CO}_2$  and their interaction.

Commented [ORJ18]: RC2 minor comment 12.

Commented [ORJ19]: RC2 minor comment 12.

Commented [ORJ20]: RC2 minor comment 13.

Commented [ORJ21]: RC2 minor comment 19.

375  
376 JULES was run with prescribed annual mean atmospheric CO<sub>2</sub> concentrations. Pre-industrial global CO<sub>2</sub>  
377 concentrations (1900 to 1960) were taken from Etheridge et al. (1996), 1960 to 2002 were from Mauna Loa  
378 (Keeling and Whorf, 2004), as calculated by the Global Carbon Project (Le Quéré et al., 2016), and 2003-2050  
379 were based on the IPCC SRES A1B scenario and were linearly interpolated to gap fill missing years (Fig. 1).

380  
381 JULES was run including dynamic vegetation with a land cover mask giving the fraction of agriculture in each  
382 0.5° x 0.5° grid cell based on the Hurtt et al. (2011) land cover database for the year 2000. [Within the agricultural  
383 mask means that, only C<sub>3</sub>/C<sub>4</sub> herbaceous PFTs are allowed to grow, with no competition from and all other PFTs  
384 , no form of land management is simulated are assumed absent. By including dynamic vegetation, grid cell PFT  
385 coverage and Leaf Area Index (LAI) is a result of resource availability and simulated competition. Following a  
386 full spin-up period (to ensure equilibrium vegetation, carbon and water states), the fractional cover of each PFT  
387 changed little over the simulation period (1901 - 2050), the land cover for 2050 is shown in Fig. S1. The model  
388 experiments in this study are run for both a high and low plant O<sub>3</sub> sensitivity: for the high plant O<sub>3</sub> sensitivity, all  
389 herbaceous PFT fractional cover uses the O<sub>3</sub> sensitivity for wheat, and for the low plant O<sub>3</sub> sensitivity, all  
390 herbaceous PFT fractional cover uses the O<sub>3</sub> sensitivity for natural grasslands.

391  
392 Tropospheric O<sub>3</sub> concentration was produced by the EMEP MSC-W model at 0.5° x 0.5° (Simpson et al., 2012),  
393 driven with meteorology from the regional climate model RCA3 (Kjellström et al., 2011; Samuelsson et al., 2011),  
394 which provides a downscaling of the ECHAM A1B-r3 (simulation 11 of Kjellström et al., 2011). This setup  
395 (EMEP+RCA3) is also used by Langner et al. (2012a), Simpson et al. (2014a), Tuovinen et al. (2013), Franz et  
396 al. (2017) and Engardt et al. (2017), where further details and model evaluation can be found. Unfortunately, the  
397 3-dimensional RCA3 data needed by the EMEP model was not available prior to 1960, but as in Engardt et al.  
398 (2017) the meteorology of 1900-1959 had to be approximated by assigning random years from 1960 to 1969. This  
399 procedure introduces some uncertainty of course, but Langner et al. (2012b) show that it is emissions change,  
400 rather than meteorological change, that drives modelled ozone concentrations. The emissions scenarios for 1900-  
401 2050 merge data from the International Institute of Applied System Analysis (IIASA) for 2005-2050 (the so-  
402 called ECLIPSE 4a scenario, Klimont et al. (2016)), recently revised EMEP data for 1990, and a scaling back  
403 from 1990 to 1900 using data from Lamarque et al. (2013). The EMEP model accounts for changes in BVOC  
404 emissions as a result of predicted ambient temperature changes, however as with all uncoupled modelling studies,  
405 there is no interaction between changes in leaf-level g, BVOCs and O<sub>3</sub> formation.

406  
407 This study used daily mean values of tropospheric O<sub>3</sub> concentration from EMEP MSC-W disaggregated down to  
408 the hourly JULES model time-step. [The daily mean O<sub>3</sub> forcing was disaggregated to follow a mean diurnal profile  
409 of O<sub>3</sub>, this was generated from hourly O<sub>3</sub> output from EMEP MSC-W for the two land cover categories across the  
410 same domain as in this study. Hourly O<sub>3</sub> values allow for variation in the diurnal response to O<sub>3</sub> exposure resulting  
411 in more accurate estimation of O<sub>3</sub> uptake. O<sub>3</sub> concentrations from EMEP were calculated at canopy height for two  
412 land-cover categories: forest and grassland (Fig. S3 and Fig. S4), which are taken as surrogates for high and low  
413 vegetation, respectively. These canopy-height specific concentrations allow for the large gradients in O<sub>3</sub>  
414 concentration that can occur in the lowest 10s of metres, giving lower O<sub>3</sub> for grasslands than seen at e.g. 20 m in

Commented [ORJ22]: RC2 minor comment 16.

Commented [ORJ23]: RC2 2)

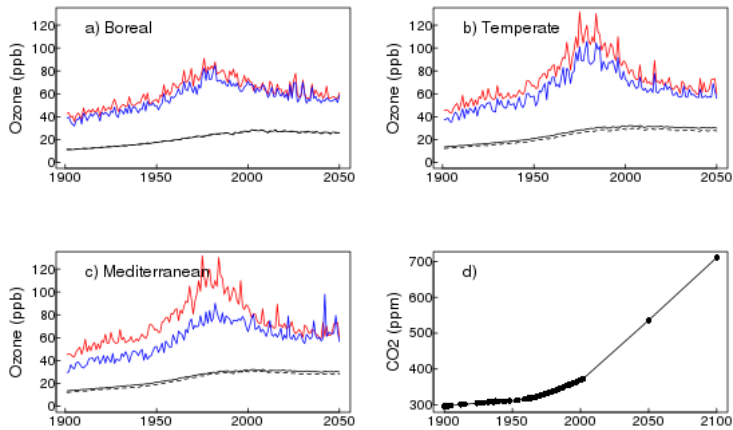
Commented [ORJ24]: RC2 minor comment 14.

415 a forest canopy (Simpson et al., 2012;Tuovinen et al., 2009). Figure 1 shows the regional mean annual O<sub>3</sub>  
416 concentration (regions are depicted in Fig. S5) along with the annual maximum. Together these clearly show the  
417 trend of increasing O<sub>3</sub> concentration on pre-industrial levels in all regions, although notably lower increases in the  
418 Boreal region. Around the 1990's O<sub>3</sub> concentrations stabilise and then start to decrease into the future.

419  
420 Figure 1 shows large increases in tropospheric O<sub>3</sub> from pre-industrial to present day (2001), this is in line with  
421 modelling studies (Young et al., 2013) and site observations (Derwent et al., 2008;Logan et al., 2012;Parrish et  
422 al., 2012), and is predominantly a result of increasing anthropogenic emissions (Young et al., 2013). Figure's S3  
423 and S4 show this large increase in ground-level O<sub>3</sub> concentrations from 1901 to 2001 occurs in all seasons. Present  
424 day O<sub>3</sub> concentration show a strong seasonal cycle, with a spring/summer peak in concentrations in the mid-  
425 latitudes of the Northern Hemisphere (Derwent et al., 2008;Parrish et al., 2012;Vingarzan, 2004). This is largely  
426 related to the seasonal cycle of photochemical O<sub>3</sub> production which is highest during periods of high radiation and  
427 temperature (Young et al., 2013), although increased stratospheric input is also thought to contribute (Vingarzan  
428 2004). Anthropogenic emissions, especially NO<sub>x</sub>, contribute to the seasonal cycle of O<sub>3</sub> through traffic, energy  
429 production and residential heating and cooling demands (Royal-Society, 2008). Biogenic emissions are also  
430 seasonal which contributes to the seasonal change in O<sub>3</sub> concentrations (Pacifico et al., 2012;Young et al., 2009),  
431 and dry deposition, driven by plant productivity also has a strong seasonal component. How the seasonality of  
432 ground level O<sub>3</sub> changes in the future will depend on how these multiple different drivers change and interact.  
433 Modelling studies such as Dentener et al. (2006) and Young et al. (2013) suggest that anthropogenic emissions  
434 will be the main factor controlling the evolution of future O<sub>3</sub> concentrations, and in the recent study of Young et  
435 al., (2013) most scenarios suggest reduced O<sub>3</sub> burden in the future as a result predominantly of reduced precursor  
436 emissions. Seasonally, the O<sub>3</sub> concentrations used in the simulations in this study show increased O<sub>3</sub> levels in  
437 winter and in some regions in autumn and spring in 2050 compared to present day, this may be due to reduced  
438 titration of O<sub>3</sub> by NO as a result of reduced NO<sub>x</sub> emissions in the future (Royal Society, 2008). Summer O<sub>3</sub>  
439 concentrations are lower in 2050 however, compared to 2001. Our simulations use a fixed climate, so we do not  
440 include the effect of climate change on shifting plant phenology. Therefore, our results may underestimate plant  
441 O<sub>3</sub> damage, since if the growing season started earlier or finished later, plants in some regions would be exposed  
442 to higher O<sub>3</sub> concentrations.

Commented [ORJ25]: RC2 5)

443  
444



445  
 446 **Figure 1.** Regional time series of canopy height O<sub>3</sub> (ppb) forcing from EMEP a) to c), and d) global atmospheric  
 447 CO<sub>2</sub> (ppm) concentration (this does not vary regionally; black dots show data points, the black line shows  
 448 interpolated points). Each panel for the O<sub>3</sub> forcing shows the regional annual average (woody PFTs, black solid  
 449 line; herbaceous PFTs, black dashed line) and the annual maximum O<sub>3</sub> concentration above: woody PFTs (red)  
 450 and herbaceous PFTs (blue).

451  
 452 **2.4.2 Spin up and factorial experiments**

453  
 454 JULES was spun-up by recycling the climate from the early part of the twentieth century (1901 to 1920) using  
 455 atmospheric CO<sub>2</sub> (296.1 ppm) and O<sub>3</sub> concentrations from 1901 (Fig. S3 & Fig. S4). Model spin-up was 2000  
 456 years by which point the carbon pools and fluxes were in steady state with zero mean net land – atmosphere CO<sub>2</sub>  
 457 flux. We performed the following transient simulations for the period 1901 to 2050 with continued recycling of  
 458 the climate as used in the spin-up, for both high and low plant O<sub>3</sub> sensitivities:

- 459 • **O3** : Fixed 1901 CO<sub>2</sub>, Varying O<sub>3</sub>
- 460 • **CO2** : Varying CO<sub>2</sub>, Fixed 1901 O<sub>3</sub>
- 461 • **CO2 + O3** : Varying CO<sub>2</sub>, Varying O<sub>3</sub>

462  
 463  
 464 We use these simulations to investigate the direct effects of changing atmospheric CO<sub>2</sub> and O<sub>3</sub> concentrations,  
 465 individually and combined, on plant physiology through the twentieth century and into the future, specifically  
 466 over three time periods: historical (1901-2001), future (2001-2050) and over the full time series (1901-2050). See  
 467 [more details in the SI section S6 for calculation of the effects due to O<sub>3</sub>, CO<sub>2</sub> and O<sub>3</sub> + CO<sub>2</sub>. We also use paired](#)  
 468 [t-test to determine statistically significant differences between the different \(high and low\) plant O<sub>3</sub> sensitivities.](#)

Commented [ORJ26]: RC1 13)

469  
 470 **2.4.3 Evaluation**

471 To evaluate our JULES simulations we compare mean GPP from 1991 to 2001 for each of the JULES scenarios  
472 and both high and low plant O<sub>3</sub> sensitivities against the observation based globally extrapolated Flux Network  
473 model tree ensemble (MTE) (Jung et al., 2011). We use paired t-test to determine statistically significant  
474 differences in the mean responses.

Commented [ORJ27]: RC2 3)

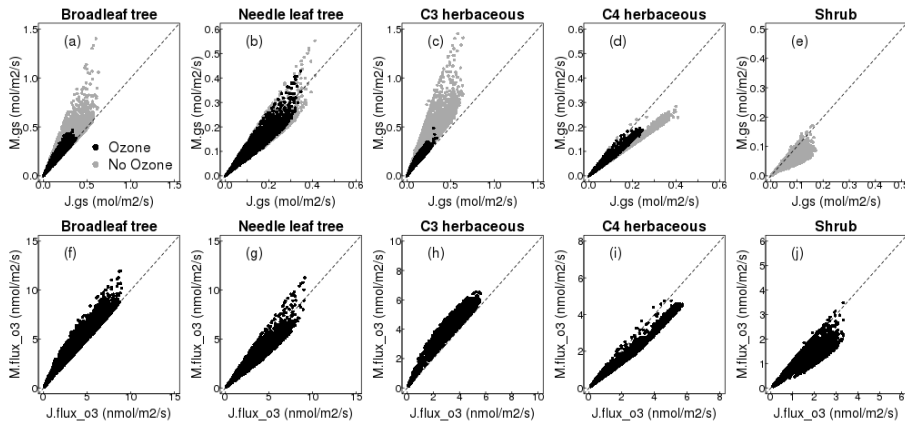
### 476 3 Results

#### 478 3.1 Impact of g<sub>s</sub> model formulation

479 The impact of g<sub>s</sub> model on simulated g<sub>s</sub> is shown for the wet site (Fig. 2). For the broadleaf tree and C<sub>3</sub> herbaceous  
480 PFT, the MEDedlyn-g<sub>s</sub> model simulates a significantly larger conductance compared to the JACaeobs-g<sub>s</sub> model.  
481 In other words, with the MEDedlyn-g<sub>s</sub> model these two PFTs are parameterised with a less conservative water use  
482 strategy, which, for the grid point shown in Fig. 2 used in the simulation, increased the annual mean leaf-level  
483 water use by 3522% (±29%) and 45% (±32%), respectively. In contrast, the needle leaf tree, C<sub>4</sub> herbaceous and  
484 shrub PFTs are parameterised with a more conservative water use strategy with the MEDedlyn-g<sub>s</sub> model, and the  
485 mean annual g<sub>s</sub> was decreased by 136% (±12%), -2732% (±10%) and 3641% (±13%), respectively, compared  
486 to the JACaeobs-g<sub>s</sub> model. This comparison was also done for a dry site, and similar results were found (Fig. S6),  
487 suggesting these results are representative across the domain. The effect of g<sub>s</sub> formulation model on simulated  
488 photosynthesis was much smaller because of the lower sensitivity of the limiting rates of photosynthesis to  
489 changes in c<sub>i</sub> in the model compared to the effect of the same change in c<sub>i</sub> on modelled g<sub>s</sub> (Fig. S7 & S8). Changes  
490 in leaf-level g<sub>s</sub> impact the partitioning of simulated energy fluxes. In general, increased g<sub>s</sub> results in increased  
491 latent heat and thus decreased sensible heat flux, and vice versa where g<sub>s</sub> is decreased (Fig. S7 & S8). Also shown  
492 is the effect of the MEDedlyn-g<sub>s</sub> model on O<sub>3</sub> flux into the leaf (Fig. 2 and Fig. S6, bottom panels). For the  
493 broadleaf tree and C<sub>3</sub> herbaceous PFT, the MEDedlyn model simulates a larger conductance and therefore a  
494 greater flux of O<sub>3</sub> through stomata compared to JACaeobs, and this is indicative of the potential for greater  
495 reductions in photosynthesis (Fig. S7 & S8). The reverse is seen for the needle leaf tree, C<sub>4</sub> herbaceous and shrub  
496 PFTs. See SI section S4 for site level evaluation of the seasonal cycles of latent and sensible heat with both JAC  
497 and MED models compared to FLUXNET observations.

Commented [ORJ28]: RC1 10)

Commented [ORJ29]: RC1 11)



500  
 501 **Figure 2.** Comparison of simulated  $g_s$  with the MEDeDlyn *et al.*, (2011) (y axis) versus the JACaeobs (1994)  
 502 formulation (x axis) currently used in JULES for all five JULES PFTs at one grid point (lat: 48.25; lon: 5.25)  
 503 shown are hourly values for the year 2000 (see SI section S3 for further details). Shown are s for stomatal  
 504 conductance ( $g_s$ , top row), and the flux of  $O_3$  through the stomata (flux\_o3, bottom row).

505  
 506 **3.2 Evaluation of the JULES  $O_3$  model**

507 For all JULES scenarios similar spatial patterns of GPP are simulated compared to MTE (Fig. 3 and Fig. S10).  
 508 MTE estimates a mean GPP for present day in Europe of  $938 \text{ gC m}^{-2} \text{ yr}^{-1}$  (Fig. 3). JULES tends to under-predict  
 509 GPP relative to the MTE product, estimates of GPP from JULES with both transient  $CO_2$  and  $O_3$  give a mean  
 510 across Europe of  $813 \text{ gC m}^{-2} \text{ yr}^{-1}$  (high plant  $O_3$  sensitivity) to  $881 \text{ gC m}^{-2} \text{ yr}^{-1}$  (low plant  $O_3$  sensitivity), both of  
 511 which are significantly different to the MTE product ( $t=27, d.f.=5750, p<2.2e^{-16}$  (high);  $t=4.3, d.f.=5750, p<1.5e^{-05}$   
 512 (low); Fig. 3). Forcing with  $CO_2$  alone (fixed 1901  $O_3$ ) gives a mean GPP across Europe of 900 to  $923 \text{ gC m}^{-2}$   
 513  $yr^{-1}$  (high and low plant  $O_3$  sensitivity respectively), and  $O_3$  alone (without the protective effect of  $CO_2$ ) reduces  
 514 estimated GPP to 732 to  $799 \text{ gC m}^{-2} \text{ yr}^{-1}$  (Fig. S10). At latitudes  $>45^\circ N$  JULES has a tendency to under-predict  
 515 MTE-GPP, and at latitudes  $<45^\circ N$  JULES tends to over-predict MTE-GPP (Fig. S11). These regional differences  
 516 are highlighted in Fig. S12, where in the Mediterranean region, JULES tends to over-predict MTE-GPP, so  
 517 simulations with  $O_3$  reduce the simulated GPP bringing it closer to MTE. In the temperate region however, JULES  
 518 tends to under-estimate MTE-GPP, so the addition of  $O_3$  reduces simulated GPP further (Fig. S12). In the boreal  
 519 region, JULES under-predicts GPP, but to a lesser extent than in the temperate region, and the addition of  $O_3$  has  
 520 less impact on reducing the GPP further (Fig. S12).

521

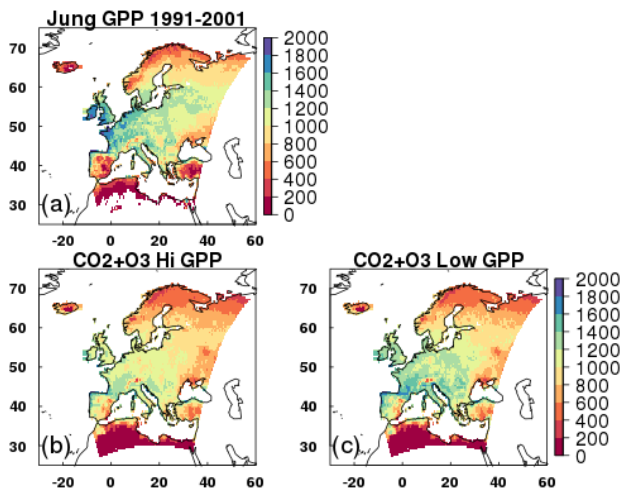


Figure 3. Mean GPP ( $\text{g C m}^{-2} \text{ yr}^{-1}$ ) from 1991 to 2001 for a) the observationally based globally extrapolated Flux Network model tree ensemble (MTE) (Jung *et al.*, 2011); b, c) model simulations with transient  $\text{CO}_2$  and transient  $\text{O}_3$ , high and low plant  $\text{O}_3$  sensitivity respectively.

Commented [ORJ30]: RC2 3)

### 3.3 European simulations - Historical Period: 1901-2001

Over the historical period (1901-2001), the physiological effect of  $\text{O}_3$  reduced GPP (-3% to -9%) for the low and high plant  $\text{O}_3$  sensitivity parameterizations, respectively (Table 1). The difference in plant  $\text{O}_3$  sensitivity was significant ( $t=102.2$ ,  $df=6270$ ,  $p<2.2e^{-16}$ ). Figure 43 highlights regional variations, however, where simulated reductions in GPP are up to 20% across large areas of Europe, and up to 30% in some Mediterranean regions under the high plant  $\text{O}_3$  sensitivity. Some Boreal and Mediterranean regions show small increases in increased GPP over this period, associated with  $\text{O}_3$  induced stomatal closure enhancing water availability in these drier regions (Fig. 54). This allows for greater enhancing stomatal conductance later in the year when soil moisture may otherwise have been limiting to growth (up to 10%, Fig. 5), and therefore higher GPP, but these regions comprise only a small area of the entire domain. Indeed, over much of the Europe,  $\text{O}_3$ -induced stomatal closure led to reduced  $g_s$  (up to 20%) across large areas of temperate Europe and the Mediterranean, and even greater reductions in some smaller regions of southern Mediterranean (Fig. 65), and these are not associated with notable significant increases in soil moisture availability (Fig. 54), resulting in depressed GPP over much of Europe as described above. Under the low plant  $\text{O}_3$  sensitivity, similar spatial patterns occur, but the magnitude of GPP change (up to -10% across much of Europe) and  $g_s$  change (-5% to -10%) are lower compared to the high sensitivity. Over the twentieth century the land carbon sink is significantly suppressed (-2% to -6%, Table 1). Large regional variation is shown in Figure 43, with temperate and Mediterranean Europe seeing a large reduction in land carbon storage, particularly under the high plant  $\text{O}_3$  sensitivity (up to -15%). Combined, the physiological

Commented [ORJ31]: RC1 13)

Commented [ORJ32]: RC1 12)



547 response to changing CO<sub>2</sub> and O<sub>3</sub> concentrations results in a net loss of land carbon over the twentieth century  
548 under the high plant O<sub>3</sub> sensitivity (-2%, Table 1), dominated by loss of soil carbon (Table S32). This reflects the  
549 large increases in tropospheric O<sub>3</sub> concentration observed over this period (Fig. 1). Under the low plant O<sub>3</sub>  
550 sensitivity, the land carbon sink has started to recover by 2001 (+1.5%) owing to the recovery of the soil carbon  
551 pool beyond 1901 values over this period (Table S32).

552  
553 To gain perspective on the magnitude of the O<sub>3</sub> induced flux of carbon from the land to the atmosphere we relate  
554 changes in total land carbon to carbon emissions from fossil fuel combustion and cement production for the EU-  
555 28-plus countries from the data of Boden et al. (2013). We recognise that our simulation domain is slightly larger  
556 than the EU28-plus as it includes a small area of western Russia so direct comparisons cannot be made, but this  
557 still provides a useful measure of the size of the carbon flux. For the period 1970 to 1979 the simulated loss of  
558 carbon from the European terrestrial biosphere due to O<sub>3</sub> effects on vegetation physiology was on average 1.32  
559 Pg C (high vegetation sensitivity) and 0.71 Pg C (low vegetation sensitivity) (Table 2). This O<sub>3</sub> induced reduced  
560 C uptake of the land surface is equivalent to around 8% to 16% of the emissions of carbon from fossil fuel  
561 combustion and cement production over the same period for the EU28-plus countries (Table 2). Currently the  
562 emissions data availability goes up to 2011, so over the last observable decade (2002 to 2011) this land carbon  
563 loss has declined but is still equivalent to 2% to 4% of the emissions of carbon from fossil fuels and cement  
564 production for the EU28-plus countries (Table 2). Therefore, the indirect O<sub>3</sub> effect on the land carbon sink  
565 potentially represents a significant additional source of anthropogenic carbon.

### 566 3.43 European simulations - Future Period: 2001-2050

567  
568  
569 Over the 2001 to 2050 period, region-wide GPP with O<sub>3</sub> only changing increased marginally (+0.1% to +0.2%,  
570 high and low plant O<sub>3</sub> sensitivity, Table 1, with a significant difference between the two plant O<sub>3</sub> sensitivities  
571 ( $t=57, df=6270, p<2.2e^{-16}$ ), although with large spatial variability (Fig. 43g & h). This reflects changes in  
572 tropospheric O<sub>3</sub> concentration as emission control policies reduce O<sub>3</sub> concentrations. Figures S34 and S45 show  
573 that despite decreased tropospheric O<sub>3</sub> concentrations by 2050 in summer compared to 2001 levels, all regions are  
574 exposed to an increase in O<sub>3</sub> over the wintertime, and some regions of Europe, particularly  
575 temperate/Mediterranean experience increases in O<sub>3</sub> concentration in spring and autumn. Therefore, although  
576 increased GPP (dominantly 10%, but up to 20% in some areas) on 2001 levels is simulated across large areas of  
577 Europe, decreases of up to 21% are simulated in some areas of the Mediterranean, up to 15% in some areas of the  
578 boreal region and up to 27% in the temperate zone (Fig. 4g & h). When O<sub>3</sub> and CO<sub>2</sub> effects are combined,  
579 simulated GPP increases (+15% to +18%, high/low plant O<sub>3</sub> sensitivities respectively, Table 1). This increase is  
580 greater than the enhancement simulated when CO<sub>2</sub> affects plant growth independently, because additional O<sub>3</sub>  
581 induced stomatal closure increases soil water availability in some regions, which enhances growth more in the O<sub>3</sub>  
582 and CO<sub>2</sub> simulations, compared to the CO<sub>2</sub> only run. Nevertheless, although the percentage gain is larger, the  
583 absolute value of GPP by 2050 remains lower compared to GPP with CO<sub>2</sub> only changing (Table S43).

584  
585 Despite small increases in GPP in the O<sub>3</sub>-only simulation, the land carbon sink continues to decline from 2001  
586 levels (-0.7% to -1.6%, low and high plant O<sub>3</sub> sensitivity respectively, Table 1). This is because the soil and

Commented [ORJ33]: RC1 13)

587 vegetation carbon pools continue to lose carbon as they adjust slowly to small changes in input (GPP), i.e. the soil  
588 carbon pool is not in equilibrium in 2001, and is declining in response to reduced litter input as a result of 20<sup>th</sup> C  
589 O<sub>3</sub> impacts on GPP. Nevertheless, the negative effect of O<sub>3</sub> on the future land sink is markedly reduced relative  
590 to the historical period. Figure 4e & f3 however highlights regional differences. Boreal regions and parts of central  
591 Europe see minimal O<sub>3</sub> damage, whereas some areas of southern and northern Europe see further losses of up to  
592 8% on 2001 levels. The combined O<sub>3</sub> and CO<sub>2</sub> effects are dominated by the physiological effects of changing  
593 CO<sub>2</sub>, with land carbon sink increases of up to 7% (Table 1).

Commented [ORJ34]: RC1 16)

### 595 3.5.4 European simulations - Anthropocene: 1901-2050

596  
597 Over the Anthropocene, O<sub>3</sub> reduces GPP (-4% to -9%, with a significant difference between the low and high  
598 plant O<sub>3</sub> sensitivity ( $t=95, d.f.=6270, p<2.2e^{-16}$ )) and land carbon storage (-3% to -7%, Table 1, Fig. S139).  
599 Regionally, O<sub>3</sub> damage is lowest in the boreal zone, GPP decreases are largely between 5% to 8% / 2% to 4% for  
600 the high/low plant O<sub>3</sub> sensitivity respectively, with large areas minimally affected by O<sub>3</sub> damage (Figure 76),  
601 consistent with lower g<sub>s</sub> of needle leaf trees that dominate this region, and so lower O<sub>3</sub> uptake (Fig. S140 & S154).  
602 In the temperate region, O<sub>3</sub> damage is extensive with reductions in GPP dominantly from 10% to 15% for the low  
603 and high plant O<sub>3</sub> sensitivity respectively. Across significant areas of this region reductions in GPP are up to 20%  
604 under high plant O<sub>3</sub> sensitivity (Figure 76). In the Mediterranean region, O<sub>3</sub> damage reduces GPP by 5% to 15%  
605 / 3% to 6% for the high/low plant O<sub>3</sub> sensitivity respectively, with some areas seeing greater losses of up to 20%  
606 under the high plant O<sub>3</sub> sensitivity, but this is less extensive than that seen in the temperate zone (Figure 76). In  
607 these drier regions, O<sub>3</sub> induced stomatal closure can increase available soil moisture (Fig. S140 & S154).

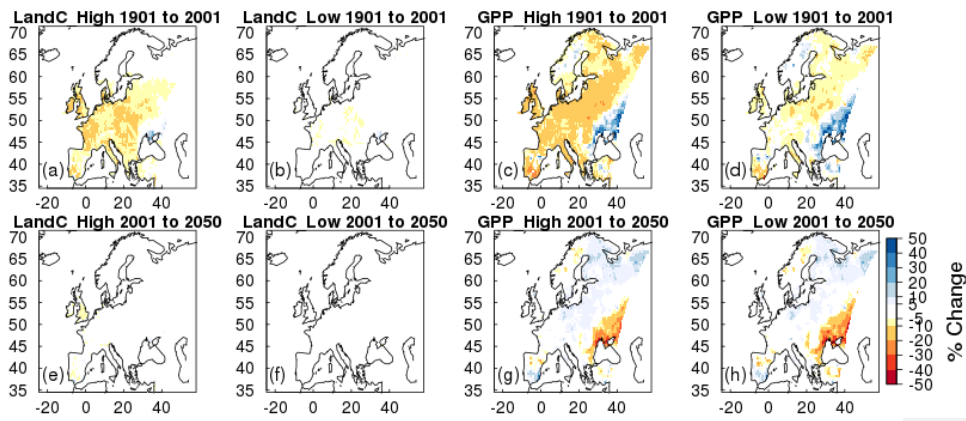
Commented [ORJ35]: RC1 13)

608  
609 Varying CO<sub>2</sub> and O<sub>3</sub> together shows that CO<sub>2</sub> induced stomatal closure can help alleviate O<sub>3</sub> damage by reducing  
610 the uptake of O<sub>3</sub> (Table S65). In these simulations, CO<sub>2</sub>-induced stomatal closure was found to offset O<sub>3</sub>-  
611 suppression of GPP, such that GPP by 2050 is 3% to 7% lower due to O<sub>3</sub> exposure, rather than 4% to 9% lower  
612 in the absence of increasing CO<sub>2</sub> (Table S65). Figure 6 shows this spatially, O<sub>3</sub> damage is reduced when the effect  
613 of atmospheric CO<sub>2</sub> on stomatal closure is accounted for, however despite this, the land carbon sink and GPP  
614 remain significantly reduced due to O<sub>3</sub> exposure.

Commented [ORJ36]: RC1 2)

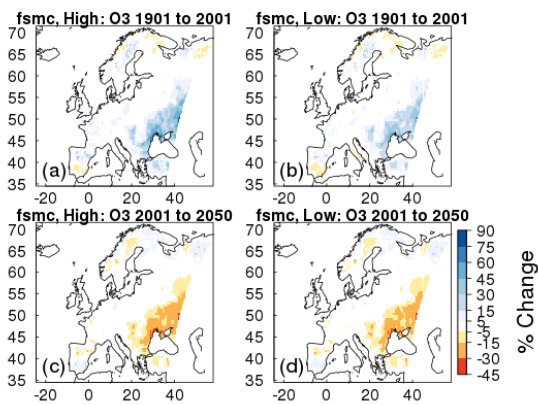
615  
616 Over the Anthropocene, changing O<sub>3</sub> and CO<sub>2</sub> in tandem results in an increase in European land carbon uptake  
617 (+5% to +9%), and an increase in GPP (+20% to +23%) by 2050 for the high and low plant O<sub>3</sub> sensitivity,  
618 respectively (Table 1). Nevertheless, despite this increase there remains a large negative impact of O<sub>3</sub> on the  
619 European land carbon sink (Fig. S139). By 2050 the simulated enhancement of land carbon and GPP in response  
620 to elevated CO<sub>2</sub> alone is reduced by 3% to 6% (land carbon) and 4% to 9% (GPP) for the low and high plant O<sub>3</sub>  
621 sensitivity respectively, when O<sub>3</sub> is also accounted for (Table 1). This is a large significant reduction in the ability  
622 of the European terrestrial biosphere to sequester carbon.

623



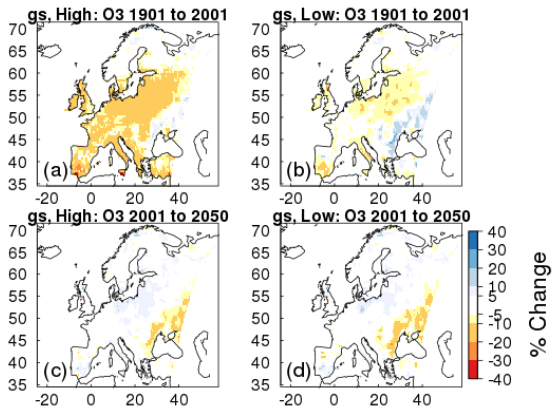
624

625 **Figure 43.** Simulated percentage change in total carbon stocks (Land C) and gross primary productivity (GPP)  
 626 due to O<sub>3</sub> effects at fixed pre-industrial atmospheric CO<sub>2</sub> concentration. Changes are shown for the periods 1901  
 627 to 2001, and 2001 to 2050 for the high and low plant O<sub>3</sub> sensitivity.  
 628



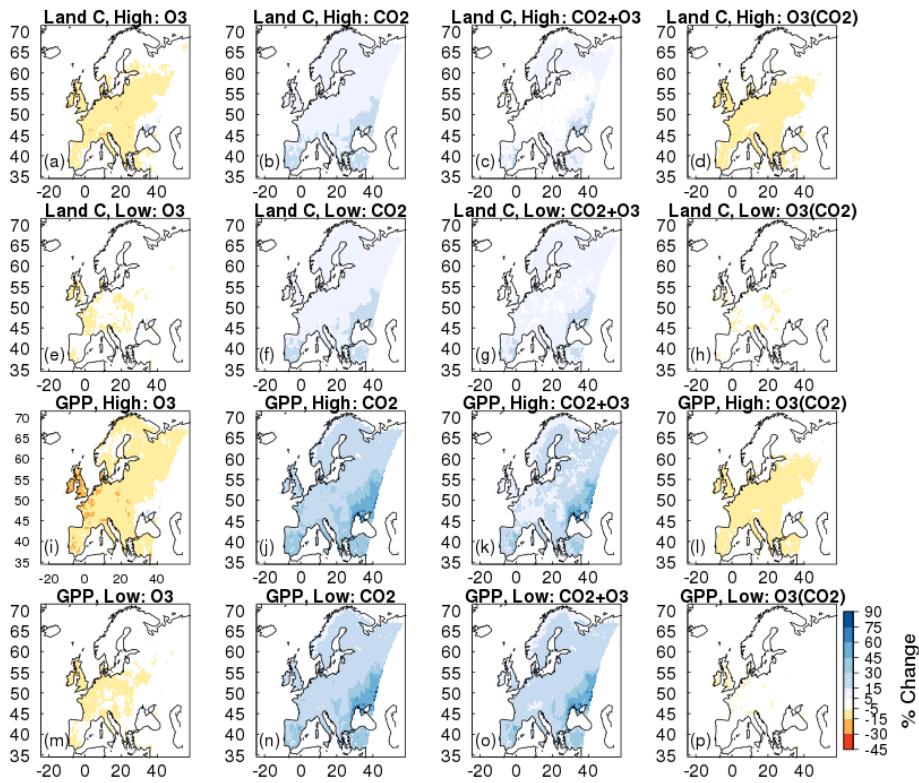
629

630 **Figure 54.** Simulated percentage change in plant available soil moisture (*fsmc*) due to O<sub>3</sub> effects at fixed pre-  
 631 industrial atmospheric CO<sub>2</sub> concentration. Changes are shown for the periods 1901 to 2001, and 2001 to 2050 for  
 632 the high and low plant O<sub>3</sub> sensitivity.  
 633



634

635 **Figure 6.5.** Simulated percentage change in stomatal conductance ( $g_s$ ) due to  $O_3$  effects at fixed pre-industrial  
 636 atmospheric  $CO_2$  concentration. Changes are shown for the periods 1901 to 2001, and 2001 to 2050 for the high  
 637 and low plant  $O_3$  sensitivity.  
 638



639

640 **Figure 76.** Simulated percentage change in total carbon stocks (Land C) and gross primary productivity (GPP)  
 641 due to i) (a, e, i, m) O<sub>3</sub> effects at fixed pre-industrial atmospheric CO<sub>2</sub> concentration (O<sub>3</sub>), ii) (b, f, j, n) CO<sub>2</sub>  
 642 fertilisation at fixed pre-industrial O<sub>3</sub> concentration (CO<sub>2</sub>), iii) (c, g, k, o) the interaction between O<sub>3</sub> and CO<sub>2</sub>  
 643 effects (CO<sub>2</sub> + O<sub>3</sub>) iv) (d, h, l, p) O<sub>3</sub> effects with changing atmospheric CO<sub>2</sub> concentration (i.e. O<sub>3</sub> damage  
 644 accounting for the effect of CO<sub>2</sub> induced stomatal closure; O<sub>3</sub>(CO<sub>2</sub>)). Changes are depicted for the periods 1901  
 645 to 2050 for high and lower ozone plant sensitivity.

646

647

648

649

650

651

652

	High Plant O <sub>3</sub> Sensitivity					
	1901 - 2001		2001 - 2050		1901 - 2050	
	GPP (Pg C yr <sup>-1</sup> )	Land C (Pg C)	GPP (Pg C yr <sup>-1</sup> )	Land C (Pg C)	GPP (Pg C yr <sup>-1</sup> )	Land C (Pg C)
Value in 1901:	9.05	167	-	-	9.05	167
Absolute Change:						
O <sub>3</sub>	-0.81	-9.21	0.01	-2.44	-0.80	-11.65
CO <sub>2</sub>	1.16	4.24	1.42	12.98	2.58	17.22
CO <sub>2</sub> + O <sub>3</sub>	0.13	-3.28	1.66	11.11	1.79	7.83
% Change:						
O <sub>3</sub>	-8.95	-5.51	0.12	-1.55	-8.84	-6.98
CO <sub>2</sub>	12.82	2.54	13.91	7.58	28.51	10.31
CO <sub>2</sub> + O <sub>3</sub>	1.44	-1.96	18.08	6.79	19.78	4.69
	Low Plant O <sub>3</sub> Sensitivity					
	1901 - 2001		2001 - 2050		1901 - 2050	
	GPP (Pg C yr <sup>-1</sup> )	Land C (Pg C)	GPP (Pg C yr <sup>-1</sup> )	Land C (Pg C)	GPP (Pg C yr <sup>-1</sup> )	Land C (Pg C)
Value in 1901:	9.34	167.5	-	-	9.34	167.5
Absolute Change:						
O <sub>3</sub>	-0.30	-3.59	0.02	-1.07	-0.40	-4.66
CO <sub>2</sub>	1.15	6.43	1.35	13.14	2.50	19.57
CO <sub>2</sub> + O <sub>3</sub>	0.65	2.50	1.50	12.35	2.15	14.85
% Change:						
O <sub>3</sub>	-3.21	-2.14	0.22	-0.65	-4.28	-2.78
CO <sub>2</sub>	12.31	3.84	12.87	7.55	26.77	11.68
CO <sub>2</sub> + O <sub>3</sub>	6.96	1.49	15.02	7.26	23.02	8.87

653

654 **Table 1.** Simulated changes in the European land carbon cycle due to changing O<sub>3</sub> and CO<sub>2</sub> concentrations  
655 (independently and together). Shown are changes in total carbon stocks (Land C) and gross primary productivity  
656 (GPP), over three different periods (historical: 1901 to 2001, future: 2001 to 2050, and Anthropocene: 1901 to  
657 2050). Absolute (top) and relative (bottom) differences are shown. For 2001 to 2050, please refer to Table S43  
658 for the initial value for each run. See the SI for details of the estimation of the O<sub>3</sub> and CO<sub>2</sub> effects and their  
659 interaction.

660

661

662

663

664

665

666

667

668

	Mean (Pg C)				
	1970-1979	1980-1989	1990-1999	2000-2009	2002-2011
<b>Modelled O<sub>3</sub> effect on land C sink :</b>					
Higher sensitivity	-1.32	-1.01	-0.97	-0.53	-0.50
Low sensitivity	-0.71	-0.58	-0.50	-0.29	-0.26
<b>Sum of C emissions from fossil fuel combustion and cement production (Pg C)</b>					
	8.39	8.63	12.26	12.83	12.75
<b>C lost from O<sub>3</sub> effect as a % of fossil fuel and cement emissions (%):</b>					
Higher sensitivity	-15.73	-11.70	-7.91	-4.13	-3.92
Low sensitivity	-8.46	-6.72	-4.08	-2.26	-2.04

670

671 **Table 2.** Simulated change in total land carbon due to O<sub>3</sub> damage with changing atmospheric CO<sub>2</sub> concentration  
672 for the two vegetation sensitivities. The sum of carbon emissions for each decade from fossil fuel combustion and  
673 cement production for the EU-28 countries plus Albania, Bosnia and Herzegovina, Iceland, Belarus, Serbia,  
674 Moldova, Norway, Turkey, Ukraine, Switzerland and Macedonia (EU28-plus) are shown, the data is from Boden  
675 *et al.*, 2013. The simulated change in land carbon as a result of O<sub>3</sub> damage is depicted as a percentage of the EU28-  
676 plus emissions to demonstrate the magnitude of the additional source of carbon to the atmosphere from plant O<sub>3</sub>  
677 damage.

678

## 679 4 Discussion

680

### 681 4.1 Comparison of *g<sub>s</sub>* models

682

683 Comparison of the new *g<sub>s</sub>* model implemented in this study (MEDedlyn *et al.*, 2014) with the *g<sub>s</sub>* model currently  
684 used as standard in JULES (JACaeobs-1994) revealed large differences in leaf-level *g<sub>s</sub>* for each PFT, principally  
685 as a result of the data-based parameterisation of the new model. Leaf-level water use increased for the broadleaf  
686 tree and C<sub>3</sub> herbaceous PFTs using the MEDedlyn-*g<sub>s</sub>* model compared to JACaeobs, but decreased for the needle  
687 leaf tree, C<sub>4</sub> herbaceous and shrub PFTs which displayed a more conservative water use strategy compared to the  
688 Jacobs parameterisation. These changes are in line with the work of De Kauwe *et al.* (2015) who found a reduction  
689 in annual transpiration for evergreen needle leaf, tundra and C<sub>4</sub> grass regions when implementing the Medlyn *g<sub>s</sub>*  
690 model into the Australian land surface scheme CABLE. Changes in leaf-level *g<sub>s</sub>* in this study resulted in  
691 differences in latent and sensible heat fluxes. Changes in the partitioning of energy fluxes at the land surface could  
692 potentially have consequences for the intensity of heatwaves (Cruz *et al.*, 2010; Kala *et al.*, 2016), runoff (Betts *et al.*,  
693 2007; Gedney *et al.*, 2006) and rainfall patterns (de Arellano *et al.*, 2012), although fully coupled simulations  
694 would be necessary to detect these effects. The differences in effect of the *g<sub>s</sub>* model on simulated *g<sub>s</sub>* stomatal  
695 conductance led to differences in the uptake of O<sub>3</sub> between the two *g<sub>s</sub>* models because the leaf-level rate of *g<sub>s</sub>*  
696 is the predominant determinant of the flux of O<sub>3</sub> through stomata. Higher O<sub>3</sub> uptake is indicative of greater damage.  
697 Therefore, given that C<sub>3</sub> herbaceous vegetation is the dominant land cover class across the European domain used

698 in this study, this suggests a greater O<sub>3</sub> impact for Europe ~~would be simulated with the MED edlyn-g<sub>s</sub>~~  
699 ~~model compared to JAC, and that studies using the Jacobs g<sub>s</sub> formulation may underestimate the O<sub>3</sub> impact for~~  
700 ~~Europe.~~

Commented [ORJ37]: RC2 3)

#### 701 **4.2 Lower than expected O<sub>3</sub> damage?**

702 We compare results from the present study to values found in literature. The Wittig et al. (2007) meta-analysis of  
703 temperate and boreal tree species showed future concentrations of O<sub>3</sub> predicted for 2050 significantly reduced leaf  
704 level light saturated net photosynthetic uptake (-19%, range: -3% to -28%) and g<sub>s</sub> (-10%, range: +5% to -23%) in  
705 both broadleaf and needle-leaf tree species. In the Feng et al. (2008) meta-analysis of wheat, projected O<sub>3</sub>  
706 concentrations for the future reduced aboveground biomass (-18%, CI -13% to -24%), photosynthetic rate (-20%)  
707 and g<sub>s</sub> (-22%). One of few long-term field-based O<sub>3</sub> exposure studies (AspenFACE) showed that after 11 years of  
708 exposing mature trees to elevated O<sub>3</sub> concentrations, O<sub>3</sub> decreased ecosystem carbon content (-9%), and decreased  
709 NPP (-10%), although the O<sub>3</sub> effect decreased through time (Falhelm et al., 2014). GPP was reduced (-12% to  
710 -19%) at two Mediterranean ecosystems (dominated by either *Pinus* species or *Citrus* species) studied by Fares et  
711 al. (2013). Biomass of mature beech trees was reduced (-44%) after 8 years of exposure to elevated O<sub>3</sub> (Matyssek  
712 et al., 2010a). After 5 years of O<sub>3</sub> exposure in a semi-natural grassland, annual biomass production was reduced  
713 (-23%), and in a Mediterranean annual pasture O<sub>3</sub> exposure significantly reduced total aboveground biomass (up  
714 to -25%) (Calvete-Sogo et al., 2014). Results from the present study suggest projected O<sub>3</sub> concentrations for 2050  
715 will reduce mean GPP for Europe (-4% to -9%), NPP (-6% to -11%), total carbon content (-3% to -7%) and g<sub>s</sub> (-  
716 4% to -9%). Using GPP as a proxy for  $A_{max}$  (these variables are not identical but they are related), our mean GPP  
717 and g<sub>s</sub> estimates fall within the range given by the meta-analysis of Wittig et al. (2007). The remaining studies are  
718 not meta-analyses, so are site- and species-specific, our estimates appear to compare more conservatively with  
719 these, however these are a mean value for Europe and spatially our estimates show greater variability.

720  
721 The impact of O<sub>3</sub> on present day European GPP simulated in this study is slightly lower compared to previous  
722 ~~modelled estimates studies~~. Our estimates suggest present day O<sub>3</sub> reduced GPP by 3% to 9% on average across  
723 Europe and NPP by 5% to 11% (Table S3). Anav et al. (2011) simulated a 22% reduction of GPP across Europe  
724 for 2002 using the ORCHIDEE model. Present day O<sub>3</sub> exposure reduced GPP by 10% to 25% in Europe, and  
725 10.8% globally in the study by Lombardozzi et al. (2015) using the Community land model (CLM). O<sub>3</sub> reduced  
726 NPP by 11.2% in Europe from 1989 to 1995 using the Terrestrial Ecosystem Model (TEM) (Felzer et al., 2005).  
727 Globally, concentrations of O<sub>3</sub> predicted for 2100 reduced GPP by 14% to 23% using a former parameterisation  
728 of O<sub>3</sub> sensitivity in JULES (Sitch et al., 2007). The recent study by Franz et al. (2017) showed mean GPP declined  
729 by 4.7% over the period 2001 to 2010 using the OCN model over the same European domain used in this study.  
730 These ~~similar similarly 'lower than expected'~~ results are likely the result of using the same domain, and, more  
731 importantly, O<sub>3</sub> forcing produced by the same model (EMEP MSC-W).

#### 733 **4.3 Impacts of O<sub>3</sub> at the land surface**

734  
735 In this study, O<sub>3</sub> has a detrimental effect on the size of the land carbon sink for Europe. This is primarily through  
736 a decrease in the size of the soil carbon pool as a result of reduced litter input to the soil, consistent with reduced  
737 GPP/NPP. Field studies show that in some regions of Europe, soil carbon stocks are decreasing (Bellamy et al.,



738 2005;Capriel, 2013;Heikkinen et al., 2013;Sleutel et al., 2003). The study of Bellamy et al. (2005), for example,  
739 showed that carbon was lost from soils across England and Wales between 1978 to 2003 at a mean rate of 0.6%  
740 per year with little effect of land use on the rate of carbon loss, suggesting a possible link to climate change. It is  
741 understood that climate change is likely to affect soil carbon turnover. Increased temperatures increase microbial  
742 decomposition activity in the soil, and therefore increase carbon losses through higher rates of respiration (Cox et  
743 al., 2000;Friedlingstein et al., 2006;Jones et al., 2003). However, some studies have found that O<sub>3</sub> can decrease  
744 soil carbon content. Talhelm et al. (2014), for example, found O<sub>3</sub> reduced carbon content in near surface mineral  
745 soil of forest soils exposed to 11 years of O<sub>3</sub> fumigation. Hofmockel et al. (2011) found elevated O<sub>3</sub> reduced the  
746 carbon content in more stable soil organic matter pools, and Loya et al. (2003) showed that the fraction of soil  
747 carbon formed in forest soils over a 4 year experimental period when fumigated with both CO<sub>2</sub> and O<sub>3</sub> was reduced  
748 by 51% compared to the soil fumigated with CO<sub>2</sub> alone. It is agreed that amongst other factors that change with  
749 O<sub>3</sub> exposure such as litter quality and composition, reduced litter quantity also has significant detrimental  
750 consequences for soil carbon stocks (Andersen, 2003;Lindroth, 2010;Loya et al., 2003). Results from this study  
751 therefore suggest that increasing tropospheric O<sub>3</sub> may be a contributing factor to the declining soil carbon stocks  
752 observed across Europe as a result of reduced litter input to the soil carbon pool consistent with reduced NPP.

753  
754 We acknowledge, however, that our model simulations do not include coupling of Nitrogen and Carbon cycles,  
755 or land management practices. Although we include a representation of agricultural regions through the model  
756 calibration against the wheat O<sub>3</sub> sensitivity function (CLRTAP, 2017), wheat is known to be one of the most O<sub>3</sub>  
757 sensitive crop species. As with all uncoupled modelling studies, a change in  $g_s$  and flux will impact the O<sub>3</sub>  
758 concentration itself. Therefore adopting the Medlyn formulation with a higher  $g_s$  and subsequently higher O<sub>3</sub> flux  
759 for broadleaf and C<sub>3</sub> PFTs (Fig 2) would lead to reduced O<sub>3</sub> concentration, which in turn would act to dampen the  
760 effect of higher  $g_s$  on O<sub>3</sub> flux. Essentially this study provides an 'upper bound' as in the high plant O<sub>3</sub> sensitivity  
761 scenario, all C<sub>3</sub>/C<sub>4</sub> fractional cover uses the wheat O<sub>3</sub> sensitivity. Additionally, this version of JULES does not  
762 have a crop module; it has no land management practices such as harvesting, ploughing or crop rotation –  
763 processes which may have counteracting effects on the land carbon sink. Further, without a coupled Carbon and  
764 Nitrogen cycle, it is likely that the CO<sub>2</sub> fertilisation response of GPP and the land carbon sink is over estimated in  
765 some regions of our simulations since nitrogen availability limits terrestrial carbon sequestration of natural  
766 ecosystems in the temperate and boreal zone (Zaehle, 2013). This would have consequences for our modelled O<sub>3</sub>  
767 impact, particularly into the future where the large CO<sub>2</sub> fertilisation effect was responsible for partly offsetting  
768 the negative impact of O<sub>3</sub>. Although in our simulations a high fraction of land cover is agricultural which we  
769 assume would be optimally fertilised. Nevertheless, we emphasise that this study provides a sensitivity assessment  
770 of the impact of plant O<sub>3</sub> damage on GPP and the land carbon sink.

771  
772 Another caveat we fully acknowledge is that at the leaf-level JULES is parameterised to reduce  $g_s$  with O<sub>3</sub>  
773 exposure. Whilst this response is commonly observed (Wittig et al., 2007;Ainsworth et al., 2012), there is evidence  
774 to suggest that O<sub>3</sub> impairs stomata in some species, making them non-responsive to environmental stimuli (Hayes  
775 et al., 2012;Hoshika et al., 2012a;Mills et al., 2009;Paoletti and Grulke, 2010). In drought conditions the  
776 mechanism is thought to involve O<sub>3</sub> stimulated ethylene production which interferes with the stomatal response  
777 to ABA signalling (Wilkinson and Davies, 2009;Wilkinson and Davies, 2010). Such stomatal sluggishness can

Commented [ORJ38]: RC2 minor comment 16.

778 result in higher O<sub>3</sub> uptake and injury, increased water-loss, and therefore greater vulnerability to environmental  
779 stresses (Mills et al., 2016). McLaughlin (2007a;2007b) and Sun et al. (2012) provide evidence of increased  
780 transpiration and reduced streamflow in forests at the regional scale in response to ambient levels of O<sub>3</sub>, and  
781 suggest this could increase the frequency and severity of droughts. (Hoshika et al., 2012b) Hoshika et al 2012  
782 however found that despite sluggish stomatal control in O<sub>3</sub> exposed trees, whole tree water use was lower in these  
783 trees because of lower gas exchange and premature leaf shedding of injured leaves. To our knowledge, the study  
784 of Hoshika et al. (2015) is the first to include an explicit representation of sluggish stomatal control in a land-  
785 atmosphere model, they show that sluggish stomatal behaviour has significant implications for carbon and water  
786 cycling in ecosystems. However, it is by no means a ubiquitous response, and it is not fully understood which  
787 species respond this way and under what conditions (Mills et al., 2016; Wittig et al., 2007). Nevertheless, this  
788 remains an important area of future work.

789  
790 The calculation of O<sub>3</sub> deposition in the EMEP model uses the stomatal conductance formulation presented in  
791 Emberson et al. (2000;2001), which depends on temperature, light, humidity and soil moisture (commonly  
792 referred to as DO<sub>3</sub>SE). Because we link two different model systems, the g<sub>s</sub> values in the EMEP model differ from  
793 those obtained using the Medlyn formulation. We acknowledge this inconsistency as a caveat of our study,  
794 however comparison of g<sub>max</sub> (maximum g<sub>s</sub>) values from both models (EMEP and JULES) suggests the  
795 differences are small for deciduous forest (EMEP 150-200, JULES ~180, all units in mmole O<sub>3</sub>/m<sup>2</sup> (PLA)/s), and  
796 C<sub>3</sub>/C<sub>4</sub> crops (EMEP 270-300, JULES ~260-390 – the dominant land cover in our simulations), but are larger for  
797 coniferous forest (EMEP 140-200, JULES ~60-70) and shrubs (EMEP 60-200, JULES 360-390). The role of  
798 EMEP in this study is not to provide g<sub>s</sub>, however, but to provide O<sub>3</sub> at the top of the vegetation canopy. The main  
799 driver of such O<sub>3</sub> levels is the regional-scale production and transport of O<sub>3</sub>, and the main impact of g<sub>s</sub> is in  
800 affecting the vertical O<sub>3</sub> gradients just above the plant canopy. Differences in g<sub>s</sub> are known to have minimal impact  
801 on canopy-top O<sub>3</sub> for trees, mainly due to the efficient turbulent mixing above tall canopies, but also due to non-  
802 stomatal sink processes. For shorter vegetation, substantial O<sub>3</sub> gradients, driven by deposition, occur in the lowest  
803 10s of metres of the atmosphere, and stomatal sinks (as given by g<sub>s</sub>) can have a significant role. However,  
804 calculations of such gradients made with the EMEP model for CLRTAP (2017) showed that differences amounted  
805 to only ca. 10% when comparing O<sub>3</sub> concentrations at 1m height above high-g<sub>s</sub> crops compared to moderate-g<sub>s</sub>  
806 (g<sub>max</sub> = 450 and 270 mmole O<sub>3</sub>/m<sup>2</sup> (PLA)/s respectively), therefore this uncertainty is small.

Commented [ORJ39]: RC2 4)

807  
808 These offline simulations show the sensitivity of GPP and the land carbon sink to tropospheric O<sub>3</sub>, suggesting that  
809 O<sub>3</sub> is an important predictor of future GPP and the land carbon store across Europe. There are uncertainties in our  
810 estimates however from the use of uncoupled tropospheric chemistry, meteorology and stomatal function. For  
811 example, increased frequency of drought in the future would reduce stomatal conductance (assuming no sluggish  
812 stomatal response) and thus O<sub>3</sub> uptake. Since our offline simulations do not include this feedback it is possible the  
813 O<sub>3</sub> effect is over estimated here. Given the complexity of potential interactions and feedbacks it remains difficult  
814 to diagnose the importance of individual factors (e.g. the direct physiological response) in a fully coupled  
815 simulation. Once the importance of a process is demonstrated offline, it provides evidence of the need to  
816 incorporate such process in coupled regional and global simulations.

Commented [ORJ40]: RC1 2)

Commented [ORJ41]: RC2 1)

#### 818 4.4 O<sub>3</sub> as a missing component of carbon cycle assessments?

819  
820 Comprehensive analyses of the European carbon balance suggest a ~~large significant~~ biogenic carbon sink  
821 (Janssens et al., 2003;Luyssaert et al., 2012;Schulze et al., 2009). However, estimates are hampered by large  
822 uncertainties in key components of the land carbon balance, such as estimates of soil carbon gains and losses  
823 (Ciais et al., 2010;Janssens et al., 2003;Schulze et al., 2009;Schulze et al., 2010). We suggest that the effect of O<sub>3</sub>  
824 on plant physiology is a contributing factor to the decline in soil carbon stores observed across Europe, and as  
825 such this O<sub>3</sub> effect is a missing component of European carbon cycle assessments. Over the Anthropocene, our  
826 results show elevated O<sub>3</sub> concentrations reduce the amount of carbon that can be stored in the soil by 3% to 9%  
827 (low and high plant O<sub>3</sub> sensitivity, respectively), which almost completely offsets the beneficial effects of CO<sub>2</sub>  
828 fertilisation on soil carbon storage under the high plant O<sub>3</sub> sensitivity . This would contribute to a ~~significant~~  
829 change in the size of a key carbon sink for Europe, and is particularly important when we consider the evolution  
830 of the land carbon sink into the future given the impact of O<sub>3</sub> on soil carbon sequestration and the high uncertainty  
831 of future tropospheric O<sub>3</sub> concentrations. Schulze et al. (2009) and Luyssaert et al. (2012) extended their analysis  
832 of the European carbon balance to include additional non-CO<sub>2</sub> greenhouse gases (CH<sub>4</sub> and N<sub>2</sub>O). Both studies  
833 found that emissions of these offset the biogenic carbon sink, reducing the climate mitigation potential of  
834 European ecosystems. This highlights the importance of accounting for all fluxes and stores in carbon/greenhouse  
835 gas balance assessments, of which O<sub>3</sub> and its indirect effect on the CO<sub>2</sub> flux via direct effects on plant physiology  
836 is currently missing.

#### 837 4.5 The interaction between O<sub>3</sub> and CO<sub>2</sub>

839  
840 We looked at the interaction between CO<sub>2</sub> and O<sub>3</sub> effects. Our results support the hypothesis that elevated  
841 atmospheric CO<sub>2</sub> provides some protection against O<sub>3</sub> damage because of lower g<sub>s</sub> that reduces uptake of O<sub>3</sub>  
842 through stomata (Harmens et al., 2007;Wittig et al., 2007). In the present study, reductions in GPP and the land  
843 carbon store due to O<sub>3</sub> exposure were lower when simulated with concurrent changes in atmospheric CO<sub>2</sub>. Despite  
844 acclimation of photosynthesis after long-term exposure to elevated atmospheric CO<sub>2</sub> of field grown plants  
845 (Ainsworth and Long, 2005;Medlyn et al., 1999), there is no evidence to suggest that g<sub>s</sub> acclimates (Ainsworth et  
846 al., 2003;Medlyn et al., 2001). This suggests the protective effect of elevated atmospheric CO<sub>2</sub> against O<sub>3</sub> damage  
847 will be sustained in the long term. However, although meta-analysis suggest a general trend of reduced g<sub>s</sub> with  
848 elevated CO<sub>2</sub> (Ainsworth and Long, 2005;Medlyn et al., 1999), this is not a universal response. Stomatal responses  
849 on exposure to elevated CO<sub>2</sub> with FACE treatment varied with genotype and growth stage in a fast-growing poplar  
850 community (Bernacchi et al., 2003;Tricker et al., 2009). In other mature forest stands, limited stomatal response  
851 to elevated CO<sub>2</sub> was observed after canopy closure (Ellsworth, 1999;Uddling et al., 2009). Also, some studies  
852 found that stomatal responses to CO<sub>2</sub> were significant only under high atmospheric humidity (Cech et al.,  
853 2003;Leuzinger and Körner, 2007;Wullschleger et al., 2002). These examples illustrate that stomatal responses to  
854 elevated atmospheric CO<sub>2</sub> are not universal, and as such the protective effect of CO<sub>2</sub> against O<sub>3</sub> injury cannot be  
855 assumed for all species, at all growth stages under wide ranging environmental conditions.

#### 856 **5 Conclusion**

858  
859 What is abundantly clear is that plant responses to both CO<sub>2</sub> and O<sub>3</sub> are complicated by a host of factors that are  
860 only partly understood, and it remains difficult to identify general, global patterns given that effects of both gases  
861 on plant communities and ecological interactions are highly context and species specific (Ainsworth and Long,  
862 2005;Fuhrer et al., 2016;Matyssek et al., 2010b). This study quantifies the sensitivity of the land carbon sink for  
863 Europe and GPP to changing concentrations of atmospheric CO<sub>2</sub> and O<sub>3</sub> from 1901 to 2050. We have used a state  
864 of the art land surface model calibrated for European vegetation to give our best estimates of this sensitivity within  
865 the limits of data availability to calibrate the model for O<sub>3</sub> sensitivity, current knowledge and model structure. In  
866 summary, this study has shown that potential gains in terrestrial carbon sequestration over Europe resulting from  
867 elevated CO<sub>2</sub> can be partially offset by concurrent rises in tropospheric O<sub>3</sub> over 1901-2050. Specifically, we have  
868 shown that the negative effect of O<sub>3</sub> on the land carbon sink was greatest over the twentieth century, when O<sub>3</sub>  
869 concentrations increased rapidly from pre-industrial levels. Over this period soil carbon stocks were ~~significantly~~  
870 diminished over agricultural areas, consistent with reduced NPP and litter input. This loss of soil carbon was  
871 largely responsible for the decrease in the size of the land carbon sink over Europe. The O<sub>3</sub> effect on the land  
872 carbon store and flux was reduced into the future as CO<sub>2</sub> concentration rose considerably and changes in O<sub>3</sub>  
873 concentration were less pronounced. However, there remained a large cumulative negative impact on the land  
874 carbon sink for Europe by 2050. The interaction between the two gases was found to reduce O<sub>3</sub> injury owing to  
875 reduced stomatal opening in elevated atmospheric CO<sub>2</sub>. However, primary productivity and land carbon storage  
876 remained ~~significantly~~ suppressed by 2050 due to plant O<sub>3</sub> damage. Expressed as a percentage of the emissions  
877 from fossil fuel and cement production for the EU28-plus countries, the ~~additional~~ carbon emissions from O<sub>3</sub>-  
878 induced plant injury ~~are~~ is a potential significant additional source of anthropogenic carbon previously not  
879 accounted for in carbon cycle assessments. Our results demonstrate the sensitivity of modelled terrestrial carbon  
880 dynamics to the direct effect of tropospheric O<sub>3</sub> and its interaction with atmospheric CO<sub>2</sub> on plant physiology.  
881 demonstrating this process is an important predictor of future GPP and trends in the land-carbon sink.  
882 Nevertheless, this process remains largely unconsidered in regional and global climate model simulations that are  
883 used to model carbon sources and sinks and carbon-climate feedbacks.

Commented [ORJ42]: RC2 1)

884  
885  
886 ~~, highlighting that such effects of O<sub>3</sub> on plant physiology significantly add to the uncertainty of future trends in~~  
887 ~~the land carbon sink and climate carbon feedbacks. Given the potential to limit the climate mitigation effect of~~  
888 ~~European terrestrial ecosystems, we suggest plant O<sub>3</sub> damage should be incorporated into carbon cycle~~  
889 ~~assessments.~~

#### 890 **Data availability**

891  
892  
893 The JULES model can be downloaded from the Met Office Science Repository Service  
894 (<https://code.metoffice.gov.uk/trac/jules> - see here for a helpful how to [http://jules.jchmr.org/content/getting-](http://jules.jchmr.org/content/getting-started)  
895 started). Model output data presented in this paper and the exact version of JULES with namelists are available  
896 upon request from the corresponding author.  
897

898 **Supplementary Information**

899

900 Supplementary\_Information\_Oliver\_et\_al.docx

901

902 **Competing Interests**

903 The authors declare that they have no conflict of interest

904

905 **Acknowledgements**

906

907 RJO and LMM were supported by the EU FP7 (ECLAIRE, 282910) and JWCRP (UKESM, NEC05816). This  
908 work was also supported by EMEP under UNECE. SS and LMM acknowledge the support of the NERC  
909 SAMBBA project (NE/J010057/1). The UK Met Office contribution was funded by BEIS under the Hadley Centre  
910 Climate Programme (GA01101). GAF also acknowledges funding from the EU's Horizon 2020 research and  
911 innovation programme (CRESCENDO, 641816). We also thank Magnuz Engardt of SMHI for providing the  
912 RCA3 climate dataset.

913

914 **References**

915

916 Ainsworth, E., and Long, S.: What have we learned from 15 years of free-air CO<sub>2</sub> enrichment (FACE)?  
917 A meta-analytic review of the responses of photosynthesis, canopy properties and plant production  
918 to rising CO<sub>2</sub>, New Phytologist, 165, 351-372, 2005.

919 Ainsworth, E. A., Davey, P. A., Hymus, G. J., Osborne, C. P., Rogers, A., Blum, H., Nosberger, J., and  
920 Long, S. P.: Is stimulation of leaf photosynthesis by elevated carbon dioxide concentration  
921 maintained in the long term? A test with *Lolium perenne* grown for 10 years at two nitrogen  
922 fertilization levels under Free Air CO<sub>2</sub> Enrichment (FACE), *Plant, Cell and Environment*, 26, 705-714,  
923 2003.

924 Ainsworth, E. A.: Rice production in a changing climate: a meta-analysis of responses to elevated  
925 carbon dioxide and elevated ozone concentration, *Global Change Biology*, 14, 1642-1650,  
926 10.1111/j.1365-2486.2008.01594.x, 2008.

927 Ainsworth, E. A., Yendrek, C. R., Sitch, S., Collins, W. J., and Emberson, L. D.: The Effects of  
928 Tropospheric Ozone on Net Primary Productivity and Implications for Climate Change, *Annual*  
929 *Review of Plant Biology*, 63, 637-661, doi:10.1146/annurev-arplant-042110-103829, 2012.

930 Anav, A., Menut, L., Khvorostyanov, D., and Viovy, N.: Impact of tropospheric ozone on the Euro-  
931 Mediterranean vegetation, *Global change biology*, 17, 2342-2359, 2011.

932 Andersen, C. P.: Source-sink balance and carbon allocation below ground in plants exposed to  
933 ozone, *New Phytologist*, 157, 213-228, 10.1046/j.1469-8137.2003.00674.x, 2003.

934 Arneth, A., Harrison, S. P., Zaehle, S., Tsigaridis, K., Menon, S., Bartlein, P. J., Feichter, J., Korhola, A.,  
935 Kulmala, M., O'Donnell, D., Schurgers, G., Sorvari, S., and Vesala, T.: Terrestrial biogeochemical  
936 feedbacks in the climate system, *Nature Geosci*, 3, 525-532,  
937 [http://www.nature.com/ngeo/journal/v3/n8/supinfo/ngeo905\\_S1.html](http://www.nature.com/ngeo/journal/v3/n8/supinfo/ngeo905_S1.html), 2010.

938 Avnery, S., Mauzerall, D. L., Liu, J., and Horowitz, L. W.: Global crop yield reductions due to surface  
939 ozone exposure: 1. Year 2000 crop production losses and economic damage, *Atmospheric*  
940 *Environment*, 45, 2284-2296, <https://doi.org/10.1016/j.atmosenv.2010.11.045>, 2011.

Field Code Changed

941 Baig, S., Medlyn, B. E., Mercado, L. M., and Zaehle, S.: Does the growth response of woody plants to  
942 elevated CO<sub>2</sub> increase with temperature? A model-oriented meta-analysis, *Global Change Biology*,  
943 21, 4303-4319, 10.1111/gcb.12962, 2015.

944 Bellamy, P. H., Loveland, P. J., Bradley, R. I., Lark, R. M., and Kirk, G. J.: Carbon losses from all soils  
945 across England and Wales 1978–2003, *Nature*, 437, 245-248, 2005.

946 Bernacchi, C. J., Calfapietra, C., Davey, P. A., Wittig, V. E., Scarascia-Mugnozza, G. E., Raines, C. A.,  
947 and Long, S. P.: Photosynthesis and stomatal conductance responses of poplars to free-air CO<sub>2</sub>  
948 enrichment (PopFACE) during the first growth cycle and immediately following coppice., *New*  
949 *Phytologist*, 159, 609-621, 2003.

950 Best, M. J., Pryor, M., Clark, D. B., Rooney, G. G., Essery, R. L. H., Menard, C. B., Edwards, J. M.,  
951 Hendry, M. A., Porson, N., Gedney, N., Mercado, L. M., Sitch, S., Blyth, E., Boucher, O., Cox, P. M.,  
952 Grimmond, C. S. B., and Harding, R. J.: The Joint UK Land Environment Simulator (JULES), Model  
953 description - Part 1: Energy and water fluxes, *Geoscientific Model Development Discussions*, 4, 595-  
954 640, 10.5194/GMDD-4-595-2011, 2011.

955 Betts, R. A., Boucher, O., Collins, M., Cox, P. M., Falloon, P. D., Gedney, N., Hemming, D. L.,  
956 Huntingford, C., Jones, C. D., and Sexton, D. M.: Projected increase in continental runoff due to plant  
957 responses to increasing carbon dioxide, *Nature*, 448, 1037-1041, 2007.

958 Boden, T. A., Marland, G., and Andres, R. J.: Global, Regional, and National Fossil-Fuel CO<sub>2</sub> Emissions,  
959 Oak Ridge National Laboratory, U.S. Department of Energy, Oak Ridge, Tenn., USA, 2013.

960 Büker, P., Feng, Z., Uddling, J., Briolat, A., Alonso, R., Braun, S., Elvira, S., Gerosa, G., Karlsson, P. E.,  
961 Le Thiec, D., Marzuoli, R., Mills, G., Oksanen, E., Wieser, G., Wilkinson, M., and Emberson, L. D.: New  
962 flux based dose-response relationships for ozone for European forest tree species, *Environmental*  
963 *Pollution*, 163-174, 2015.

964 Calvete-Sogo, H., Elvira, S., Sanz, J., González-Fernández, I., García-Gómez, H., Sánchez-Martín, L.,  
965 Alonso, R., and Bermejo-Bermejo, V.: Current ozone levels threaten gross primary production and  
966 yield of Mediterranean annual pastures and nitrogen modulates the response, *Atmospheric*  
967 *Environment*, 95, 197-206, <http://dx.doi.org/10.1016/j.atmosenv.2014.05.073>, 2014.

968 Capriel, P.: Trends in organic carbon and nitrogen contents in agricultural soils in Bavaria (south  
969 Germany) between 1986 and 2007, *European Journal of Soil Science*, 64, 445-454, 2013.

970 Cech, P. G., Pepin, S., and Korner, C.: Elevated CO<sub>2</sub> reduces sap flux in mature deciduous forest trees,  
971 *Oecologia*, 137, 258-268, 2003.

972 Ceulemans, R., and Mousseau, M.: Effects of elevated atmospheric CO<sub>2</sub> on woody plants, *New*  
973 *Phytologist*, 127, 1994.

974 Ciais, P., Wattenbach, M., Vuichard, N., Smith, P., Piao, S., Don, A., Luysaert, S., Janssens, I.,  
975 Bondeau, A., and Dechow, R.: The European carbon balance. Part 2: croplands, *Global Change*  
976 *Biology*, 16, 1409-1428, 2010.

977 Ciais, P., Sabine, C., Bala, G., Bopp, L., Brovkin, V., Canadell, J., Chhabra, A., DeFries, R., Galloway, J.,  
978 Heimann, M., Jones, C., Le Quéré, C., Myneni, R. B., Piao, S., and Thornton, P.: Carbon and Other  
979 Biogeochemical Cycles. In: *Climate Change 2013: The Physical Science Basis. Contribution of Working*  
980 *Group I to the Fifth Assessment Report of the Intergovernmental Panel on Climate Change* [Stocker,  
981 T.F., D. Qin, G.-K. Plattner, M. Tignor, S.K. Allen, J. Boschung, A. Nauels, Y. Xia, V. Bex and P.M.  
982 Midgley (eds.)]. Cambridge University Press, Cambridge, United Kingdom and New York, NY, USA.,  
983 2013.

984 Clark, D. B., Mercado, L. M., Sitch, S., Jones, C. D., Gedney, N., Best, M. J., Pryor, M., Rooney, G. G.,  
985 Essery, R. L. H., Blyth, E., Boucher, O., Harding, R. J., and Cox, P. M.: The Joint UK Land Environment  
986 Simulator (JULES), Model description - Part 2: Carbon fluxes and vegetation, *Geoscientific Model*  
987 *Development Discussions*, 4, 641-688, 10.5194/gmdd-4-641-2011, 2011.

988 CLRTAP: The UNECE Convention on Long-range Transboundary Air Pollution. Manual on  
989 Methodologies and Criteria for Modelling and Mapping Critical Loads and Levels and Air Pollution  
990 Effects, Risks and Trends: Chapter III Mapping Critical Levels for Vegetation, accessed via,

991 [http://icpvegetation.ceh.ac.uk/publications/documents/Chapter3-](http://icpvegetation.ceh.ac.uk/publications/documents/Chapter3-Mappingcriticallevelsforvegetation_000.pdf)  
992 [Mappingcriticallevelsforvegetation\\_000.pdf](http://icpvegetation.ceh.ac.uk/publications/documents/Chapter3-Mappingcriticallevelsforvegetation_000.pdf), 2017.

993 Collins, W. J., Sitch, S., and Boucher, O.: How vegetation impacts affect climate metrics for ozone  
994 precursors, *Journal of Geophysical Research: Atmospheres*, 115, D23308, 10.1029/2010JD014187,  
995 2010.

996 Collins, W. J., Bellouin, N., Doutriaux-Boucher, M., Gedney, N., Halloran, P., Hinton, T., Hughes, J.,  
997 Jones, C. D., Joshi, M., Liddicoat, S., Martin, G., O'Connor, F., Rae, J., Senior, C., Sitch, S., Totterdell, I.,  
998 Wiltshire, A., and Woodward, S.: Development and evaluation of an Earth-System model –  
999 HadGEM2, *Geosci. Model Dev.*, 4, 1051-1075, 10.5194/gmd-4-1051-2011, 2011.

1000 Cooper, O. R., Parrish, D. D., Stohl, A., Trainer, M., Nedelec, P., Thouret, V., Cammas, J. P., Oltmans,  
1001 S. J., Johnson, B. J., Tarasick, D., Leblanc, T., McDermid, I. S., Jaffe, D., Gao, R., Stith, J., Ryerson, T.,  
1002 Aikin, K., Campos, T., Weinheimer, A., and Avery, M. A.: Increasing springtime ozone mixing ratios in  
1003 the free troposphere over western North America, *Nature*, 463, 344-348,  
1004 [http://www.nature.com/nature/journal/v463/n7279/supinfo/nature08708\\_S1.html](http://www.nature.com/nature/journal/v463/n7279/supinfo/nature08708_S1.html), 2010.

1005 Cooper, O. R., Parrish, D., Ziemke, J., Balashov, N., Cupeiro, M., Galbally, I., Gilge, S., Horowitz, L.,  
1006 Jensen, N., and Lamarque, J.-F.: Global distribution and trends of tropospheric ozone: An  
1007 observation-based review, *Elementa: Science of the Anthropocene*, 2, 000029, 2014.

1008 Cox, P. M., Betts, R. A., Jones, C. D., Spall, S. A., and Totterdell, I. J.: Acceleration of global warming  
1009 due to carbon-cycle feedbacks in a coupled climate model, *Nature*, 408, 184-187, 2000.

1010 Cox, P. M.: Description of the TRIFFID dynamic global vegetation model, Hadley Centre technical  
1011 note 24, 2001.

1012 Cruz, F. T., Pitman, A. J., and Wang, Y. P.: Can the stomatal response to higher atmospheric carbon  
1013 dioxide explain the unusual temperatures during the 2002 Murray-Darling Basin drought?, *Journal of*  
1014 *Geophysical Research: Atmospheres*, 115, 2010.

1015 de Arellano, J. V.-G., van Heerwaarden, C. C., and Lelieveld, J.: Modelled suppression of boundary-  
1016 layer clouds by plants in a CO<sub>2</sub>-rich atmosphere, *Nature geoscience*, 5, 701-704, 2012.

1017 De Kauwe, M., Kala, J., Lin, Y.-S., Pitman, A., Medlyn, B., Duursma, R., Abramowitz, G., Wang, Y.-P.,  
1018 and Miralles, D.: A test of an optimal stomatal conductance scheme within the CABLE land surface  
1019 model, 8, 431-452, 2015.

1020 Dentener, F., Stevenson, D., Ellingsen, K., van Noije, T., Schultz, M., Amann, M., Atherton, C., Bell, N.,  
1021 Bergmann, D., Bey, I., Bouwman, L., Butler, T., Cofala, J., Collins, B., Drevet, J., Doherty, R., Eickhout,  
1022 B., Eskes, H., Fiore, A., Gauss, M., Hauglustaine, D., Horowitz, L., Isaksen, I. S. A., Josse, B., Lawrence,  
1023 M., Krol, M., Lamarque, J. F., Montanaro, V., Müller, J. F., Peuch, V. H., Pitari, G., Pyle, J., Rast, S.,  
1024 Rodriguez, J., Sanderson, M., Savage, N. H., Shindell, D., Strahan, S., Szopa, S., Sudo, K., Van  
1025 Dingenen, R., Wild, O., and Zeng, G.: The Global Atmospheric Environment for the Next Generation,  
1026 *Environmental Science & Technology*, 40, 3586-3594, 10.1021/es0523845, 2006.

1027 Derwent, R. G., Stevenson, D. S., Doherty, R. M., Collins, W. J., Sanderson, M. G., and Johnson, C. E.:  
1028 Radiative forcing from surface NO<sub>x</sub> emissions: spatial and seasonal variations, *Climatic Change*, 88,  
1029 385-401, 10.1007/s10584-007-9383-8, 2008.

1030 Ellsworth, D. S.: CO<sub>2</sub> enrichment in a maturing pine forest: are CO<sub>2</sub> exchange and water status in the  
1031 canopy affected?, *Plant, Cell and Environment*, 22, 461-472, 1999.

1032 Emberson, L. D., Ashmore, M. R., Cambridge, H. M., Simpson, D., and Tuovinen, J.-P.: Modelling  
1033 stomatal ozone flux across Europe, *Environmental Pollution*, 109, 403-413, 2000.

1034 Emberson, L. D., Simpson, D., Tuovinen, J.-P., Ashmore, M. R., and Cambridge, H. M.: Modelling and  
1035 mapping ozone deposition in Europe, *Water Air Soil Pollution*, 130, 577-582, 2001.

1036 Engardt, M., Simpson, D., Schwikowski, M., and Granat, L.: Deposition of sulphur and nitrogen in  
1037 Europe 1900-2050. Model calculations and comparison to historical observations, *Tellus B: Chem.*  
1038 *Phys. Meteor.*, 69, 2017.

1039 Etheridge, D. M., Steele, L. P., Langenfelds, R. L., Francey, R. J., M., B., and Morgan, V. I.: Natural and  
1040 anthropogenic changes in atmospheric CO<sub>2</sub> over the last 1000 years from air in Antarctic ice and firn,  
1041 *Journal of Geophysical Research*, 101(D2), 4115-4128, doi:10.1029/95JD03410, 1996.

1042 Fagnano, M., Maggio, A., and Fumagalli, I.: Crops' responses to ozone in Mediterranean  
1043 environments, *Environmental Pollution*, 157, 1438-1444, 2009.

1044 Fares, S., Vargas, R., Detto, M., Goldstein, A. H., Karlik, J., Paoletti, E., and Vitale, M.: Tropospheric  
1045 ozone reduces carbon assimilation in trees: estimates from analysis of continuous flux  
1046 measurements, *Global change biology*, 19, 2427-2443, 2013.

1047 Felzer, B., Reilly, J., Melillo, J., Kicklighter, D., Sarofim, M., Wang, C., Prinn, R., and Zhuang, Q.: Future  
1048 Effects of Ozone on Carbon Sequestration and Climate Change Policy Using a Global Biogeochemical  
1049 Model, *Climatic Change*, 73, 345-373, 10.1007/s10584-005-6776-4, 2005.

1050 Felzer, B. S. F., Kicklighter, D. W., Melillo, J. M., Wang, C., Zhuang, Q., and Prinn, R. G.: Ozone effects  
1051 on net primary productivity and carbon sequestration in the conterminous United States using a  
1052 biogeochemistry model, *Tellus*, 56B, 230-248, 2004.

1053 Feng, Z., Kobayashi, K., and Ainsworth, E. A.: Impact of elevated ozone concentration on growth,  
1054 physiology, and yield of wheat (*Triticum aestivum* L.): a meta-analysis, *Global Change Biology*, 14,  
1055 2696-2708, 10.1111/j.1365-2486.2008.01673.x, 2008.

1056 Fowler, D., Flechard, C., Cape, J. N., Storeton-West, R. L., and Coyle, M.: Measurements of Ozone  
1057 Deposition to Vegetation Quantifying the Flux, the Stomatal and Non-Stomatal Components, *Water,  
1058 Air, and Soil Pollution*, 130, 63-74, 10.1023/a:1012243317471, 2001.

1059 Fowler, D., Pilegaard, K., Sutton, M., Ambus, P., Raivonen, M., Duyzer, J., Simpson, D., Fagerli, H.,  
1060 Fuzzi, S., and Schjørring, J. K.: Atmospheric composition change: ecosystems-atmosphere  
1061 interactions, *Atmospheric Environment*, 43, 5193-5267, 2009.

1062 Franz, M., Simpson, D., Arneth, A., and Zaehle, S.: Development and evaluation of an ozone  
1063 deposition scheme for coupling to a terrestrial biosphere model, *Biogeosciences*, 14, 45-71,  
1064 doi:10.5194/bg-14-45-2017, 2017.

1065 Friedlingstein, P., Cox, P., Betts, R., Bopp, L., von Bloh, W., Brovkin, V., Cadule, P., Doney, S., Eby, M.,  
1066 Fung, I., Bala, G., John, J., Jones, C., Joos, F., Kato, T., Kawamiya, M., Knorr, W., Lindsay, K.,  
1067 Matthews, H. D., Raddatz, T., Rayner, P., Reick, C., Roeckner, E., Schnitzler, K. G., Schnur, R.,  
1068 Strassmann, K., Weaver, A. J., Yoshikawa, C., and Zeng, N.: Climate-Carbon Cycle Feedback Analysis:  
1069 Results from the C4MIP Model Intercomparison, *Journal of Climate*, 19, 3337-3353,  
1070 10.1175/jcli3800.1, 2006.

1071 Fuhrer, J., Val Martin, M., Mills, G., Heald, C. L., Harmens, H., Hayes, F., Sharps, K., Bender, J., and  
1072 Ashmore, M. R.: Current and future ozone risks to global terrestrial biodiversity and ecosystem  
1073 processes, *Ecology and Evolution*, 6, 8785-8799, 10.1002/ece3.2568, 2016.

1074 Gedney, N., Cox, P. M., Bett, R. A., Boucher, O., Huntingford, C., and Stott, P. A.: Detection of a direct  
1075 carbon dioxide effect in continental river runoff records, *Nature*, 439, 835-838, 2006.

1076 Grantz, D., Gunn, S., and VU, H. B.: O<sub>3</sub> impacts on plant development: a meta-analysis of root/shoot  
1077 allocation and growth, *Plant, cell & environment*, 29, 1193-1209, 2006.

1078 Harmens, H., Mills, G., Emberson, L. D., and Ashmore, M. R.: Implications of climate change for the  
1079 stomatal flux of ozone: A case study for winter wheat, *Environmental Pollution*, 146, 763-770,  
1080 <http://dx.doi.org/10.1016/j.envpol.2006.05.018>, 2007.

1081 Hayes, F., Wagg, S., Mills, G., Wilkinson, S., and Davies, W.: Ozone effects in a drier climate:  
1082 implications for stomatal fluxes of reduced stomatal sensitivity to soil drying in a typical grassland  
1083 species, *Global Change Biology*, 18, 948-959, 2012.

1084 Heikkinen, J., Ketoja, E., Nuutinen, V., and Regina, K.: Declining trend of carbon in Finnish cropland  
1085 soils in 1974-2009, *Global Change Biology*, 19, 1456-1469, 10.1111/gcb.12137, 2013.

1086 Hofmockel, K. S., Zak, D. R., Moran, K. K., and Jastrow, J. D.: Changes in forest soil organic matter  
1087 pools after a decade of elevated CO<sub>2</sub> and O<sub>3</sub>, *Soil Biology and Biochemistry*, 43, 1518-1527,  
1088 <http://dx.doi.org/10.1016/j.soilbio.2011.03.030>, 2011.

1089 Hoshika, Y., Watanabe, M., Inada, N., and Koike, T.: Ozone-induced stomatal sluggishness develops  
1090 progressively in Siebold's beech (*Fagus crenata*), *Environmental Pollution*, 166, 152-156, 2012a.



1091 Hoshika, Y., Omasa, K., and Paoletti, E.: Whole-Tree Water Use Efficiency Is Decreased by Ambient  
1092 Ozone and Not Affected by O<sub>3</sub>-Induced Stomatal Sluggishness, PLOS ONE, 7, e39270,  
1093 10.1371/journal.pone.0039270, 2012b.

1094 Hoshika, Y., Watanabe, M., Inada, N., and Koike, T.: Model-based analysis of avoidance of ozone  
1095 stress by stomatal closure in Siebold's beech (*Fagus crenata*), Annals of Botany, 112, 1149-1158,  
1096 2013.

1097 Hoshika, Y., Katata, G., Deushi, M., Watanabe, M., Koike, T., and Paoletti, E.: Ozone-induced stomatal  
1098 sluggishness changes carbon and water balance of temperate deciduous forests., Scientific Reports,  
1099 doi:10.1038/srep09871, 2015.

1100 Hurtt, G., Chini, L. P., Froking, S., Betts, R., Feddema, J., Fischer, G., Fisk, J., Hibbard, K., Houghton,  
1101 R., Janetos, A., and Jones, C. D.: Harmonization of land-use scenarios for the period 1500–2100: 600  
1102 years of global gridded annual land-use transitions, wood harvest, and resulting secondary lands,  
1103 Climatic Change, 109, 117-161, 2011.

1104 IPCC: Climate change 2013: The Physical Science Basis, IPCC Working Group I Contribution to AR5,  
1105 2013.

1106 Jacobs, C. M. J.: Direct impact of atmospheric CO<sub>2</sub> enrichment on regional transpiration, Wageningen  
1107 Agricultural University, 1994.

1108 Janssens, I. A., Freibauer, A., Ciais, P., Smith, P., Nabuurs, G.-J., Folberth, G., Schlamadinger, B.,  
1109 Hutjes, R. W. A., Ceulemans, R., Schulze, E.-D., Valentini, R., and Dolman, A. J.: Europe's Terrestrial  
1110 Biosphere Absorbs 7 to 12% of European Anthropogenic CO<sub>2</sub> Emissions, Science, 300, 1538-1542,  
1111 10.1126/science.1083592, 2003.

1112 Jones, C. D., Cox, P., and Huntingford, C.: Uncertainty in climate–carbon-cycle projections associated  
1113 with the sensitivity of soil respiration to temperature, Tellus B, 55, 642-648, 10.1034/j.1600-  
1114 0889.2003.01440.x, 2003.

1115 Jung, M., Reichstein, M., Margolis, H. A., Cescatti, A., Richardson, A. D., Arain, M. A., Arneth, A.,  
1116 Bernhofer, C., Bonal, D., Chen, J., Gianelle, D., Gobron, N., Kiely, G., Kutsch, W., Lasslop, G., Law, B.  
1117 E., Lindroth, A., Merbold, L., Montagnani, L., Moors, E. J., Papale, D., Sottocornola, M., Vaccari, F.,  
1118 and Williams, C.: Global patterns of land-atmosphere fluxes of carbon dioxide, latent heat, and  
1119 sensible heat derived from eddy covariance, satellite, and meteorological observations, Journal of  
1120 Geophysical Research: Biogeosciences, 116, n/a-n/a, 10.1029/2010JG001566, 2011.

1121 Kala, J., De Kauwe, M. G., Pitman, A. J., Medlyn, B. E., Wang, Y. P., Lorenz, R., and Perkins-Kirkpatrick,  
1122 S. E.: Impact of the representation of stomatal conductance on model projections of heatwave  
1123 intensity., Scientific Reports, 1-7, 10.1038/srep23418, 2016.

1124 Karlsson, P. E., Braun, S., Broadmeadow, M., Elvira, S., Emberson, L., Gimeno, B. S., Le Thiec, D.,  
1125 Novak, K., Oksanen, E., Schaub, M., Uddling, J., and Wilkinson, M.: Risk assessments for forest trees:  
1126 The performance of the ozone flux versus the AOT concepts, Environmental Pollution, 146, 608-616,  
1127 <http://dx.doi.org/10.1016/j.envpol.2006.06.012>, 2007.

1128 Karnosky, D., Percy, K. E., Xiang, B., Callan, B., Noormets, A., Mankovska, B., Hopkin, A., Sober, J.,  
1129 Jones, W., and Dickson, R.: Interacting elevated CO<sub>2</sub> and tropospheric O<sub>3</sub> predisposes aspen  
1130 (*Populus tremuloides* Michx.) to infection by rust (*Melampsora medusae* f. sp. *tremuloideae*), Global  
1131 Change Biology, 8, 329-338, 2002.

1132 Karnosky, D. F., Skelly, J. M., Percy, K. E., and Chappelka, A. H.: Perspectives regarding 50years of  
1133 research on effects of tropospheric ozone air pollution on US forests, Environmental Pollution, 147,  
1134 489-506, 2007.

1135 Keeling, C. D., and Whorf, T. P.: Atmospheric CO<sub>2</sub> records from sites in the SIO air sampling network.  
1136 In Trends: A Compendium of Data on Global Change, Carbon Dioxide Information Analysis Center,  
1137 Oak Ridge National Laboratory, Oak Ridge, Tenn., U.S.A. , 2004.

1138 Kitao, M., Löw, M., Heerd, C., Grams, T. E., Häberle, K.-H., and Matyssek, R.: Effects of chronic  
1139 elevated ozone exposure on gas exchange responses of adult beech trees (*Fagus sylvatica*) as related  
1140 to the within-canopy light gradient, Environmental Pollution, 157, 537-544, 2009.

1141 Kjellström, E., Nikulin, G., Hansson, U., Strandberg, G., and Ullerstig, A.: 21st century changes in the  
 1142 European climate: uncertainties derived from an ensemble of regional climate model simulations,  
 1143 *Tellus A*, 63, 24-40, 2011.  
 1144 Kubiske, M., Quinn, V., Marquardt, P., and Karnosky, D.: Effects of Elevated Atmospheric CO<sub>2</sub> and/or  
 1145 O<sub>3</sub> on Intra- and Interspecific Competitive Ability of Aspen, *Plant biology*, 9, 342-355, 2007.  
 1146 Lamarque, J., Shindell, D. T., Josse, B., Young, P., Cionni, I., Eyring, V., Bergmann, D., Cameron-Smith,  
 1147 P., Collins, W. J., and Doherty, R.: The Atmospheric Chemistry and Climate Model Intercomparison  
 1148 Project (ACCMIP): overview and description of models, simulations and climate diagnostics,  
 1149 *Geoscientific Model Development*, 6, 179-206, 2013.  
 1150 Langner, J., Engardt, M., Baklanov, A., Christensen, J. H., Gauss, M., Geels, C., Hedegaard, G. B.,  
 1151 Nuterman, R., Simpson, D., and Soares, J.: A multi-model study of impacts of climate change on  
 1152 surface ozone in Europe, *Atmospheric Chemistry and Physics*, 12, 10423-10440, 2012a.  
 1153 Langner, J., Engardt, M., and Andersson, C.: European summer surface ozone 1990–2100,  
 1154 *Atmospheric Chemistry and Physics*, 12, 10097-10105, 2012b.  
 1155 Le Quéré, C., Moriarty, R., Andrew, R. M., Peters, G. P., Ciais, P., Friedlingstein, P., Jones, S. D., Sitch,  
 1156 S., Tans, P., Arneeth, A., Boden, T. A., Bopp, L., Bozec, Y., Canadell, J. G., Chini, L. P., Chevallier, F.,  
 1157 Cosca, C. E., Harris, I., Hoppema, M., Houghton, R. A., House, J. I., Jain, A. K., Johannessen, T., Kato,  
 1158 E., Keeling, R. F., Kitidis, V., Klein Goldewijk, K., Koven, C., Landa, C. S., Landschützer, P., Lenton, A.,  
 1159 Lima, I. D., Marland, G., Mathis, J. T., Metzl, N., Nojiri, Y., Olsen, A., Ono, T., Peng, S., Peters, W., Pfeil,  
 1160 B., Poulter, B., Raupach, M. R., Regnier, P., Rödenbeck, C., Saito, S., Salisbury, J. E., Schuster, U.,  
 1161 Schwinger, J., Séférian, R., Segsneider, J., Steinhoff, T., Stocker, B. D., Sutton, A. J., Takahashi, T.,  
 1162 Tilbrook, B., van der Werf, G. R., Viovy, N., Wang, Y. P., Wanninkhof, R., Wiltshire, A., and Zeng, N.:  
 1163 Global carbon budget 2014, *Earth Syst. Sci. Data*, 7, 47-85, 10.5194/essd-7-47-2015, 2015.  
 1164 Le Quéré, C., Andrew, R. M., Canadell, J. G., Sitch, S., Korsbakken, J. I., Peters, G. P., Manning, A. C.,  
 1165 Boden, T. A., Tans, P. P., Houghton, R. A., Keeling, R. F., Alin, S., Andrews, O. D., Anthoni, P., Barbero,  
 1166 L., Bopp, L., Chevallier, F., Chini, L. P., Ciais, P., Currie, K., Delire, C., Doney, S. C., Friedlingstein, P.,  
 1167 Gkritzalis, T., Harris, I., Hauck, J., Haverd, V., Hoppema, M., Klein Goldewijk, K., Jain, A. K., Kato, E.,  
 1168 Körtzinger, A., Landschützer, P., Lefèvre, N., Lenton, A., Lienert, S., Lombardozi, D., Melton, J. R.,  
 1169 Metzl, N., Millero, F., Monteiro, P. M. S., Munro, D. R., Nabel, J. E. M. S., Nakaoka, S. I., O'Brien, K.,  
 1170 Olsen, A., Omar, A. M., Ono, T., Pierrot, D., Poulter, B., Rödenbeck, C., Salisbury, J., Schuster, U.,  
 1171 Schwinger, J., Séférian, R., Skjelvan, I., Stocker, B. D., Sutton, A. J., Takahashi, T., Tian, H., Tilbrook, B.,  
 1172 van der Laan-Luijckx, I. T., van der Werf, G. R., Viovy, N., Walker, A. P., Wiltshire, A. J., and Zaehle, S.:  
 1173 Global Carbon Budget 2016, *Earth Syst. Sci. Data*, 8, 605-649, 10.5194/essd-8-605-2016, 2016.  
 1174 Le Quéré, C., Andrew, R. M., Friedlingstein, P., Sitch, S., Pongratz, J., Manning, A. C., Korsbakken, J. I.,  
 1175 Peters, G. P., Canadell, J. G., Jackson, R. B., Boden, T. A., Tans, P. P., Andrews, O. D., Arora, V. K.,  
 1176 Bakker, D. C. E., Barbero, L., Becker, M., Betts, R. A., Bopp, L., Chevallier, F., Chini, L. P., Ciais, P.,  
 1177 Cosca, C. E., Cross, J., Currie, K., Gasser, T., Harris, I., Hauck, J., Haverd, V., Houghton, R. A., Hunt, C.  
 1178 W., Hurtt, G., Ilyina, T., Jain, A. K., Kato, E., Kautz, M., Keeling, R. F., Klein Goldewijk, K., Körtzinger,  
 1179 A., Landschützer, P., Lefèvre, N., Lenton, A., Lienert, S., Lima, I., Lombardozi, D., Metzl, N., Millero,  
 1180 F., Monteiro, P. M. S., Munro, D. R., Nabel, J. E. M. S., Nakaoka, S.-I., Nojiri, Y., Padín, X. A., Pregon,  
 1181 A., Pfeil, B., Pierrot, D., Poulter, B., Rehder, G., Reimer, J., Rödenbeck, C., Schwinger, J., Séférian, R.,  
 1182 Skjelvan, I., Stocker, B. D., Tian, H., Tilbrook, B., van der Laan-Luijckx, I. T., van der Werf, G. R., van  
 1183 Heuven, S., Viovy, N., Vuichard, N., Walker, A. P., Watson, A. J., Wiltshire, A. J., Zaehle, S., and Zhu,  
 1184 D.: Global Carbon Budget 2017, *Earth Syst. Sci. Data Discuss*, in review, 2017.  
 1185 Leuzinger, S., and Körner, C.: Water savings in mature deciduous forest trees under elevated CO<sub>2</sub>,  
 1186 *Global Change Biology*, 13, 2498-2508, doi:10.1111/j.1365-2486.2007.01467.x, 2007.  
 1187 Lin, Y.-S., Medlyn, B. E., Duursma, R. A., Prentice, I. C., Wang, H., Baig, S., Eamus, D., de Dios, V. R.,  
 1188 Mitchell, P., and Ellsworth, D. S.: Optimal stomatal behaviour around the world, *Nature Climate  
 1189 Change*, 5, 459-464, 2015.

1190 Lindroth, R. L.: Impacts of Elevated Atmospheric CO<sub>2</sub> and O<sub>3</sub> on Forests: Phytochemistry, Trophic  
1191 Interactions, and Ecosystem Dynamics, *Journal of Chemical Ecology*, 36, 2-21, 10.1007/s10886-009-  
1192 9731-4, 2010.

1193 Logan, J. A., Staehelin, J., Megretskaia, I. A., Cammas, J. P., Thouret, V., Claude, H., De Backer, H.,  
1194 Steinbacher, M., Scheel, H. E., Stübi, R., Fröhlich, M., and Derwent, R.: Changes in ozone over  
1195 Europe: Analysis of ozone measurements from sondes, regular aircraft (MOZAIC) and alpine surface  
1196 sites, *Journal of Geophysical Research*, 117, 1-23, 2012.

1197 Lombardozi, D., Levis, S., Bonan, G., Hess, P. G., and Sparks, J. P.: The Influence of Chronic Ozone  
1198 Exposure on Global Carbon and Water Cycles, *Journal of Climate*, 28, 292-305, 10.1175/jcli-d-14-  
1199 00223.1, 2015.

1200 Long, S. P., Ainsworth, E. A., Leakey, A. D. B., Nosberger, J., and Ort, D. R.: Food for Thought: Lower-  
1201 Than-Expected Crop Yield Stimulation with Rising CO<sub>2</sub> Concentrations, *Science*, 312, 1918-1921,  
1202 10.1126/science.1114722, 2006.

1203 Löw, M., Herbinger, K., Nunn, A., Häberle, K.-H., Leuchner, M., Heerd, C., Werner, H., Wipfler, P.,  
1204 Pretzsch, H., and Tausz, M.: Extraordinary drought of 2003 overrules ozone impact on adult beech  
1205 trees (*Fagus sylvatica*), *Trees*, 20, 539-548, 2006.

1206 Loya, W. M., Pregitzer, K. S., Karberg, N. J., King, J. S., and Giardina, C. P.: Reduction of soil carbon  
1207 formation by tropospheric ozone under increased carbon dioxide levels., *Nature*, 425, 705-707,  
1208 2003.

1209 Luysaert, S., Abril, G., Andres, R., Bastviken, D., Bellassen, V., Bergamaschi, P., Bousquet, P.,  
1210 Chevallier, F., Ciais, P., Corazza, M., Dechow, R., Erb, K. H., Etiope, G., Fortems-Cheiney, A., Grassi, G.,  
1211 Hartmann, J., Jung, M., Lathière, J., Lohila, A., Mayorga, E., Moosdorf, N., Njakou, D. S., Otto, J.,  
1212 Papale, D., Peters, W., Peylin, P., Raymond, P., Rödenbeck, C., Saarnio, S., Schulze, E. D., Szopa, S.,  
1213 Thompson, R., Verkerk, P. J., Vuichard, N., Wang, R., Wattenbach, M., and Zaehle, S.: The European  
1214 land and inland water CO<sub>2</sub>, CO, CH<sub>4</sub> and N<sub>2</sub>O balance between 2001 and 2005, *Biogeosciences*, 9,  
1215 3357-3380, 10.5194/bg-9-3357-2012, 2012.

1216 Massman, W. J.: A review of the molecular diffusivities of H<sub>2</sub>O, CO<sub>2</sub>, CH<sub>4</sub>, CO, O<sub>3</sub>, SO<sub>2</sub>, NH<sub>3</sub>, N<sub>2</sub>O,  
1217 NO, and NO<sub>2</sub> in air, O<sub>2</sub> and N<sub>2</sub> near STP, *Atmospheric Environment*, 32, 1111-1127,  
1218 [http://dx.doi.org/10.1016/S1352-2310\(97\)00391-9](http://dx.doi.org/10.1016/S1352-2310(97)00391-9), 1998.

1219 Matyssek, R., Wieser, G., Ceulemans, R., Rennenberg, H., Pretzsch, H., Haberer, K., Löw, M., Nunn,  
1220 A., Werner, H., and Wipfler, P.: Enhanced ozone strongly reduces carbon sink strength of adult beech  
1221 (*Fagus sylvatica*)—Resume from the free-air fumigation study at Kranzberg Forest, *Environmental*  
1222 *Pollution*, 158, 2527-2532, 2010a.

1223 Matyssek, R., Karnosky, D., Wieser, G., Percy, K., Oksanen, E., Grams, T., Kubiske, M., Hanke, D., and  
1224 Pretzsch, H.: Advances in understanding ozone impact on forest trees: messages from novel  
1225 phytotron and free-air fumigation studies, *Environmental Pollution*, 158, 1990-2006, 2010b.

1226 McLaughlin, S. B., Nosal, M., Wullschleger, S. D., and Sun, G.: Interactive effects of ozone and climate  
1227 on tree growth and water use in a southern Appalachian forest in the USA, *New Phytologist*, 174,  
1228 109-124, 10.1111/j.1469-8137.2007.02018.x, 2007a.

1229 McLaughlin, S. B., Wullschleger, S. D., Sun, G., and Nosal, M.: Interactive effects of ozone and climate  
1230 on water use, soil moisture content and streamflow in a southern Appalachian forest in the USA,  
1231 *New Phytologist*, 174, 125-136, 10.1111/j.1469-8137.2007.01970.x, 2007b.

1232 Medlyn, B. E., Badeck, F. W., De Pury, D. G. G., Barton, C. V. M., Broadmeadow, M., Ceulemans, R.,  
1233 De Angelis, P., Forstreuter, M., Jach, M. E., Kellomaki, S., Laitat, E., Marek, M., Philippot, S., Rey, A.,  
1234 Strassmeyer, J., Laitinen, K., Liozon, R., Portier, B., Roberntz, P., Wang, K., and Jstbid, P. G.: Effects  
1235 of elevated [CO<sub>2</sub>] on photosynthesis in European forest species: a meta-analysis of model  
1236 parameters, *Plant, Cell & Environment*, 22, 1475-1495, doi:10.1046/j.1365-3040.1999.00523.x, 1999.

1237 Medlyn, B. E., Barton, C. V. M., Broadmeadow, M. S. J., Ceulemans, R., De Angelis, P., Forstreuter,  
1238 M., Freeman, M., Jackson, S. B., Kellomaki, S., Laitat, E., Rey, A., Roberntz, P., Sigurdsson, B. D.,  
1239 Strassmeyer, J., Wang, K., Curtis, P. S., and Jarvis, P. G.: Stomatal conductance of forest species

1240 after long-term exposure to elevated CO<sub>2</sub> concentration: a synthesis, *New Phytologist*, 149, 247-264,  
 1241 2001.  
 1242 Medlyn, B. E., Duursma, R. A., Eamus, D., Ellsworth, D. S., Prentice, I. C., Barton, C. V., Crous, K. Y., de  
 1243 Angelis, P., Freeman, M., and Wingate, L.: Reconciling the optimal and empirical approaches to  
 1244 modelling stomatal conductance, *Global Change Biology*, 17, 2134-2144, 2011.  
 1245 Mercado, L. M., Bellouin, N., Sitch, S., Boucher, O., Huntingford, C., Wild, M., and Cox, P. M.: Impact  
 1246 of changes in diffuse radiation on the global land carbon sink, *Nature*, 458, 1014-1017,  
 1247 [http://www.nature.com/nature/journal/v458/n7241/supinfo/nature07949\\_S1.html](http://www.nature.com/nature/journal/v458/n7241/supinfo/nature07949_S1.html), 2009.  
 1248 Mills, G., Hayes, F., Wilkinson, S., and Davies, W. J.: Chronic exposure to increasing background  
 1249 ozone impairs stomatal functioning in grassland species, *Global Change Biology*, 15, 1522-1533,  
 1250 2009.  
 1251 Mills, G., Hayes, F., Simpson, D., Emberson, L., Norris, D., Harmens, H., and BÜKer, P.: Evidence of  
 1252 widespread effects of ozone on crops and (semi-)natural vegetation in Europe (1990–2006) in  
 1253 relation to AOT40- and flux-based risk maps, *Global Change Biology*, 17, 592-613, 10.1111/j.1365-  
 1254 2486.2010.02217.x, 2011b.  
 1255 Mills, G., Harmens, H., Wagg, S., Sharps, K., Hayes, F., Fowler, D., Sutton, M., and Davies, B.: Ozone  
 1256 impacts on vegetation in a nitrogen enriched and changing climate, *Environmental Pollution*, 208,  
 1257 898-908, 2016.  
 1258 Norby, R. J., Wullschlegel, S. D., Gunderson, C. A., Johnson, D. W., and Ceulemans, R.: Tree responses  
 1259 to rising CO<sub>2</sub> in field experiments: implications for the future forest, *Plant, Cell and Environment*, 22,  
 1260 683-714, 1999.  
 1261 Norby, R. J., DeLucia, E. H., Gielen, B., Calfapietra, C., Giardina, C. P., King, J. S., Ledford, J., McCarthy,  
 1262 H. R., Moore, D. J. P., Ceulemans, R., De Angelis, P., Finzi, A. C., Karnosky, D. F., Kubiske, M. E., Lukac,  
 1263 M., Pregitzer, K. S., Scarascia-Mugnozza, G. E., Schlesinger, W. H., and Oren, R.: Forest response to  
 1264 elevated CO<sub>2</sub> is conserved across a broad range of productivity, *Proc. Natl. Acad. Sci. U. S. A.*, 102,  
 1265 18052-18056, 10.1073/pnas.0509478102, 2005.  
 1266 Nunn, A. J., Reiter, I. M., Häberle, K.-H., Langebartels, C., Bahnweg, G., Pretzsch, H., Sandermann, H.,  
 1267 and Matyssek, R.: Response patterns in adult forest trees to chronic ozone stress: identification of  
 1268 variations and consistencies, *Environmental Pollution*, 136, 365-369, 2005.  
 1269 Pacifico, F., Folberth, G. A., Jones, C. D., Harrison, S. P., and Collins, W. J.: Sensitivity of biogenic  
 1270 isoprene emissions to past, present, and future environmental conditions and implications for  
 1271 atmospheric chemistry, *Journal of Geophysical Research: Atmospheres*, 117, n/a-n/a,  
 1272 10.1029/2012JD018276, 2012.  
 1273 Paoletti, E., and Grulke, N. E.: Ozone exposure and stomatal sluggishness in different plant  
 1274 physiognomic classes, *Environmental Pollution*, 158, 2664-2671, 2010.  
 1275 Parrish, D. D., Law, K. S., Staehelin, J., Derwent, R., Cooper, O. R., Tanimoto, H., Volz-Thomas, A.,  
 1276 Gilge, S., Scheel, H. E., Steinbacher, M., and Chan, E.: Long-term changes in lower tropospheric  
 1277 baseline ozone concentrations at northern mid-latitudes, *Atmos. Chem. Phys.*, 12, 11485-11504,  
 1278 10.5194/acp-12-11485-2012, 2012.  
 1279 Percy, K. E., Awmack, C. S., Lindroth, R. L., Kubiske, M. E., Kopper, B. J., Isebrands, J., Pregitzer, K. S.,  
 1280 Hendrey, G. R., Dickson, R. E., and Zak, D. R.: Altered performance of forest pests under atmospheres  
 1281 enriched by CO<sub>2</sub> and O<sub>3</sub>, *Nature*, 420, 403-407, 2002.  
 1282 Royal-Society: Ground-level ozone in the 21st century: future trends, impacts and policy  
 1283 implications, *Science Policy Report 15/08*, 2008.  
 1284 Samuelsson, P., Jones, C. G., Willén, U., Ullerstig, A., Gollvik, S., Hansson, U., Jansson, C., Kjellström,  
 1285 E., Nikulin, G., and Wyser, K.: The Rossby Centre Regional Climate model RCA3: model description  
 1286 and performance, *Tellus A*, 63, 4-23, 2011.  
 1287 Saxe, H., Ellsworth, D. S., and Heath, J.: Tree and forest functioning in an enriched CO<sub>2</sub> atmosphere,  
 1288 *New Phytologist*, 139, 395-436, doi:10.1046/j.1469-8137.1998.00221.x, 1998.

1289 Schulze, E.-D., Ciais, P., Luyssaert, S., Schrumppf, M., Janssens, I. A., Thiruchittampalam, B., Theloke, J.,  
1290 Saurat, M., Bringezu, S., and Lelieveld, J.: The European carbon balance. Part 4: integration of carbon  
1291 and other trace-gas fluxes, *Global Change Biology*, 16, 1451-1469, 2010.  
1292 Schulze, E. D., Luyssaert, S., Ciais, P., Freibauer, A., Janssens, I. A., and et al.: Importance of methane  
1293 and nitrous oxide for Europe's terrestrial greenhouse-gas balance, *Nature Geosci*, 2, 842-850,  
1294 [http://www.nature.com/ngeo/journal/v2/n12/supinfo/ngeo686\\_S1.html](http://www.nature.com/ngeo/journal/v2/n12/supinfo/ngeo686_S1.html), 2009.  
1295 Sicard, P., De Marco, A., Troussier, F., Renoua, C., Vas, N., and Paoletti, E.: Decrease in surface ozone  
1296 concentrations at Mediterranean remote sites and increase in the cities, *Atmospheric Environment*,  
1297 79, 705-715, 2013.  
1298 Simpson, D., Benedictow, A., Berge, H., Bergström, R., Emberson, L. D., Fagerli, H., Flechard, C. R.,  
1299 Hayman, G. D., Gauss, M., and Jonson, J. E.: The EMEP MSC-W chemical transport model—technical  
1300 description, *Atmospheric Chemistry and Physics*, 12, 7825-7865, 2012.  
1301 Simpson, D., Andersson, C., Christensen, J. H., Engardt, M., Geels, C., Nyiri, A., Posch, M., Soares, J.,  
1302 Sofiev, M., and Wind, P.: Impacts of climate and emission changes on nitrogen deposition in Europe:  
1303 a multi-model study, *Atmospheric Chemistry and Physics*, 14, 6995-7017, 2014a.  
1304 Simpson, D., Arneth, A., Mills, G., Solberg, S., and Uddling, J.: Ozone—the persistent menace:  
1305 interactions with the N cycle and climate change, *Current Opinion in Environmental Sustainability*, 9,  
1306 9-19, 2014b.  
1307 Sitch, S., Cox, P. M., Collins, W. J., and Huntingford, C.: Indirect radiative forcing of climate change  
1308 through ozone effects on the land-carbon sink, *Nature*, 448, 791-794,  
1309 [http://www.nature.com/nature/journal/v448/n7155/supinfo/nature06059\\_S1.html](http://www.nature.com/nature/journal/v448/n7155/supinfo/nature06059_S1.html), 2007.  
1310 Sitch, S., Friedlingstein, P., Gruber, N., Jones, S. D., Murray-Tortarolo, G., Ahlström, A., Doney, S. C.,  
1311 Graven, H., Heinze, C., Huntingford, C., Levis, S., Levy, P. E., Lomas, M., Poulter, B., Viovy, N., Zaehle,  
1312 S., Zeng, N., Arneth, A., Bonan, G., Bopp, L., Canadell, J. G., Chevallier, F., Ciais, P., Ellis, R., Gloor, M.,  
1313 Peylin, P., Piao, S. L., Le Quéré, C., Smith, B., Zhu, Z., and Myneni, R.: Recent trends and drivers of  
1314 regional sources and sinks of carbon dioxide, *Biogeosciences*, 12, 653-679, 10.5194/bg-12-653-2015,  
1315 2015.  
1316 Sleutel, S., De Neve, S., and Hofman, G.: Estimates of carbon stock changes in Belgian cropland., *Soil*  
1317 *Use and Management*, 19, 166-171, 10.1079/SUM2003187, 2003.  
1318 Sun, G. E., McLaughlin, S. B., Porter, J. H., Uddling, J., Mulholland, P. J., Adams, M. B., and Pederson,  
1319 N.: Interactive influences of ozone and climate on streamflow of forested watersheds, *Global Change*  
1320 *Biology*, 18, 3395-3409, 10.1111/j.1365-2486.2012.02787.x, 2012.  
1321 Tai, P. K. A., Val Martin, M., and Heald, C. L.: Threat to future global food security from climate  
1322 change and ozone air pollution, *Nature Climate Change*, 4, 817 - 821, 2014.  
1323 Talhelm, A. F., Pregitzer, K. S., Kubiske, M. E., Zak, D. R., Campany, C. E., Burton, A. J., Dickson, R. E.,  
1324 Hendrey, G. R., Isebrands, J. G., Lewin, K. F., Nagy, J., and Karnosky, D. F.: Elevated carbon dioxide  
1325 and ozone alter productivity and ecosystem carbon content in northern temperate forests, *Global*  
1326 *Change Biology*, 20, 2492-2504, 10.1111/gcb.12564, 2014.  
1327 Tricker, P. J., Pecchiari, M., Bunn, S. M., Vaccari, F. P., Peressotti, A., Miglietta, F., and Taylor, G.:  
1328 Water use of a bioenergy plantation increases in a future high CO<sub>2</sub> world, *Biomass and Bioenergy*,  
1329 33, 200-208, 2009.  
1330 Tuovinen, J.-P., Emberson, L., and Simpson, D.: Modelling ozone fluxes to forests for risk assessment:  
1331 status and prospects, *Annals of Forest Science*, 66, 1-14, 2009.  
1332 Tuovinen, J., Hakola, H., Karlsson, P., and Simpson, D.: Air pollution risks to Northern European  
1333 forests in a changing climate, *Climate Change, Air Pollution and Global Challenges Understanding*  
1334 *and Perspectives from Forest Research*, 2013.  
1335 Uddling, J., Teclaw, R. M., Pregitzer, K. S., and Ellsworth, D. S.: Leaf and canopy conductance in aspen  
1336 and aspen-birch forests under free-air enrichment of carbon dioxide and ozone, *Tree Physiology*, 29,  
1337 1367-1380, 2009.

1338 Verstraeten, W. W., Neu, J. L., Williams, J. E., Bowman, K. W., Worden, J. R., and Boersma, K. F.:  
1339 Rapid increases in tropospheric ozone production and export from China, *Nature Geoscience* 8, 690-  
1340 695, 2015.

1341 Vingarzan, R.: A review of surface ozone background levels and trends, *Atmospheric Environment*,  
1342 38, 3431-3442, <https://doi.org/10.1016/j.atmosenv.2004.03.030>, 2004.

1343 Weedon, G. P., Gomes, S., Viterbo, P., Österle, H., Adam, J. C., Bellouin, N., Boucher, O., and Best, M.  
1344 J.: The WATCH Forcing Data 1958-2001: a meteorological forcing dataset for land surface- and  
1345 hydrological models. , *WATCH Tech. Rep. 22*, 41p (available at [www.eu-watch.org/publications](http://www.eu-watch.org/publications) ).  
1346 2010.

1347 Weedon, G. P., Gomes, S., Viterbo, P., Shuttleworth, W. J., Blyth, E., Österle, H., Adam, J. C., Bellouin,  
1348 N., Boucher, O., and Best, M.: Creation of the WATCH Forcing data and its use to assess global and  
1349 regional reference crop evaporation over land during the twentieth century, *Journal of*  
1350 *Hydrometeorology*, 12, 823-848, doi: 10.1175/2011JHM1369.1., 2011.

1351 Wilkinson, S., and Davies, W. J.: Ozone suppresses soil drying-and abscisic acid (ABA)-induced  
1352 stomatal closure via an ethylene-dependent mechanism, *Plant, Cell & Environment*, 32, 949-959,  
1353 2009.

1354 Wilkinson, S., and Davies, W. J.: Drought, ozone, ABA and ethylene: new insights from cell to plant to  
1355 community, *Plant, Cell & Environment*, 33, 510-525, 10.1111/j.1365-3040.2009.02052.x, 2010.

1356 Wittig, V. E., Ainsworth, E. A., and Long, S. P.: To what extent do current and projected increases in  
1357 surface ozone affect photosynthesis and stomatal conductance of trees? A meta-analytic review of  
1358 the last 3 decades of experiments, *Plant, Cell & Environment*, 30, 1150-1162, 10.1111/j.1365-  
1359 3040.2007.01717.x, 2007.

1360 Wittig, V. E., Ainsworth, E. A., Naidu, S. L., Karnosky, D. F., and Long, S. P.: Quantifying the impact of  
1361 current and future tropospheric ozone on tree biomass, growth, physiology and biochemistry: a  
1362 quantitative meta-analysis, *Global Change Biology*, 15, 396-424, 10.1111/j.1365-2486.2008.01774.x,  
1363 2009.

1364 Wullschleger, S. D., Gunderson, C. A., Hanson, P. J., Wilson, K. B., and Norby, R. J.: Sensitivity of  
1365 stomatal and canopy conductance to elevated CO<sub>2</sub> concentration; interacting variables and  
1366 perspectives of scale, *New Phytologist*, 153, 485-496, doi:10.1046/j.0028-646X.2001.00333.x, 2002.

1367 Young, P., Arneth, A., Schurgers, G., Zeng, G., and Pyle, J. A.: The CO<sub>2</sub> inhibition of terrestrial isoprene  
1368 emission significantly affects future ozone projections, *Atmospheric Chemistry and Physics*, 9, 2793-  
1369 2803, 2009.

1370 Young, P., Archibald, A., Bowman, K., Lamarque, J.-F., Naik, V., Stevenson, D., Tilmes, S., Voulgarakis,  
1371 A., Wild, O., and Bergmann, D.: Pre-industrial to end 21st century projections of tropospheric ozone  
1372 from the Atmospheric Chemistry and Climate Model Intercomparison Project (ACCMIP),  
1373 *Atmospheric Chemistry and Physics*, 13, 2063-2090, 2013.

1374 Zaehle, S.: Terrestrial nitrogen-carbon cycle interactions at the global scale, *Philosophical*  
1375 *Transactions of the Royal Society B: Biological Sciences*, 368, 20130125, 10.1098/rstb.2013.0125,  
1376 2013.

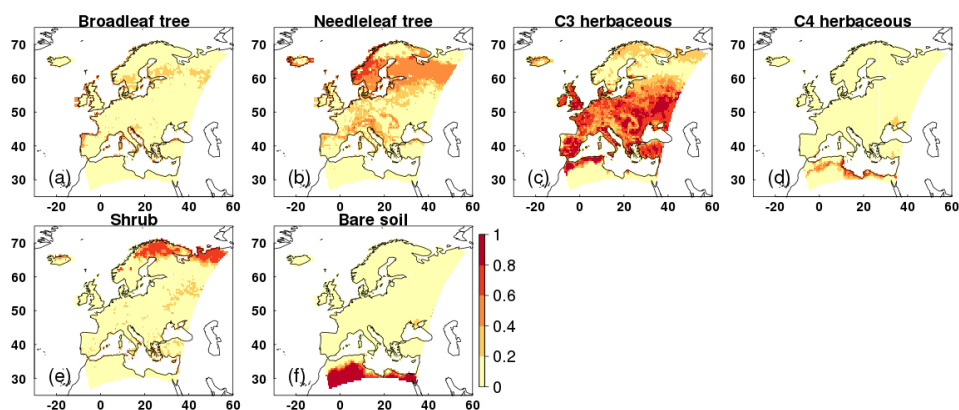
1377 Zak, D. R., Pregitzer, K. S., Kubiske, M. E., and Burton, A. J.: Forest productivity under elevated CO<sub>2</sub>  
1378 and O<sub>3</sub>: positive feedbacks to soil N cycling sustain decade-long net primary productivity  
1379 enhancement by CO<sub>2</sub>, *Ecology Letters*, 14, 1220-1226, 10.1111/j.1461-0248.2011.01692.x, 2011.

1380  
1381  
1382  
1383  
1384  
1385  
1386

1387 **Supplementary Information**

1388

1389 **S1 Fractional cover of JULES PFTs**



1390

1391 **Figure S1.** Fractional cover of each JULES PFT and bare soil at  $0.5^\circ \times 0.5^\circ$  resolution.

1392

1393

1394 **S2 Calibration of  $O_3$  uptake model for European vegetation**

1395

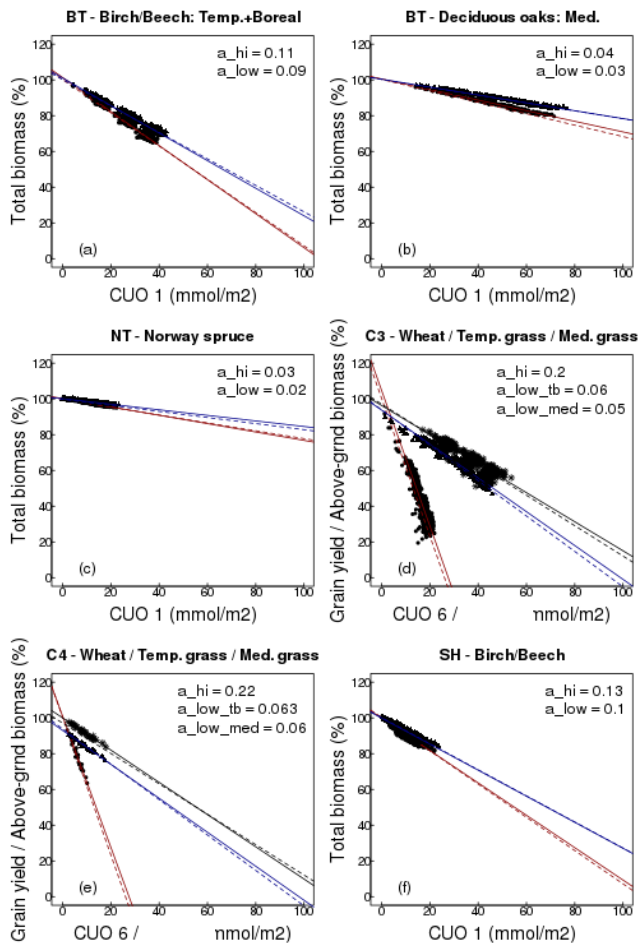
1396 Here we use the latest literature on  $O_3$  dose-response relationships derived from observed field data across Europe  
1397 (CLRTAP, 2017) to calculate the key PFT-specific parameters. Data comes from the UNECE CLRTAP (2017)  
1398 report which is a synthesis of the latest peer reviewed literature, collated by a panel of experts and so is considered  
1399 the state-of the art knowledge. Each PFT was calibrated for a high and low plant  $O_3$  sensitivity to account for  
1400 uncertainty in the sensitivity of different plant species to  $O_3$ , using the approach of Sitch *et al.*, (2007). In addition,  
1401 where possible owing to available data, a distinction was made for Mediterranean regions. This was because the  
1402 work of B ker *et al.* (2015) showed that different  $O_3$  dose-response relationships are needed to describe the  $O_3$   
1403 sensitivity of dominant Mediterranean trees. For the  $C_3$  herbaceous PFT – the dominant land cover type across  
1404 the European domain in this study (Fig. S1) - the  $O_3$  sensitivity was calibrated against observations for wheat to  
1405 give a representation of agricultural regions (high plant  $O_3$  sensitivity), versus natural grassland (low plant  $O_3$   
1406 sensitivity), with a separate function for Mediterranean grasslands (low plant  $O_3$  sensitivity), all taken from  
1407 CLRTAP (2017). Tree/shrub PFTs were calibrated against observed  $O_3$  dose-response functions for the high plant  
1408  $O_3$  sensitivity (BT = Birch/Beech, BT-Med = deciduous oaks, NT = Norway spruce, shrub = Birch/Beech) all

1409 from CLRTAP (2017). The low plant O<sub>3</sub> sensitivity functions for trees/shrubs were calibrated as being 20 % less  
1410 sensitive based on the difference in sensitivity between high and low sensitive tree species in the Karlsson et al.  
1411 (2007) study. Due to limitations in data availability, the shrub parameterisation uses the observed dose-response  
1412 functions for broadleaf trees. Similarly, the parameterisation for C<sub>4</sub> herbaceous uses the observed dose-responses  
1413 for C<sub>3</sub> herbaceous, however the fractional cover of C<sub>4</sub> herbs across Europe is low (Fig. S1), so this assumption  
1414 affects a very small percentage of land cover. See Table S1 and Figure S2.  
1415

1416 To calibrate the O<sub>3</sub> uptake model for the fast carbon fluxes, e.g. net primary productivity (NPP), JULES was run  
1417 across Europe forced using the WFDEI observational climate dataset (Weedon, 2013) at 0.5° X 0.5° spatial and  
1418 three hour temporal resolution. JULES uses interpolation to disaggregate the forcing data down from 3 hours to  
1419 an hourly model time step. The model was spun-up over the period 1979 to 1999 with a fixed atmospheric CO<sub>2</sub>  
1420 concentration of 368.33 ppm (1999 value from Mauna Loa observations, (Tans and Keeling)). Zero tropospheric  
1421 ozone concentration was assumed for the control simulation, for the simulations with O<sub>3</sub>, spin-up used spatially  
1422 explicit fields of present day O<sub>3</sub> concentration produced using the UK Chemistry and Aerosol (UKCA) model  
1423 with standard chemistry from the run evaluated by O'Connor et al. (2014). A fixed land cover map was used based  
1424 on IGBP (International Geosphere-Biosphere Programme) land cover classes (IGBP-DIS), therefore as the  
1425 vegetation distribution was fixed and the calibration was not looking at carbon stores, a short spin-up was adequate  
1426 to equilibrate soil temperature and soil moisture. JULES was then run for year 2000 with a corresponding CO<sub>2</sub>  
1427 concentration of 369.52 ppm (from Mauna Loa observations, (Tans and Keeling)) and monthly fields of spatially  
1428 explicit tropospheric O<sub>3</sub> (O'Connor et al., 2014) as necessary.  
1429

1430 Calibration was performed using four simulations: with i) zero tropospheric O<sub>3</sub> concentration, this was the control  
1431 simulation (NPP\_control), ii) tropospheric O<sub>3</sub> at current ambient concentration (NPP\_O3), iii) ambient +20 ppb  
1432 (NPP\_O3+20) and iv) ambient +40 ppb (NPP\_O3+40). The different O<sub>3</sub> simulations (i.e. ambient, ambient + 20  
1433 and ambient + 40 ppb) were used to capture the range of O<sub>3</sub> conditions used in constructing the observed O<sub>3</sub> dose-  
1434 response relationships deployed for calibration, often these had been constructed under artificially manipulated  
1435 conditions of ambient + 40 ppb O<sub>3</sub> for example. For each simulation with O<sub>3</sub>, JULES used the observed PFT-  
1436 specific threshold value of O<sub>3</sub> uptake (i.e. parameter  $F_{O_3crit}$ ), and an initial estimate of the parameter 'a' (equation  
1437 2). For each PFT and each simulation, hourly estimates of NPP and O<sub>3</sub> uptake for the top sunlit leaf in excess of  
1438  $F_{O_3crit}$  were accumulated over a PFT dependent accumulation (i.e. ~6 months for broadleaf trees and shrubs, all  
1439 year for needle leaf trees, and ~3 months for herbaceous species, through the growing season). Change in total  
1440 NPP over the accumulation period (NPP\_O3/+20/+40 divided by NPP\_control) was calculated for each O<sub>3</sub>  
1441 simulation and plotted against the cumulative uptake of O<sub>3</sub> over the same period. The linear regression of this  
1442 relationship was calculated, and slope and intercept compared against the observed dose-response relationships.  
1443 Values of the parameter 'a' were adjusted, and the procedure repeated until the linear regression through the  
1444 simulation points matched that of the observations (Fig. S2). JULES is run to be as comparable as possible to the  
1445 dose-based O<sub>3</sub> risk indicator used in CLRTAP (2017), as only the O<sub>3</sub> flux to top of canopy sunlit leaves is  
1446 accumulated (i.e. the O<sub>3</sub> flux per projected leaf area). See Table S1 Figure S2.





1447  
 1448 **Figure S2.** Calibration of JULES for O<sub>3</sub> impacts on plant productivity for each JULES PFT ; a) broadleaf tree –  
 1449 temperate/boreal, b) broadleaf tree Mediterranean, c) Needle leaf tree, d) C<sub>3</sub> herbaceous (split into  
 1450 temperate/boreal and Mediterranean for the natural grasslands), e) C<sub>4</sub> herbaceous (split into temperate/boreal and  
 1451 Mediterranean for the natural grasslands), and f) shrub. High (red) and low (blue) plant O<sub>3</sub> sensitivities are shown.  
 1452 For the herbaceous PFTs the low sensitivity calibration is separate for Mediterranean regions (black). The solid  
 1453 line is the regression line through the modelled points, the dashed line is the regression line from the observed  
 1454 dose-response relationship. [The x axis is cumulative uptake of O<sub>3</sub> (CUO) above the critical O<sub>3</sub> threshold ( $F_{O3crit}$ ).

Commented [ORJ43]: RC1 8

1455  
 1456  
 1457

1458  
1459  
1460

	High Sensitivity				
	BT	NT	C3	C4	SH
$F_{O3crit}$ (nmol/m <sup>2</sup> /s)	1.00	1.00	1.00	1.00	1.00
$a$ (mmol/m <sup>2</sup> )	0.110	0.030	0.200	0.220	0.130
Function	Birch/Beech: $y=100.2-0.93x$	Norway spruce: $y=99.8-0.22x$	Wheat: $y=100.3-3.85x$	Wheat: $y=100.3-3.85x$	Birch/Beech: $y=100.2-0.93x$
$dq_{crit}$ (kg kg <sup>-1</sup> )	0.09	0.06	0.1	0.075	0.1
$f_0$	0.875	0.875	0.9	0.8	0.9
$g_1$ (kPa <sup>0.5</sup> )	3.22	2.22	5.56	1.1	2.24
	Low Sensitivity				
	BT	NT	C3	C4	SH
$F_{O3crit}$ (nmol/m <sup>2</sup> /s)	1.00	1.00	1.00	1.00	1.00
$a$ (mmol/m <sup>2</sup> )	0.090	0.020	0.060	0.063	0.100
Function	Birch/Beech: $y=100.2-0.74x$	Norway spruce: $y=99.8-0.17x$	Temperate perennial grassland: $y=93.9-0.99x$	Temperate perennial grassland: $y=93.9-0.99x$	Birch/Beech: $y=100.2-0.74x$
	High Sensitivity				
	BT - Med.				
$F_{O3crit}$ (nmol/m <sup>2</sup> /s)	1.00				
$a$ (mmol/m <sup>2</sup> )	0.040				
Function	Dec. Oaks: $y=100.3-0.32x$				
	Low Sensitivity				
	BT - Med.	C3 - Med.	C4 - Med.		
$F_{O3crit}$ (nmol/m <sup>2</sup> /s)	1.00	1.00	1.00		
$a$ (mmol/m <sup>2</sup> )	0.030	0.050	0.060		
Function	Dec. Oaks: $y=100.3-0.22x$	Mediterranean annual pasture: $y=97.1-0.85x$	Mediterranean annual pasture: $y=97.1-0.85x$		

1461  
1462 **Table S1.** PFT-specific parameter values used in the O<sub>3</sub> uptake and  $g_s$  formulation in JULES.  $F_{O3crit}$  is the critical  
1463 O<sub>3</sub> threshold above which damage occurs,  $a$  determines the reduction in photosynthesis with O<sub>3</sub> exposure,  
1464 ‘function’ shows the regression equation for the observed functions ( $x$  is  $F_{O3crit}$ ),  $dq_{crit}$  (kg kg<sup>-1</sup>) is a PFT specific

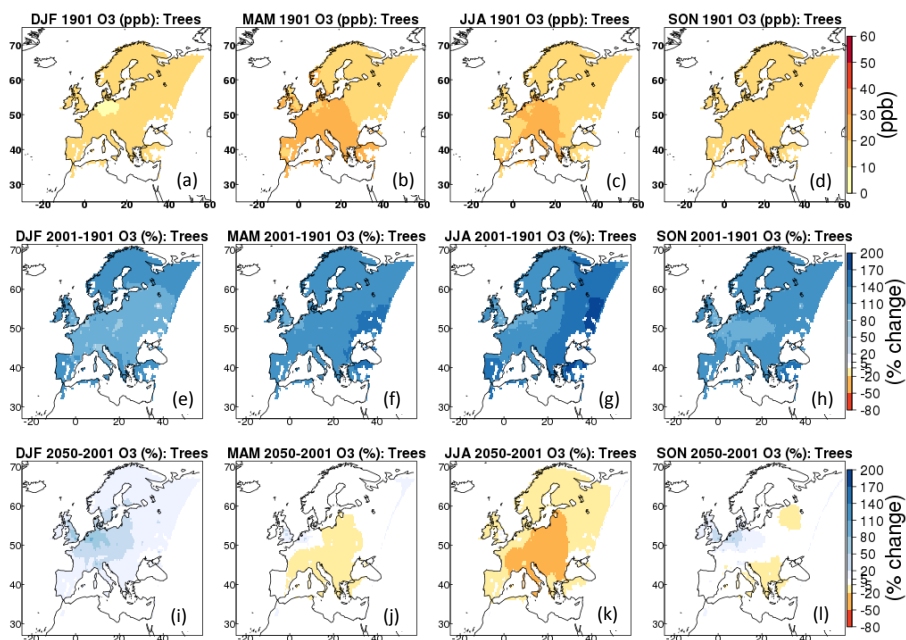
1465 parameters representing the critical humidity deficit at the leaf surface (used in the default JULES  $g_s$  model),  $f_0$  is  
 1466 the leaf internal to atmospheric CO<sub>2</sub> ratio ( $c_i/c_a$ ) at the leaf specific humidity deficit (also used in the default  
 1467 JULES  $g_s$  model), and  $g_l$  is the PFT specific parameter of the Medlyn *et al.*, (2011)  $g_s$  model. The parameters  
 1468  $dq_{crit}$ ,  $f_0$  and  $g_l$  vary by PFT, but not by O<sub>3</sub> sensitivity so are only shown once here.

1469

1470

1471

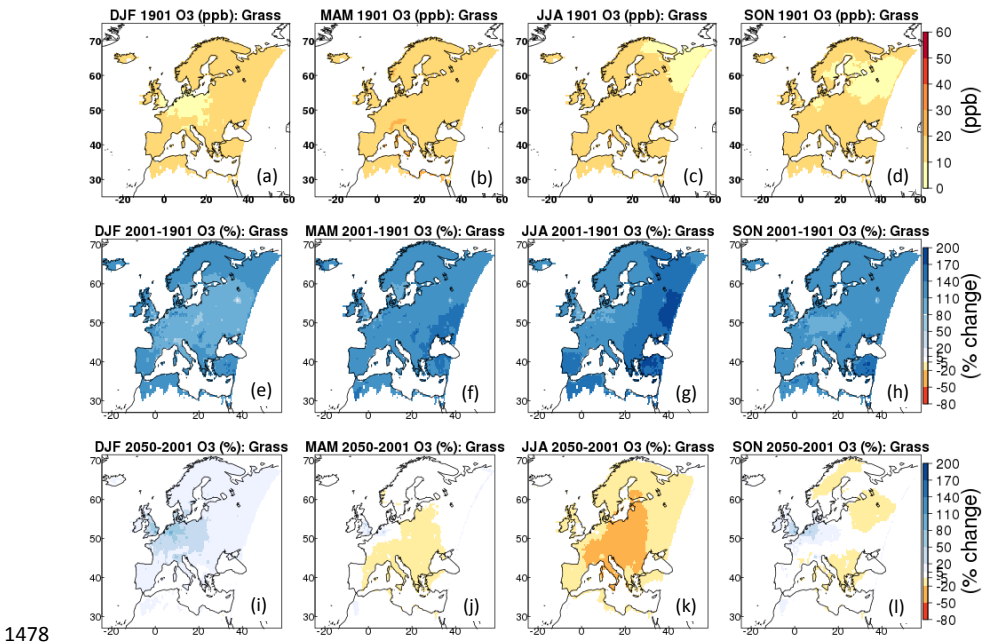
1472



1473

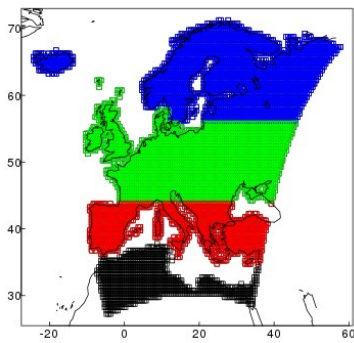
1474 **Figure S3.** (a-d) 1901 seasonal mean (DJF, MAM, JJA, SON) O<sub>3</sub> concentration (ppb) from EMEP for woody  
 1475 (tree and shrub) PFTs; (e-h) change in seasonal O<sub>3</sub> concentration (%) from 1901 to 2001; (i-l) change in seasonal  
 1476 O<sub>3</sub> concentration (%) from 2001 to 2050.

1477



1478  
 1479 **Figure S4.** (a-d) 1901 seasonal mean (DJF, MAM, JJA, SON) O<sub>3</sub> concentration (ppb) from EMEP for herbaceous  
 1480 PFTs; (e-h) change in seasonal O<sub>3</sub> concentration (%) from 1901 to 2001; (i-l) change in seasonal O<sub>3</sub> concentration  
 1481 (%) from 2001 to 2050.

1482



1483  
 1484 **Figure S5.** Regions, blue is Boreal, green is Temperate, red is Mediterranean.

1485

1486

1487 **S3 Assessing the difference between  $g_s$  model formulation**

1488

1489 Here we assess the impact of  $g_s$  model formulation, comparing the standard JULES Jacobs (1994) formulation  
1490 (equation 6; JAC) with the alternative Medlyn *et al.*, (2011) formulation (equation 7; MED). This was done for  
1491 two contrasting grid points (wet/dry) in central Europe with a fixed fractional cover of 20% for each PFT.

1492

1493 JULES was spun-up for 20 years (1979-1999) at two grid points in central Europe representing a wet (lat: 48.25;  
1494 lon.: 5.25) and a dry site (lat: 38.25; lon.: -7.75). The modelled soil moisture stress factor (fsmc) at the wet site  
1495 ranged from 0.8 to 1.0 over the year 2000 (1.0 indicates no soil moisture stress), and at the dry site fsmc steadily  
1496 declined from 0.8 at the start of the year to 0.25 by the end of the summer. The WFDEI meteorological forcing  
1497 dataset was used (Weedon, 2013), along with atmospheric CO<sub>2</sub> concentration for the year 1999 (368.33 ppm), and  
1498 either no O<sub>3</sub> (i.e. the O<sub>3</sub> damage model was switched off) for the control simulations, or spatially explicit fields of  
1499 present day O<sub>3</sub> concentration produced using the UK Chemistry and Aerosol (UKCA) model from the run  
1500 evaluated by O'Connor *et al.* (2014) for the simulations with O<sub>3</sub>. Following the spin-up period, JULES was run  
1501 for one year (2000) with corresponding atmospheric CO<sub>2</sub> concentration, and tropospheric O<sub>3</sub> concentrations as  
1502 described above. The control and ozone simulations were performed for both JAC and MED model formulations.  
1503 Land cover for the spin-up and main run was fixed at 20% for each PFT. For the simulations including O<sub>3</sub> damage,  
1504 the high plant O<sub>3</sub> sensitivity parameterisation was used. The difference between these simulations was used to  
1505 assess the impact of  $g_s$  model formulation on the leaf level fluxes of carbon and water.

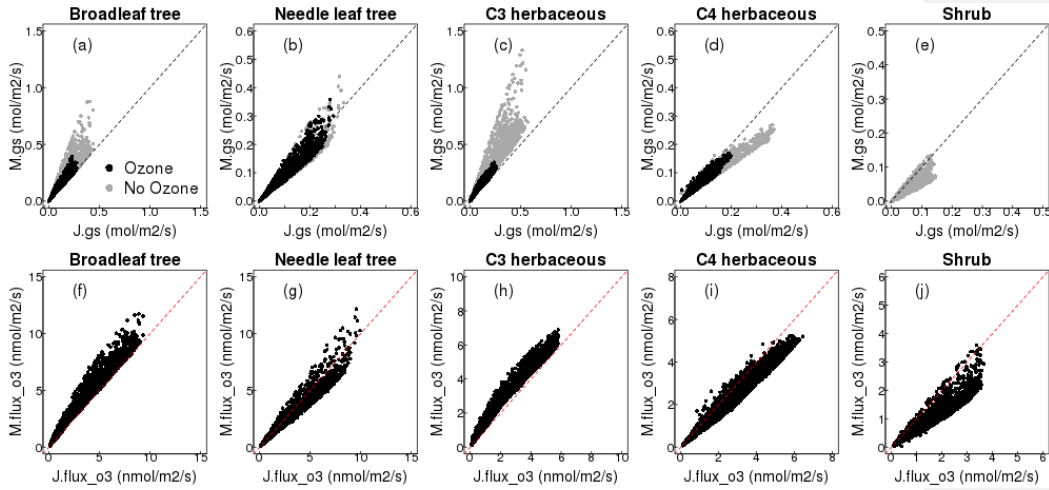
1506

1507 We calculate and report in the main manuscript (results section 3.1), the difference in mean annual leaf-level  
1508 water-use that results from the above simulation using the different  $g_s$  models. For each day of the simulation we  
1509 calculate the percentage difference in water-use between the two simulations, we then calculate the mean and  
1510 standard deviation over the year to give the annual mean leaf-level water-use.

1511

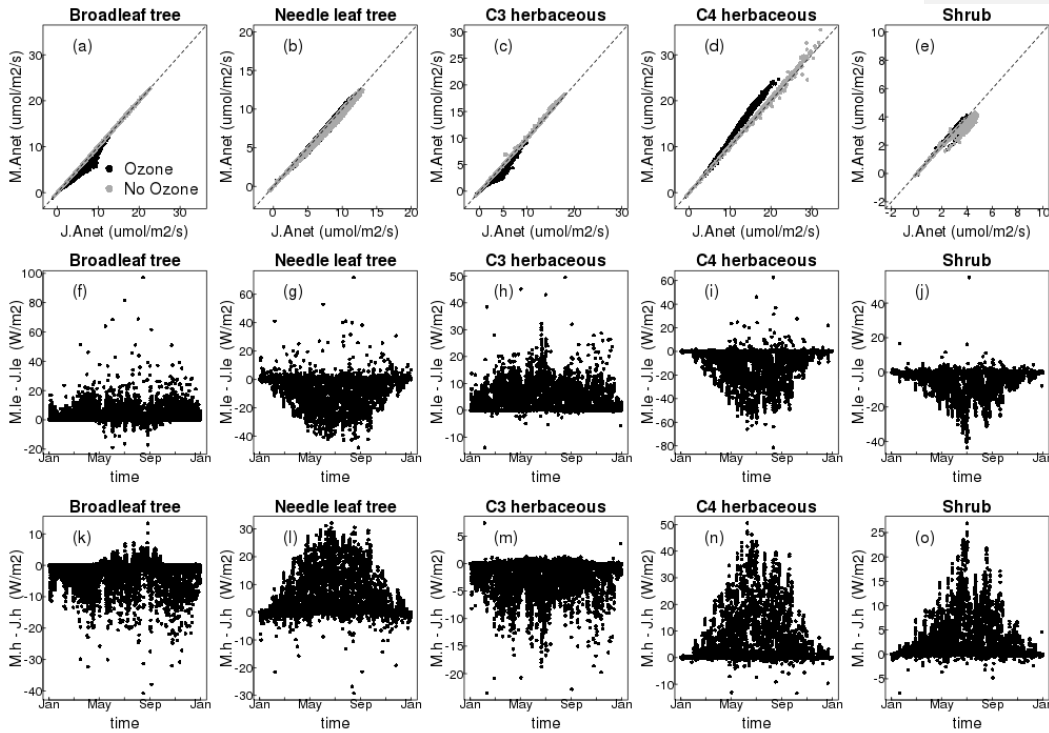
Commented [ORJ44]: RC1 10)

1512

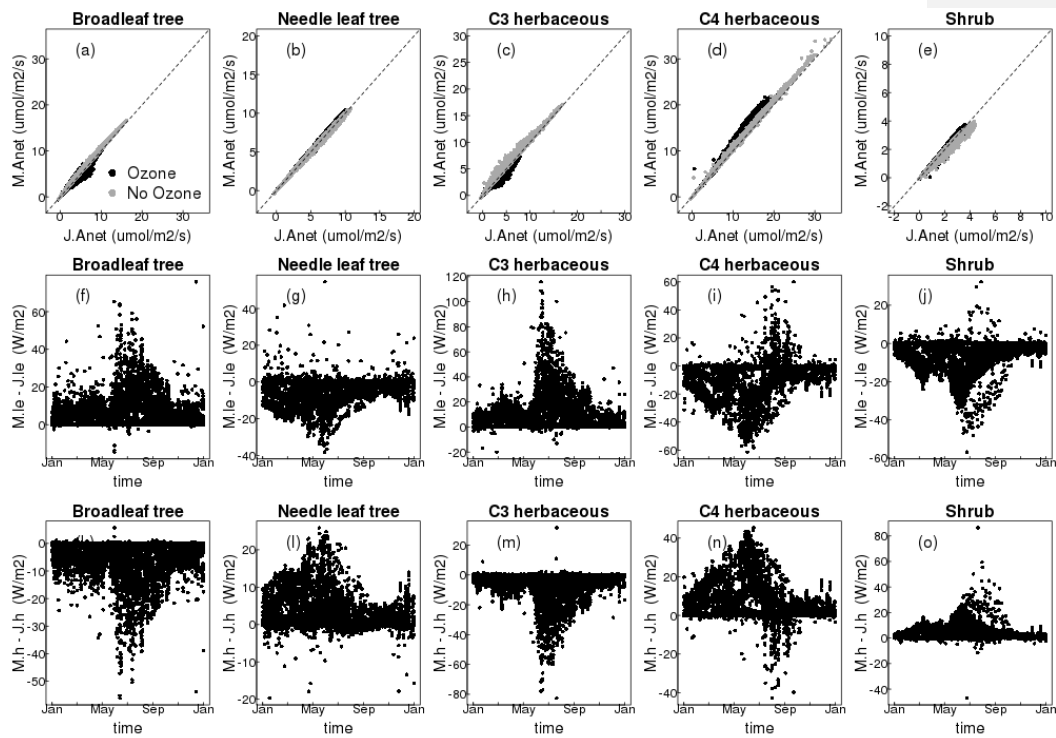


1513 **Figure S6.** Comparison of the Medlyn *et al.*, (2011)  $g_s$  model (y axis) versus the Jacobs (1994)  $g_s$  model (x axis)  
 1514 currently used in JULES for all five JULES PFTs, for stomatal conductance ( $g_s$ , top row) and the flux of  $O_3$   
 1515 through the stomata ( $flux_{o3}$ , bottom row) for a dry site.

1516



1517 **Figure S7.** Comparison of the Medlyn *et al.*, (2011)  $g_s$  model (y axis) versus the Jacobs (1994)  $g_s$  model (x axis)  
 1518 currently used in JULES for all five JULES PFTs at a wet site, for net photosynthesis (*Anet*, top row). Residual  
 1519 plots (Medlyn - Jacobs) show the difference between models over the year for latent heat (le, middle row) and  
 1520 sensible heat (h, bottom row).



1521  
 1522 **Figure S8.** Comparison of the Medlyn *et al.*, (2011)  $g_s$  model (y axis) versus the Jacobs (1994)  $g_s$  model (x axis)  
 1523 currently used in JULES for all five JULES PFTs at a dry site, for net photosynthesis (*Anet*, top row). Residual  
 1524 plots (Medlyn - Jacobs) show the difference between models over the year for latent heat (le, middle row) and  
 1525 sensible heat (h, bottom row).

1526

1527 **S4 Site level evaluation of  $g_s$  models**

1528 We carried out site-level simulations using sites from the FLUXNET2015 dataset to evaluate the seasonal cycle  
 1529 of latent and sensible heat using the two  $g_s$  models JAC and MED compared to observations. Sites were selected  
 1530 to represent a range of land cover types (Table S2). In general, at all sites the MED model improved the seasonal  
 1531 cycle of both fluxes (lower RMSE), but the magnitude of this varied from site to site. At the deciduous broadleaf  
 1532 site US-UMB, MED resulted in large improvements of the simulated seasonal cycle particularly in the summer  
 1533 months for both fluxes. At the second deciduous broadleaf site IT-CA1 however, there was almost no difference

1534 between the two  $g_s$  models. Both evergreen needleleaf forest sites (FI-Hyy and DE-Tha) saw large improvements  
 1535 in the simulated seasonal cycles of latent and sensible heat with the MED model, primarily as a result of lower  
 1536 latent heat flux in the spring and summer months, and higher sensible heat flux over the same period. With the  
 1537 MED model the monthly mean latent heat flux was improved at the C<sub>3</sub> grass site (CH-Cha) as a result of increased  
 1538 flux in the summer months, however there was no improvement in the sensible heat flux and RMSE with MED  
 1539 was increased. At the C<sub>4</sub> grass site (US-SRG), small improvements were made in the seasonal cycle of both latent  
 1540 and sensible heat with the MED model. At the deciduous savannah site (CG-Tch) which included a high  
 1541 proportion of shrub PFT in the land cover type used in the site simulation, large improvements in the seasonal  
 1542 cycle of both fluxes were simulated with the MED model, as a result of a decrease in the latent heat flux and an  
 1543 increase in the sensible heat flux.

1544

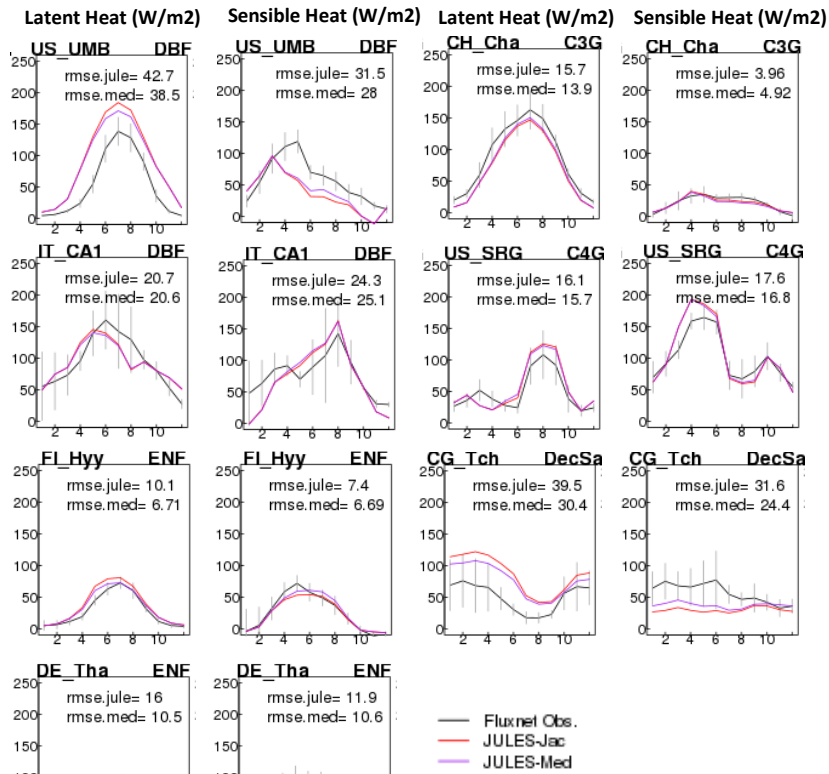
Site name	Country	Latitude	Longitude	Simulated years	Land cover	Dominant PFT(s)
US-UMB	USA	45.56	-84.71	2000-2014	Broadleaf forest	100% BT
IT-CA1	Italy	42.38	12.02	2011-2014	Broadleaf forest	100% BT
FI-Hyy	Finland	62	24.3	1996-2014	Needleleaf forest	100% NT
DE-Tha	Germany	51	13.57	1996-2014	Needleleaf forest	100% NT
CH_Ch	Switzerland	47.21	8.41	2006-2014	C <sub>3</sub> grassland	80% C <sub>3</sub> , 20% bare soil
US-SRG	USA	31.8	-110.83	2008-2014	C <sub>4</sub> grassland	80% C <sub>4</sub> , 20% bare soil 50% BT, 15% C <sub>4</sub> , 25% shrub, 10% bare soil
CG-Tch	Congo	-4.5	11.66	2006-2009	Deciduous savanna	soil

1545 **Table S2.** Sites from the FLUXNET2015 dataset used in the site simulations to evaluate  $g_s$  models.

1546  
 1547  
 1548  
 1549  
 1550  
 1551  
 1552  
 1553  
 1554  
 1555  
 1556  
 1557  
 1558



1559  
 1560  
 1561  
 1562  
 1563  
 1564  
 1565  
 1566  
 1567  
 1568  
 1569  
 1570  
 1571  
 1572  
 1573  
 1574  
 1575

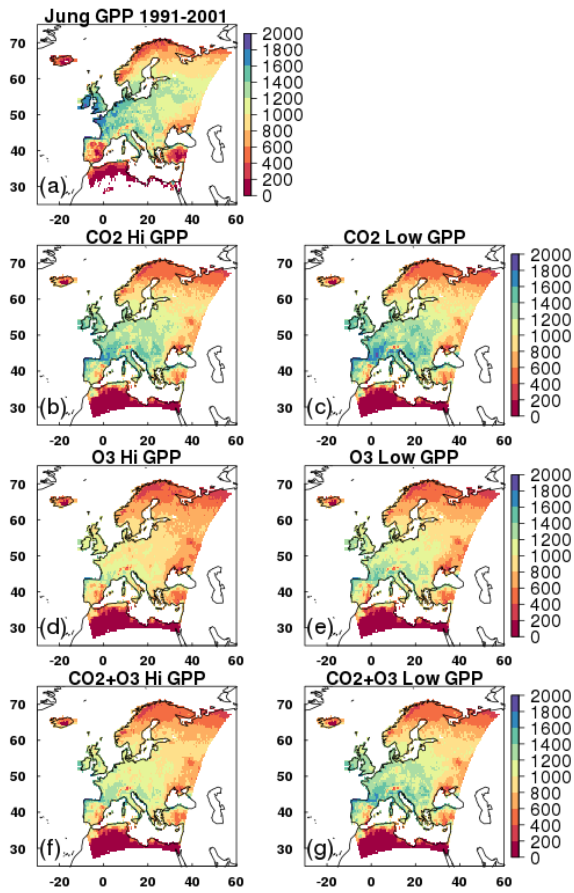


1576 **Fig. S9** Monthly mean fluxes of latent and sensible heat. Observations  $\pm$  standard deviation from  
 1577 FLUXNET2015 sites are shown as black line with grey vertical bars, JULES with the JAC  $g_s$  model is shown in  
 1578 red and JULES with the MED  $g_s$  model are shown in purple. Also shown are the root mean squared error (rmse)  
 1579 for each simulation.

Commented [ORJ45]: RC2 3)  
 Site level evaluation of the  $g_s$  formulations.

1580  
 1581  
 1582

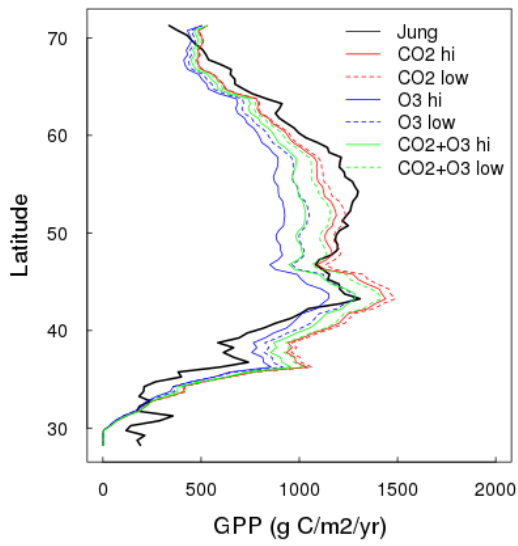
**S5 Evaluation of JULES O<sub>3</sub> model**



1583

1584 **Figure S10.** Mean GPP ( $\text{g C m}^{-2} \text{yr}^{-1}$ ) from 1991 to 2001 for a) the observations based globally extrapolated Flux  
 1585 Network model tree ensemble (MTE) (Jung et al., 2011); b, c) model simulations with transient  $\text{CO}_2$  and fixed  
 1586  $\text{O}_3$ ; d, e) model simulations with fixed  $\text{CO}_2$  and transient  $\text{O}_3$ , and f, g) our model simulations with transient  $\text{CO}_2$   
 1587 and transient  $\text{O}_3$ . All model simulations show GPP for high and low plant  $\text{O}_3$  sensitivity respectively.

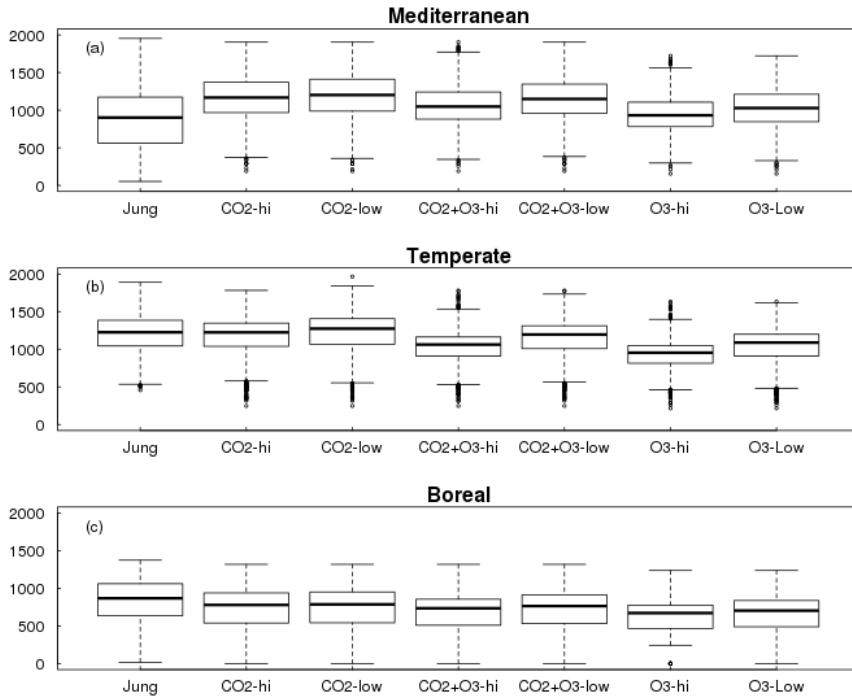
1588



1589

1590 **Figure S11.** Zonal mean GPP from 1991 to 2001 for FLUXNET-MTE (Jung) and all JULES scenario  
 1591 simulations with both high (solid lines) and low (dashed lines) plant O<sub>3</sub> sensitivity.

1592



1593

1594 **Figure S12.** Mean GPP from 1991 to 2001 shown by region, comparing MTE (Jung) and all JULES scenario  
 1595 simulations with both high and low plant O<sub>3</sub> sensitivity.

Commented [ORJ46]: RC2 3)

1596

1597 **S6 Estimation of effects due to O<sub>3</sub>, CO<sub>2</sub> and O<sub>3</sub> with CO<sub>2</sub>**

1598

1599 For each variable analysed (GPP, NPP, vegetation carbon, soil carbon, total land carbon and *g<sub>s</sub>*), we use the mean  
 1600 over 10 years to represent each time period, e.g. the mean over 2040 to 2050 is what we call 2050, 1901 to 1910  
 1601 is what we refer to as 1901. The difference between the simulations gives the effect of O<sub>3</sub> and CO<sub>2</sub> either separately  
 1602 or in combination over the different time periods. We look at the percentage change due to either O<sub>3</sub> at pre-  
 1603 industrial CO<sub>2</sub> concentration (i.e. without the additional effect of atmospheric CO<sub>2</sub> on stomatal behaviour), CO<sub>2</sub>  
 1604 (at fixed pre-industrial O<sub>3</sub> concentration) or the combined effect of both gases, which is calculated as:

$$1605$$

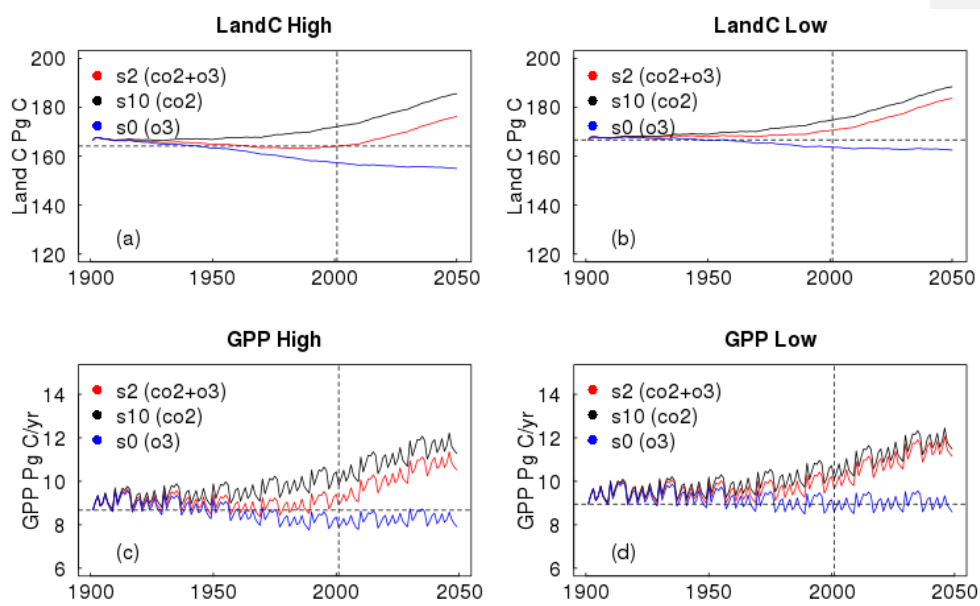
$$1606 \quad 100 * (\text{var}[y_1] - \text{var}[y_2]) / \text{var}[y_2]$$

$$1607 \quad \quad \quad (S1)$$

1608

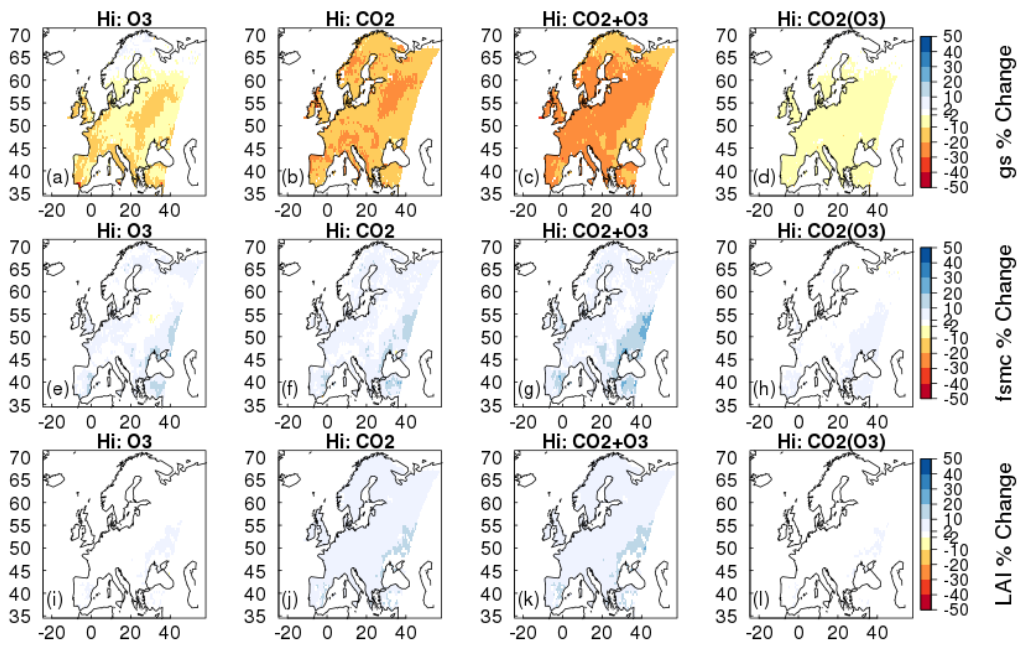
1609 Where var[*y<sub>x</sub>*] represents the variable in time period *y*, e.g.  $100 * (\text{varO}_3[2050] - \text{varO}_3[1901]) / \text{varO}_3[1901]$   
 1610 gives the O<sub>3</sub> effect (at fixed CO<sub>2</sub>) over the full experimental period. The meteorological forcing is prescribed in

1611 these simulations and is therefore the same between the model runs. Other climate factors, such as VPD,  
 1612 temperature and soil moisture availability are accounted for in our simulations, but our analysis isolates the effects  
 1613 of O<sub>3</sub>, CO<sub>2</sub> and O<sub>3</sub> + CO<sub>2</sub>.  
 1614  
 1615  
 1616



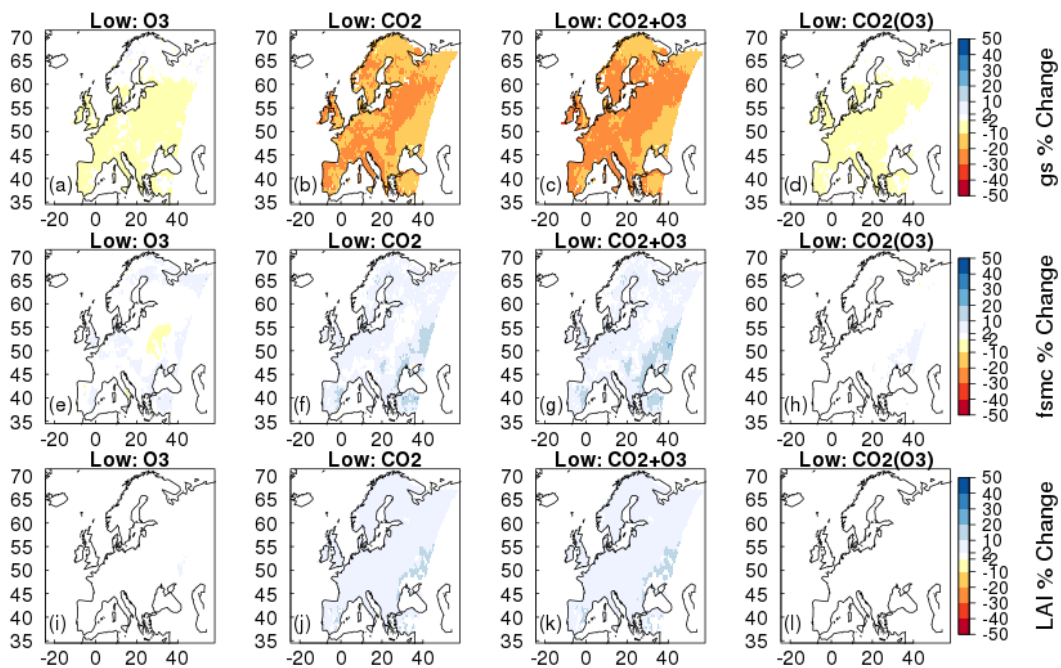
1617  
 1618 **Figure S13.** Times series (1901 to 2050) of changes in total carbon stocks (Land C) and gross primary productivity  
 1619 (GPP) due to O<sub>3</sub> effects at fixed pre-industrial atmospheric CO<sub>2</sub> concentration (O<sub>3</sub>, blue), CO<sub>2</sub> effects at fixed pre-  
 1620 industrial O<sub>3</sub> concentration (CO<sub>2</sub>, black), and effects of CO<sub>2</sub> and O<sub>3</sub> together (CO<sub>2</sub>+O<sub>3</sub>, red), for the higher and  
 1621 lower plant O<sub>3</sub> sensitivity. The horizontal dashed line shows the pre-industrial value, and the vertical dashed line  
 1622 marks the year 2001.

1623  
 1624  
 1625



1626

1627 **Figure S14.** Simulated percentage change in stomatal conductance (gs) a-c), soil moisture availability factor  
 1628 (fsmc) d-e) and leaf area index (LAI) g-i) due to O<sub>3</sub> effects at fixed pre-industrial atmospheric CO<sub>2</sub> concentration  
 1629 (O<sub>3</sub>), CO<sub>2</sub> effects at fixed pre-industrial O<sub>3</sub> concentration (CO<sub>2</sub>), and effects of CO<sub>2</sub> and O<sub>3</sub> changing  
 1630 simultaneously (CO<sub>2</sub>+O<sub>3</sub>). Changes are shown for the periods 1901 to 2050 for the higher plant O<sub>3</sub> sensitivity.  
 1631



1632

1633 **Figure S15.** Simulated percentage change in stomatal conductance (gs) a-c), soil moisture availability factor  
 1634 (fsmc) d-e) and leaf area index (LAI) g-i) due to O<sub>3</sub> effects at fixed pre-industrial atmospheric CO<sub>2</sub> concentration  
 1635 (O<sub>3</sub>), CO<sub>2</sub> effects at fixed pre-industrial O<sub>3</sub> concentration (CO<sub>2</sub>), and effects of CO<sub>2</sub> and O<sub>3</sub> changing  
 1636 simultaneously (CO<sub>2</sub>+O<sub>3</sub>). Changes are shown for the periods 1901 to 2050 for the lower plant O<sub>3</sub> sensitivity.  
 1637

1638

1639

1640

1641

1642

1643

1644

1645

1646

1647

1648  
1649  
1650  
1651  
1652

Future run, constant climate (1901 - 2001)						
Hi Sensitivity						
	GPP (Pg C yr <sup>-1</sup> )	NPP (Pg C yr <sup>-1</sup> )	$g_s$ (m/s)	Veg C (Pg C)	Soil C (Pg C)	Land C (Pg C)
Value in 1901:	9.05	4.46	0.03228	41.1	125.8	167
Absolute diff. (2001 - 1901):						
<b>O<sub>3</sub></b>	-0.81	-0.47	0.00	-0.02	-9.09	-9.21
<b>CO<sub>2</sub></b>	1.16	0.76	0.00	2.82	1.52	4.24
<b>CO<sub>2</sub> + O<sub>3</sub></b>	0.13	0.12	0.00	2.37	-5.55	-3.28
Relative diff. (%)	(%)	(%)	(%)	(%)	(%)	(%)
<b>O<sub>3</sub></b>	-8.95	-10.54	-8.55	-0.05	-7.23	-5.51
<b>CO<sub>2</sub></b>	12.82	17.04	-6.07	6.86	1.21	2.54
<b>CO<sub>2</sub> + O<sub>3</sub></b>	1.44	2.69	-13.66	5.77	-4.41	-1.96
Lower Sensitivity						
	GPP (Pg C yr <sup>-1</sup> )	NPP (Pg C yr <sup>-1</sup> )	$g_s$ (m/s)	Veg C (Pg C)	Soil C (Pg C)	Land C (Pg C)
Value in 1901:	9.34	4.65	0.03319	41.1	126.4	167.5
Absolute diff. (2001 - 1901):						
<b>O<sub>3</sub></b>	-0.30	-0.21	0.00	-0.21	-3.38	-3.59
<b>CO<sub>2</sub></b>	1.15	0.74	0.00	2.73	3.70	6.43
<b>CO<sub>2</sub> + O<sub>3</sub></b>	0.65	0.43	0.00	2.21	0.29	2.50
Relative diff. (%)	(%)	(%)	(%)	(%)	(%)	(%)
<b>O<sub>3</sub></b>	-3.21	-4.52	-3.31	-0.51	-2.67	-2.14
<b>CO<sub>2</sub></b>	12.31	15.91	-6.39	6.64	2.93	3.84
<b>CO<sub>2</sub> + O<sub>3</sub></b>	6.96	9.25	-9.88	5.38	0.23	1.49

1653  
1654  
1655  
1656  
1657  
1658  
1659

**Table S3.** Simulated changes in the European land carbon cycle due to changing O<sub>3</sub> and CO<sub>2</sub> concentrations. Shown are changes in total carbon stocks (Land C), split into vegetation (Veg C) and soil (Soil C) carbon, and gross primary productivity (GPP), net primary productivity (NPP) and conductance ( $g_s$ ), between 1901 and 2001.



1660

1661

Future run, constant climate (2001 - 2050)						
Hi Sensitivity						
	GPP (Pg C yr <sup>-1</sup> )	NPP (Pg C yr <sup>-1</sup> )	$g_s$ (m/s)	Veg C (Pg C)	Soil C (Pg C)	Land C (Pg C)
Value in 2001:						
<b>O<sub>3</sub></b>	8.24	3.99	0.02952	41.08	116.71	157.79
<b>CO<sub>2</sub></b>	10.21	5.22	0.03032	43.92	127.32	171.24
<b>CO<sub>2</sub> + O<sub>3</sub></b>	9.18	4.58	0.02787	43.47	120.25	163.72
Absolute diff. (2050 - 2001):						
<b>O<sub>3</sub></b>	0.01	0.00	0.00	-0.09	-2.35	-2.44
<b>CO<sub>2</sub></b>	1.42	0.95	0.00	5.25	7.73	12.98
<b>CO<sub>2</sub> + O<sub>3</sub></b>	1.66	1.07	0.00	5.11	6.00	11.11
Relative diff. (%)						
<b>O<sub>3</sub></b>	0.12	0.00	0.00	-0.22	-2.01	-1.55
<b>CO<sub>2</sub></b>	13.91	18.20	-13.89	11.95	6.07	7.58
<b>CO<sub>2</sub> + O<sub>3</sub></b>	18.08	23.36	-11.37	11.76	4.99	6.79
Lower Sensitivity						
	GPP (Pg C yr <sup>-1</sup> )	NPP (Pg C yr <sup>-1</sup> )	$g_s$ (m/s)	Veg C (Pg C)	Soil C (Pg C)	Land C (Pg C)
Value in 2001:						
<b>O<sub>3</sub></b>	9.04	4.44	0.03	40.89	123.02	163.91
<b>CO<sub>2</sub></b>	10.49	5.39	0.03	43.83	130.1	173.93
<b>CO<sub>2</sub> + O<sub>3</sub></b>	9.99	5.08	0.02991	43.31	126.69	170
Absolute diff. (2050 - 2001):						
<b>O<sub>3</sub></b>	0.02	-0.06	0.00	-0.13	-0.94	-1.07
<b>CO<sub>2</sub></b>	1.35	0.92	0.00	5.25	7.89	13.14
<b>CO<sub>2</sub> + O<sub>3</sub></b>	1.50	1.00	0.00	5.11	7.25	12.35
Relative diff. (%)						
<b>O<sub>3</sub></b>	0.22	-1.35	-0.72	-0.32	-0.76	-0.65
<b>CO<sub>2</sub></b>	12.87	17.07	-14.64	11.98	6.06	7.55
<b>CO<sub>2</sub> + O<sub>3</sub></b>	15.02	19.69	-13.37	11.80	5.72	7.26

1662

1663 **Table S4.** Simulated changes in the European land carbon cycle due to changing O<sub>3</sub> and CO<sub>2</sub> concentrations.

1664 Shown are changes in total carbon stocks (Land C), split into vegetation (Veg C) and soil (Soil C) carbon, and

1665 gross primary productivity (GPP), net primary productivity (NPP) and conductance ( $g_s$ ), between 2001 and 2050.

1666

1667

1668

1669

Future run, constant climate (1901 - 2050)						
Hi Sensitivity						
	GPP (Pg C yr <sup>-1</sup> )	NPP (Pg C yr <sup>-1</sup> )	$g_s$ (m/s)	Veg C (Pg C)	Soil C (Pg C)	Land C (Pg C)
Value in 1901:	9.05	4.46	0.03228	41.1	125.8	167
Absolute diff. (2050 - 1901):						
<b>O<sub>3</sub></b>	-0.80	-0.47	0.00	-0.11	-11.44	-11.65
<b>CO<sub>2</sub></b>	2.58	1.71	-0.01	8.07	9.25	17.22
<b>CO<sub>2</sub> + O<sub>3</sub></b>	1.79	1.19	-0.01	7.48	0.45	7.83
Relative diff. (%)	(%)	(%)	(%)	(%)	(%)	(%)
<b>O<sub>3</sub></b>	-8.84	-10.54	-8.55	-0.27	-9.09	-6.98
<b>CO<sub>2</sub></b>	28.51	38.34	-19.11	19.64	7.35	10.31
<b>CO<sub>2</sub> + O<sub>3</sub></b>	19.78	26.68	-23.48	18.20	0.36	4.69
Lower Sensitivity						
	GPP (Pg C yr <sup>-1</sup> )	NPP (Pg C yr <sup>-1</sup> )	$g_s$ (m/s)	Veg C (Pg C)	Soil C (Pg C)	Land C (Pg C)
Value in 1901:	9.34	4.65	0.03319	41.1	126.4	167.5
Absolute diff. (2050 - 1901):						
<b>O<sub>3</sub></b>	-0.40	-0.27	0.00	-0.34	-4.32	-4.66
<b>CO<sub>2</sub></b>	2.50	1.66	-0.01	7.98	11.59	19.57
<b>CO<sub>2</sub> + O<sub>3</sub></b>	2.15	1.43	-0.01	7.32	7.54	14.85
Relative diff. (%)	(%)	(%)	(%)	(%)	(%)	(%)
<b>O<sub>3</sub></b>	-4.28	-5.81	-4.01	-0.83	-3.42	-2.78
<b>CO<sub>2</sub></b>	26.77	35.70	-20.10	19.42	9.17	11.68
<b>CO<sub>2</sub> + O<sub>3</sub></b>	23.02	30.75	-21.93	17.81	5.97	8.87

1670

1671 **Table S5.** Simulated changes in the European land carbon cycle due to changing O<sub>3</sub> and CO<sub>2</sub> concentrations.  
 1672 Shown are changes in total carbon stocks (Land C), split into vegetation (Veg C) and soil (Soil C) carbon, and  
 1673 gross primary productivity (GPP), net primary productivity (NPP) and conductance ( $g_s$ ), between 1901 and 2050.

1674

1675

1676

1677

1678

1679  
1680  
1681  
1682

	GPP_hi (Pg C yr <sup>-1</sup> )	GPP_low (Pg C yr <sup>-1</sup> )	LandC_hi (Pg C)	LandC_low (Pg C)
Value in 1901:	9.05	9.34	167.00	167.50
Value in 2050:				
<b>CO<sub>2</sub></b>	11.63	11.84	184.22	187.07
<b>O<sub>3</sub></b>	8.25	8.94	155.35	162.84
<b>CO<sub>2</sub> + O<sub>3</sub></b>	10.84	11.49	174.83	182.35
† % change due to O <sub>3</sub> at PI CO <sub>2</sub>	-8.84	-4.28	-6.98	-2.78
‡ % change due to O <sub>3</sub> at high CO <sub>2</sub>	-6.79	-2.96	-5.10	-2.52
†† Alleviation of O <sub>3</sub> damage by CO <sub>2</sub> increase (%)	2.05	1.33	1.88	0.26

1683

1684 **Table S6.** Percentage reduction in simulated GPP and Land C by 2050 due to future O<sub>3</sub> effects at pre-industrial  
1685 (PI) CO<sub>2</sub> concentration, and under increasing future CO<sub>2</sub> concentration. The difference between these defines the  
1686 alleviation of the O<sub>3</sub> effect by CO<sub>2</sub>. **O<sub>3</sub>** = Fixed 1901 CO<sub>2</sub>, Varying O<sub>3</sub> ; **CO<sub>2</sub>** = Varying CO<sub>2</sub>, Fixed 1901 O<sub>3</sub> ;  
1687 **CO<sub>2</sub> + O<sub>3</sub>** = Varying CO<sub>2</sub>, Varying O<sub>3</sub>. Calculated as: †) O<sub>3</sub> effect with fixed pre-industrial CO<sub>2</sub>:  
1688  $100 \cdot (\text{fixCO}_2\_varO_3[2050] - \text{value}[1901]) / \text{value}[1901]$ , where value[1901] represents the hypothetical value at  
1689 2050 from a run with fixCO<sub>2</sub>\_fixO<sub>3</sub> which is equivalent to the initial state, i.e. the value in 1901 ; ‡) O<sub>3</sub> effect  
1690 with increasing CO<sub>2</sub>:  $100 \cdot (\text{varCO}_2\_varO_3[2050] - \text{varCO}_2\_fixO_3[2050]) / \text{varCO}_2\_fixO_3[2050]$  ; ††) the alleviation  
1691 of O<sub>3</sub> damage by CO<sub>2</sub> is the difference between the two runs: ‡ - †.

Commented [ORJ47]: RC1 14)

1692  
1693  
1694

1695

1696

1697

1698

1699 **Acknowledgments**

1700 This work used eddy covariance data acquired and shared by the FLUXNET community, including these  
1701 networks: AmeriFlux, AfriFlux, AsiaFlux, CarboAfrica, CarboEuropeIP, CarboItaly, CarboMont, ChinaFlux,  
1702 Fluxnet-Canada, GreenGrass, ICOS, KoFlux, LBA, NECC, OzFlux-TERN, TCOS-Siberia, and USCCC. The  
1703 ERA-Interim reanalysis data are provided by ECMWF and processed by LSCE. The FLUXNET eddy covariance  
1704 data processing and harmonization was carried out by the European Fluxes Database Cluster, AmeriFlux  
1705 Management Project, and Fluxdata project of FLUXNET, with the support of CDIAC and ICOS Ecosystem  
1706 Thematic Center, and the OzFlux, ChinaFlux and AsiaFlux offices.

## 1707 **References**

1708 B ker, P., Feng, Z., Uddling, J., Briolat, A., Alonso, R., Braun, S., Elvira, S., Gerosa, G., Karlsson, P. E.,  
1709 Le Thiec, D., Marzuoli, R., Mills, G., Oksanen, E., Wieser, G., Wilkinson, M., and Emberson, L. D.: New  
1710 flux based dose-response relationships for ozone for European forest tree species, *Environmental*  
1711 *Pollution*, 163-174, 2015.

1712 CLRTAP: The UNECE Convention on Long-range Transboundary Air Pollution. Manual on  
1713 Methodologies and Criteria for Modelling and Mapping Critical Loads and Levels and Air Pollution  
1714 Effects, Risks and Trends: Chapter III Mapping Critical Levels for Vegetation, accessed via,  
1715 [http://icpvegetation.ceh.ac.uk/publications/documents/Chapter3-](http://icpvegetation.ceh.ac.uk/publications/documents/Chapter3-Mappingcriticallevelsforvegetation_000.pdf)  
1716 [Mappingcriticallevelsforvegetation\\_000.pdf](http://icpvegetation.ceh.ac.uk/publications/documents/Chapter3-Mappingcriticallevelsforvegetation_000.pdf), 2017.

1717 IGBP-DIS: International Geosphere-Biosphere Programme, Data and Information System, Potsdam,  
1718 Germany. Available from Oak Ridge National Laboratory Distributed Active Archive Center, Oak  
1719 Ridge, TN, available at: <http://www.daac.ornl.gov>.

1720 Jung, M., Reichstein, M., Margolis, H. A., Cescatti, A., Richardson, A. D., Arain, M. A., Arneth, A.,  
1721 Bernhofer, C., Bonal, D., Chen, J., Gianelle, D., Gobron, N., Kiely, G., Kutsch, W., Lasslop, G., Law, B.  
1722 E., Lindroth, A., Merbold, L., Montagnani, L., Moors, E. J., Papale, D., Sottocornola, M., Vaccari, F.,  
1723 and Williams, C.: Global patterns of land-atmosphere fluxes of carbon dioxide, latent heat, and  
1724 sensible heat derived from eddy covariance, satellite, and meteorological observations, *Journal of*  
1725 *Geophysical Research: Biogeosciences*, 116, n/a-n/a, 10.1029/2010JG001566, 2011.

1726 Karlsson, P. E., Braun, S., Broadmeadow, M., Elvira, S., Emberson, L., Gimeno, B. S., Le Thiec, D.,  
1727 Novak, K., Oksanen, E., Schaub, M., Uddling, J., and Wilkinson, M.: Risk assessments for forest trees:  
1728 The performance of the ozone flux versus the AOT concepts, *Environmental Pollution*, 146, 608-616,  
1729 <http://dx.doi.org/10.1016/j.envpol.2006.06.012>, 2007.

1730 O'Connor, F. M., Johnson, C. E., Morgenstern, O., Abraham, N. L., Braesicke, P., Dalvi, M., Folberth,  
1731 G. A., Sanderson, M. G., Telford, P. J., Voulgarakis, A., Young, P. J., Zeng, G., Collins, W. J., and Pyle, J.  
1732 A.: Evaluation of the new UKCA climate-composition model – Part 2: The Troposphere, *Geosci.*  
1733 *Model Dev.*, 7, 41-91, 10.5194/gmd-7-41-2014, 2014.

1734 Tans, P., and Keeling, R.: Dr. Pieter Tans, NOAA/ESRL ([www.esrl.noaa.gov/gmd/ccgg/trends/](http://www.esrl.noaa.gov/gmd/ccgg/trends/)) and Dr.  
1735 Ralph Keeling, Scripps Institution of Oceanography ([scrippsco2.ucsd.edu/](http://scrippsco2.ucsd.edu/)).

1736 Weedon, G. P.: Readme file for the "WFDEI" dataset.available at: [http://www.eu-](http://www.eu-watch.org/gfx_content/documents/README-WFDEI.pdf)  
1737 [watch.org/gfx\\_content/documents/README-WFDEI.pdf](http://www.eu-watch.org/gfx_content/documents/README-WFDEI.pdf), 2013.

1738

1739

1740

1741

1742 **Response to RC1:**

1743

1744 We would like to thank the reviewer for their time taken to read and comment on this manuscript. The  
1745 comments have been very helpful to improve the manuscript. We hope we have addressed the  
1746 comments to the full satisfaction of the reviewer. We attach the revised manuscript with track changes  
1747 so it can be seen what has been changed and where. In our response below, the reviewer comments  
1748 are in bold to distinguish from our responses.

1749  
1750  
1751 **This paper investigated the interaction between CO<sub>2</sub> and O<sub>3</sub>, the two greenhouse gases that**  
1752 **directly affect plant photosynthesis, and indirectly gs. The goal of the paper is to quantify the**  
1753 **impact of tropospheric O<sub>3</sub>, and its interaction with CO<sub>2</sub>, on gross primary productivity and**  
1754 **land carbon storage across Europe from 1901 to 2050 using the JULES land-surface model. In**  
1755 **principle, the analysis is highly topical and needed.**

1756  
1757 **1) Throughout the abstract, it should be more quantitative in nature. For example, line 37-38,**  
1758 **by how much does the tropospheric O<sub>3</sub> suppress terrestrial carbon uptake?**

1759 We have modified the abstract to make it more quantitative (lines 37 to 47).

1760  
1761  
1762 **2) Line 40-41, How much of the combined effects of elevated future CO<sub>2</sub> (acting to reduce**  
1763 **stomatal opening) and reductions in O<sub>3</sub> concentrations resulted in reduced O<sub>3</sub> damage?**  
1764 **Moreover, elevated future CO<sub>2</sub> will lead to climate warming simultaneously, so how do the**  
1765 **authors remove the response of GPP and land carbon uptake to climate warming due to the**  
1766 **increased CO<sub>2</sub> concentration? Warming will also increase evaporation (evapotranspiration)**  
1767 **and reduce soil water availability, is this also considered?**

1768 We have added a sentence to the abstract to show that the alleviation of O<sub>3</sub> damage by CO<sub>2</sub> induced  
1769 stomatal closure was around 1 to 2% for the low and high plant O<sub>3</sub> sensitivities respectively (for both  
1770 GPP and land C, line 42). This is discussed in more detail in the original manuscript in the Results  
1771 section 3.4 pg. 18 on lines 609 to 614 and in Table S6.

1772  
1773  
1774 This study uses a fixed climate. We cycle over the climate from 1901 to 1920 so we maintain natural  
1775 climate variability, but we do not have climate change. This allows us to focus on the direct effects of  
1776 changing atmospheric CO<sub>2</sub> and O<sub>3</sub> concentrations, and their complex interaction, on plant physiology  
1777 through the twentieth century and into the future. We acknowledge the use of a 'fixed' pre-industrial  
1778 climate omits the additional factor of the interaction between climate change and g<sub>s</sub> which will affect  
1779 the rate of O<sub>3</sub> uptake and therefore O<sub>3</sub> concentrations. Nevertheless, these simulations are an  
1780 important tool to understand the direct impacts of O<sub>3</sub> at the land surface. This work demonstrates the  
1781 sensitivity of GPP and the land carbon sink to tropospheric O<sub>3</sub>, highlighting that it is an important  
1782 predictor of future GPP. We do state in the original manuscript that we use a fixed climate (methods  
1783 section 2.4.1 line 373), but we realise that we do not make it clear enough early on in the manuscript  
1784 that we use a fixed climate, so we have amended this in the introduction (pg.6 , lines 214 to 223). We  
1785 also add a paragraph to our discussion about potential impacts on our results (section 4.3, pg. 26, lines  
1786 808 to 816).

1787  
1788  
1789 **3) Line 43, how large are the regional variations in temperate boreal regions? Overall, some**  
1790 **specific problems should be described in Introduction. For the O<sub>3</sub> effect on the land C sink,**  
1791 **what have we learned from the previous studies? What bioregions, and with what methods,**  
1792 **have been studied?**

1793 We have added a new paragraph to the introduction to discuss the findings from previous studies from  
1794 different regions (pg. 4, lines 134 to 157). Also, we have quantified the regional variations in the  
1795

1796 abstract (line 44), and in the original manuscript we discuss these spatial variations in greater detail in  
1797 the results section.

1798  
1799 **4) Line 81-83, The authors mentioned few studies have considered the simultaneous effects of**  
1800 **exposure to both O<sub>3</sub> and CO<sub>2</sub>, so what have learned from these previous studies? Please specify**  
1801 **previous findings.**

1802 See response to comment above. We have added a new paragraph to the introduction to discuss  
1803 previous studies, both field and model-based, and what has been shown from these studies (pg. 4,  
1804 lines 134 to 157).

1805  
1806  
1807  
1808 **5) Line 86-99, Please describe the O<sub>3</sub> concentration for historical and current level in quantity.**  
1809 **How does the O<sub>3</sub> change over the last decades?**

1810 We have added more information about the change in O<sub>3</sub> concentrations from historical to present  
1811 day (pg.3, lines 88 to 98).

1812  
1813  
1814 **6) Line 103-104, High levels of O<sub>3</sub> are reducing the land carbon sink. How many carbon loss**  
1815 **was led to by O<sub>3</sub> at regional and global scale based on previous studies?**

1816 We have added a paragraph to the introduction to discuss the findings of previous studies (pg. 4, lines  
1817 134 to 157).

1818  
1819  
1820 **7) Line 121-122, are you also going to study the effects of high temperature and drought?**

1821 This links to an earlier comment – in this study we have used a fixed pre-industrial climate. We cycle  
1822 over the climate from 1901 to 1920 so we maintain natural climate variability, but we do not have  
1823 climate change. This allows us to focus on the direct effects of changing atmospheric CO<sub>2</sub> and O<sub>3</sub>  
1824 concentrations, and their complex interaction, on plant physiology through the twentieth century and  
1825 into the future. We realise that we do not make it clear enough early on in the manuscript that we use  
1826 a fixed climate, so we have amended this in the introduction (pg.6 , lines 214 to 223). We also add a  
1827 paragraph to our discussion about potential impacts on our results (section 4.3, pg. 26, lines 808 to  
1828 816).

1829  
1830  
1831 **8) Please explain the CUO1 in Figure S2 caption. As shown in Table S1, the g1 parameter in NT**  
1832 **(Needle leaf tree) is similar to that of shrub. Does it mean plant water use efficiency in NT and**  
1833 **SH are same?**

1834 We have clarified this by adding the following to the Figure S2 caption: “The x axis is cumulative  
1835 uptake of O<sub>3</sub> (CUO) above the critical O<sub>3</sub> threshold ( $F_{O_3crit}$ ).”

1836  
1837 The parameter values for g1 were derived from the extensive database of Lin et al., (2015). The  
1838 parameter g1 is a measure of water-use efficiency. In the model, the plant water-use efficiencies of NT  
1839 and SH would be similar but not identical since WUE is the ratio of carbon gain to water loss and the  
1840 two PFTs have different photosynthetic rates owing to different parameter values.

1841  
1842 **9) Figure1, could you provide some O<sub>3</sub> concentration data from observations?**

1843 This links to an earlier comment #5. Comparison of these long-term O<sub>3</sub> trends with observations is  
1844 difficult for many reasons, not least lack of reliable data before recent decades, and limited  
1845 representativity and inconsistencies in data from recent years (Logan et al., 2012; Parrish et al., 2012).  
1846 For example, ozone levels at the start of the 20<sup>th</sup> century are estimated to be around 10 ppb for the site  
1847

1848 Montsouris Observatory near Paris, data for Arkona on the Baltic coast increased from ca. 15 ppb in  
1849 the 1950s to 20-27 ppb by the early 1980s, and the Irish coast site Mace Head shows around 40 ppb  
1850 by the year 2000 (Logan et al., 2012, Parrish et al., 2012, and refs within). Trends vary from site to  
1851 site though, even on a decadal basis (Logan et al., 2012; Simpson et al., 2014), depending, for  
1852 example, on local/regional trends in precursor (especially NO<sub>x</sub>) emissions, elevation, and exposure to  
1853 long-range transport. As a result of this spatial variation in O<sub>3</sub> concentrations across Europe,  
1854 comparison of the EMEP O<sub>3</sub> forcing in Fig. 1 (plotted as a mean across regions) with individual sites  
1855 would potentially be misleading.

1856  
1857

1858 **10) Line 342-345, what is the uncertainty (or SD) for these percentage number? It may be better**  
1859 **if the authors mentioned how these number are calculated in methods.**

1860  
1861 These numbers were re-calculated to get the standard deviation. Previously the annual mean for each  
1862 simulation was calculated, and this used to calculate the percentage difference. To get the standard  
1863 deviation the daily means were calculated and the percentage difference was calculated for each day,  
1864 then the mean and standard deviation were calculated, these values are now reported in the manuscript  
1865 (section 3.1, pg. 14, lines 482 to 487). We explain how these numbers are calculated in the SI section  
1866 S3 (lines 111 to 114). This re-calculation slightly changes the percentage differences in annual mean  
1867 leaf-level stomatal conductance, but the direction of change remains the same, i.e. MED increases  
1868 water-use for BT and C3, and reduced water-use for NT, C4 and SH. The standard deviations are  
1869 quite large reflecting the large spread in the data, partly due to the seasonal cycle.

1870

1871 **11) Line 352-353, For the broadleaf tree and C3 herbaceous PFT, the Medlyn model simulates a**  
1872 **larger conductance and therefore a greater flux of O<sub>3</sub> through stomata compared to Jacobs, but**  
1873 **it also led to a greater flux of CO<sub>2</sub> through stomata simultaneously, which may be helpful for**  
1874 **increasing photosynthesis.**

1875  
1876 Figures S7 and S8 (top rows) show 1:1 plots of *Anet*, plotting MED (y axis) against JAC (x axis).  
1877 These plots show that in the model, *Anet* is not as sensitive to the change in *gs* scheme as *gs* itself  
1878 (Fig. 2 and Fig. S6). Although the greater conductance for BT and C3 with MED will result in high  
1879 internal CO<sub>2</sub> concentrations, this doesn't result in a large change in modelled photosynthetic rates  
1880 because in the model, the sensitivity of the limiting rates of photosynthesis to changes in *ci* is much  
1881 lower than the sensitivity of *gs* to the same change (see section 3.1, pg. 14, lines 488 to 490 where this  
1882 is mentioned). Therefore, the WUE for BT and C3 will change, they are less WUE with MED.

1883

1884 **12) Line 366-368, Some Boreal and Mediterranean regions show increased GPP over this**  
1885 **period, associated with O<sub>3</sub> induced stomatal closure enhancing water availability. But O<sub>3</sub>**  
1886 **induced stomatal closure also reduce the flux of CO<sub>2</sub> through stomata simultaneously, which**  
1887 **have a negative impact on GPP.**

1888  
1889 This is a trade-off between the opposing effects of O<sub>3</sub> induced stomatal closure enhancing soil water  
1890 availability and also reducing GPP. The overall effect occurs seasonally, which is not shown in Figs.  
1891 4, 5, & 6. O<sub>3</sub> induced stomatal closure occurs during spring/early summer when O<sub>3</sub> concentrations are  
1892 highest, at this point GPP is reduced, but in these dry regions this leads to increased soil moisture that,  
1893 in the model, allows growth later in the year when conditions are still favourable but soil moisture  
1894 may otherwise have been limiting. We have clarified this point in the text (section 3.3, pg. 16, lines  
1895 534-538): "Some Boreal and Mediterranean regions show small increases in GPP over this period,  
1896 associated with O<sub>3</sub> induced stomatal closure enhancing water availability in these drier regions (Fig.  
1897 5). This allows for greater stomatal conductance later in the year when soil moisture may otherwise

1898 have been limiting to growth (up to 10%, Fig. 6), and therefore higher GPP, but these regions  
1899 comprise only a small area of the entire domain.”

1900  
1901 **13) Line 373-375, is the different response of GPP to low and high plant O<sub>3</sub> sensitivity are**  
1902 **significant?**

1903  
1904 On the advice of the reviewer, we carry out statistical testing of the different responses of GPP to the  
1905 low and high plant O<sub>3</sub> sensitivities. We use the software R, and use paired t-tests to determine whether  
1906 the O<sub>3</sub> effect on GPP is significantly different between the two different plant sensitivity  
1907 parameterisations (section 3.3 line 531; section 3.4 line 570; section 3.5 line 597).

1908  
1909 **14) Line 437-440, CO<sub>2</sub> induced stomatal closure can help alleviate O<sub>3</sub> damage by reducing the**  
1910 **uptake of O<sub>3</sub>, but it will also increase available soil moisture simultaneously.**

1911 We agree. The CO<sub>2</sub> induced stomatal closure is the dominant effect that helps alleviate O<sub>3</sub> damage.  
1912 Figures S14 and S15 show that in the model the effect of CO<sub>2</sub> on  $g_s$  is large, whereas the effect of CO<sub>2</sub>  
1913 on soil moisture availability ( $f_{smc}$  in these plots) is small in comparison. Simulated  $g_s$  declines with  
1914 increasing CO<sub>2</sub> which may increase available soil moisture, however CO<sub>2</sub> enhances GPP and growth  
1915 of the vegetation which can increase LAI leading to higher water-use on a leaf area basis. These  
1916 responses are all captured in our simulation however with both CO<sub>2</sub> and O<sub>3</sub> changing, and in our  
1917 calculation of the O<sub>3</sub> effect with CO<sub>2</sub> rising. We look at the difference in this simulation to the  
1918 simulation with O<sub>3</sub> changing but CO<sub>2</sub> concentration fixed at pre-industrial concentrations, this gives  
1919 us the alleviation of O<sub>3</sub> damage by increasing CO<sub>2</sub> and all associated effects, such as changes in soil  
1920 moisture, but it is the effect on stomata that dominates. We have clarified the calculation of the  
1921 alleviation of O<sub>3</sub> damage by increasing CO<sub>2</sub> in the legend to Table S6.

1922  
1923  
1924 **15) Contradictions are reported in Figure 4 and 5. In Figure 4a, the areas with great increasing**  
1925 **in plant available soil moisture have less change in  $g_s$  in Figure 5a. Why? In figure 4c, the areas**  
1926 **with decreasing in plant available soil moisture have large reduction in  $g_s$ .**

1927 The  $f_{smc}$  formulation (factor determining plant available soil moisture) varies with soil moisture  
1928 content and is non-linear. It has a value of zero below wilting point then linearly increases to a value  
1929 of 1 at field capacity, and remains at this value beyond. The wilting point and field capacity depend  
1930 on soil texture. Therefore a small percentage change in soil water content in dry regions  
1931 (Mediterranean) can result in a large percentage increase in  $f_{smc}$ . Likewise an increase in soil  
1932 moisture in mesic areas (e.g. northern Europe) may translate into relatively small percentage changes  
1933 in  $f_{smc}$ .

1934  
1935 In Figs 5a and 6a, the areas that see a large increase in plant available soil moisture see a small  
1936 increase in  $g_s$  (up to 10%). This is looking at the change over the period 1901 to 2001 when only O<sub>3</sub> is  
1937 changing. Over this period there is a large increase in O<sub>3</sub>, so the O<sub>3</sub> induced stomatal closure is large,  
1938 causing the increase in  $f_{smc}$  in this region. The changes are seasonal, these plots show the annual  
1939 mean which will average out some of the change. In this region, for example,  $g_s$  increases a lot in JJA  
1940 and DJF, but there is minimal change in SON/MAM. Figures 5c and 6c are for a different time period,  
1941 2001 to 2050. Over this period the O<sub>3</sub> effect is reduced considerably, so by 2050 plant available water  
1942 is reduced on 2001 levels because the O<sub>3</sub> induced stomatal closure is less. Stomatal conductance  
1943 decreases in this region during this period.

1944  
1945 **16) In table 1, O<sub>3</sub> increased GPP but decreased land carbon over the period 2001-2050. Why**  
1946 **does land C decrease when GPP is increasing?**

1947  
1948



1949 We refer to this in the results section (section 3.4, pg. 17, lines 585 to 589). GPP is a fast flux,  
1950 whereas the land carbon store is a slower pool of carbon, it takes longer for this carbon store to adjust  
1951 to changes in the flux, especially when those changes are fairly small as is the case here. This  
1952 highlights the importance of using a carbon cycle model to look at the impacts of O<sub>3</sub> on the terrestrial  
1953 biosphere.

1954 **The discussion could be improved by using subtitles more clearly.**

1955 We have amended this and added subtitles.

1956  
1957  
1958 **17) Line 525-541, the authors listed a lot of results from the literatures, but the reader is left to**  
1959 **decide what and why is the difference between this study and previous studies? More discussion**  
1960 **on comparing this study with previous studies in detail would be helpful.**

1961 This paragraph discusses findings from field-based studies looking at plant O<sub>3</sub> impacts. We have  
1962 removed this paragraph and put it in the introduction as it seemed more appropriate here to place our  
1963 study in context (pg. 4, lines 134 to 157).  
1964  
1965  
1966  
1967  
1968  
1969  
1970

1971 Logan, J. A., Staehelin, J., Megretskaia, I. A., Cammas, J. P., Thouret, V., Claude, H., De Backer, H.,  
1972 Steinbacher, M., Scheel, H. E., Stübi, R., Fröhlich, M., and Derwent, R.: Changes in ozone over  
1973 Europe: Analysis of ozone measurements from sondes, regular aircraft (MOZAIC) and alpine surface  
1974 sites, *Journal of Geophysical Research*, 117, 1-23, 2012.

1975 Parrish, D. D., Law, K. S., Staehelin, J., Derwent, R., Cooper, O. R., Tanimoto, H., Volz-Thomas, A.,  
1976 Gilge, S., Scheel, H. E., Steinbacher, M., and Chan, E.: Long-term changes in lower tropospheric  
1977 baseline ozone concentrations at northern mid-latitudes, *Atmos. Chem. Phys.*, 12, 11485-11504,  
1978 10.5194/acp-12-11485-2012, 2012.

1979 Simpson, D., Arneeth, A., Mills, G., Solberg, S., and Uddling, J.: Ozone—the persistent menace:  
1980 interactions with the N cycle and climate change, *Current Opinion in Environmental Sustainability*, 9,  
1981 9-19, 2014.

1982

1983

1984

1985

1986

1987

1988

1989

1990

1991

1992 **Response to RC2:**

1993

1994 We thank the reviewer for the time taken to read the manuscript and comment on it. The comments  
1995 are very helpful and improve the manuscript. We hope we have addressed all the comments to the full  
1996 satisfaction of the reviewer. We attach the revised manuscript with track changes so it can be seen  
1997 what has been changed and where.

1998  
1999 **RC) Oliver et al. quantify the impact of ozone damage to European GPP and total land carbon**  
2000 **stock on an annual basis. The authors apply a new stomatal conductance parameterization to**  
2001 **their model, and force the model with surface ozone concentrations, meteorology and global**  
2002 **CO<sub>2</sub> concentration to investigate the roles of CO<sub>2</sub> fertilization vs. O<sub>3</sub> damage on GPP and total**  
2003 **land carbon stock from 1901 to 2050. This new stomatal conductance parameterization**  
2004 **simulates higher stomatal conductance than the previous, causing higher uptake of ozone**  
2005 **through plant stomata. They find that there are spatial variations in the response of GPP and**  
2006 **land carbon stock to CO<sub>2</sub> fertilization vs. O<sub>3</sub> damage. On a regional basis, CO<sub>2</sub> fertilization**  
2007 **dominates the response (vs ozone damage) when CO<sub>2</sub> is allowed to evolve, but ozone does limit**  
2008 **the land carbon sink. The impact of ozone damage from 1901 to 2050 is dominated by 1901-**  
2009 **2001 due to increasing surface ozone concentrations during that time. Overall, it seems like**  
2010 **there is a lot more to discuss in regards to the previous work that has been done on the leaf level**  
2011 **to global scale on this topic (e.g., Karnosky et al., 2003) and how the Oliver et al. findings**  
2012 **contribute substantially to knowledge. It is not really clear how these results advance Sitch et al.**  
2013 **2007 except examining the region-scale over Europe. A huge limitation to this study is that CO<sub>2</sub>**  
2014 **and meteorology are uncoupled, as well as meteorology, ozone, and stomatal conductance.**  
2015

2016 AC: This study makes significant developments to the model from that used in Sitch et al., 2007. In  
2017 short these developments include:

2018 - Re-calibration of the model for ozone impacts on vegetation using up-to-date functions published in  
2019 2017.

2020 - A representation of ozone damage on crops and accounting for regional differences where possible  
2021 (i.e. Mediterranean regions).

2022 - A new  $g_s$  model including parameters derived from field observations which have physical meaning  
2023 (i.e. measureable quantities).

2024 - A term for non-stomatal deposition of ozone.

2025 - A diurnal cycle of ozone forcing at a much higher spatial resolution than in Sitch *et al.*, global  
2026 simulations (i.e. 0.5 x 0.5 vs 3.75x 2.5) from a high resolution atmospheric chemistry model for  
2027 Europe.

2028  
2029 The final paragraph of the introduction was re-arranged to highlight these advances (pg. 6, lines 193  
2030 to 214).

2031  
2032 We also include greater discussion on previous studies in this area and move a paragraph from the  
2033 discussion to the introduction (pg. 4, lines 134 to 157).

2034  
2035 **RC1) Using recycled early 20th C climate is problematic. I understand that the authors want to**  
2036 **isolate the physiological response of plants of CO<sub>2</sub> vs. O<sub>3</sub> here, but ozone is high during drought**  
2037 **and heat waves, and stomata close at that time. So if there is increasing aridity and hydrological**  
2038 **and temperature extremes into the 21st C, then the ozone response should be much lower than**  
2039 **the authors suggest. The authors do at some point say that their work here is an upper bound,**  
2040 **but upper bounds have already been published.**  
2041

2042 AC: The aim of these simulations was to investigate the direct effects of changing atmospheric CO<sub>2</sub>  
2043 and O<sub>3</sub> concentrations, and their complex interaction, on plant physiology through the twentieth

2044 century and into the future. These offline simulations are not coupled and therefore do not have  
2045 feedbacks between climate, O<sub>3</sub> formation and stomatal behaviour, but nonetheless they are an  
2046 important tool to understand the direct impacts of O<sub>3</sub> at the land surface. This work demonstrates the  
2047 sensitivity of GPP and the land carbon sink to tropospheric O<sub>3</sub>, highlighting that it is an important  
2048 predictor of future GPP and the land carbon sink. We do state in the original manuscript that we use a  
2049 fixed climate (methods section 2.4.1 line 373), however, we realise we do not make it clear from the  
2050 beginning that we are running offline simulations, therefore we have modified the manuscript to make  
2051 this point clear in the introduction (pg.6 , lines 214 to 223).

2052  
2053 An important point that we make in the original manuscript is: “our results demonstrate the  
2054 sensitivity of modelled terrestrial carbon dynamics to tropospheric O<sub>3</sub> and its interaction with  
2055 atmospheric CO<sub>2</sub>, highlighting that such effects of O<sub>3</sub> on plant physiology significantly add to the  
2056 uncertainty of future trends in the land carbon sink and climate-carbon feedbacks. Given the potential  
2057 to limit the climate mitigation effect of European terrestrial ecosystems, we suggest plant O<sub>3</sub> damage  
2058 should be incorporated into carbon cycle assessments”. Here the point we mean to make is that our  
2059 work shows the sensitivity of modelled GPP and land carbon to the direct effect of O<sub>3</sub> on plant  
2060 physiology, however, this process remains largely unconsidered in regional and global climate model  
2061 simulations that do account for climate-carbon feedbacks and are used to model carbon sources and  
2062 sinks even though it is likely contribute to the large uncertainty in future modelled carbon-climate  
2063 feedbacks. We modify the text to make this point more clearly at the end of the conclusions (section  
2064 5, pg. 28, lines 879 to 883).

2065  
2066 We add to the discussion a paragraph outlining the potential implications for our results of using  
2067 uncoupled simulations (section 4.3, pg. 26, lines 808 to 816).

2068  
2069 It is computationally expensive to run coupled simulations. Offline studies are valuable in  
2070 determining the relevance of individual responses and are relatively cheap computationally. Once the  
2071 importance of a process is demonstrated off line, it provides evidence of the need to incorporate such  
2072 processes in coupled simulations.

2073  
2074 **RC2) Further, Langner et al. 2012 is not the appropriate work here to justify the authors’  
2075 approach. Langner et al. examine the impact of climate change following the A1B scenario on  
2076 surface ozone (they do not consider changes in anthropogenic precursor emissions from present  
2077 to future under A1B). Langner et al. use biogenic emissions to explain some of the cross-model  
2078 differences in changes from present to future in ozone due to climate. This is quite different  
2079 from using the full A1B scenario which considers changes in climate & anthropogenic precursor  
2080 emissions, which is what Oliver et al. do.**

2081  
2082 AC: This should be a different Langer et al., 2012 reference here, this has now been corrected:

2083  
2084 Langner, J., Engardt, M. & Andersson, C. European summer surface ozone 1990–2100, *Atmos. Chem.  
2085 Physics*, **2012b**, 12, 10097-10105

2086  
2087 Section 2.4.1, pg. 11, line 399.

2088  
2089 **RC3) The authors change their stomatal conductance parameterization but do not explain why.  
2090 Their phrasing implies that the new gs model is truth, whereas the Jacobs 1994 model is not  
2091 (e.g., "studies using the Jacobs [1994] formulation may underestimate" on line 523). I  
2092 understand that parameterizations of stomatal conductance are uncertain in general, and hard**

2093 **to evaluate, but it seems like there should be some reasoning and evaluation here. Further,**  
2094 **please clarify the re-calibration (lines 130-133). This seems like a major part of your analysis**  
2095 **and I think evaluation & inclusion of this evaluation in the main part of the paper is warranted.**  
2096

2097 AC: The main advance of the Medlyn model over Jacobs, and other empirical  $g_s$  formulations, is the  
2098 availability of observational-derived parameters for European vegetation. We discuss the advantages  
2099 of the Medlyn model over the Jacobs formulation in the original text and that is our reasoning for  
2100 using it in these simulations. We apologise if this is not clear, and have moved this to a separate  
2101 paragraph in the introduction and expanded our reasoning (pg. 6, lines 181 to 191). We do not mean  
2102 to imply that the Medlyn model is truth compared to Jacobs, and have changed the wording on line  
2103 697 (section 4.1, pg. 26) accordingly to read “studies using the Jacobs  $g_s$  formulation would simulate  
2104 a lower O<sub>3</sub> impact for Europe”.

2105  
2106 We have included site level evaluation of the seasonal cycle of latent and sensible heat at some  
2107 FLUXNET sites comparing the two  $g_s$  models against observations. This is in the supplementary  
2108 information, section S4 (Fig. S9 and Table S2). We refer to this evaluation in the main text (section  
2109 2.3, pg. 10, line 365 and section 3.1, pg. 14, line 497).

2110  
2111 We mention the calibration in the introduction, but we do not feel here is the place to expand or  
2112 clarify further. We expand upon the re-calibration in the Methods (section 2.2), and have updated this  
2113 section in the manuscript to clarify it further. We put additional details in the supplementary  
2114 information because these are quite technical details so we feel they are not necessary in the main  
2115 text.

2116  
2117 Validation of land-surface models such as JULES for O<sub>3</sub> impacts is not straightforward because of  
2118 small scale, site specific biotic and abiotic factors that affect the growth response of vegetation to O<sub>3</sub>.  
2119 These include competition within and between species leading to differential O<sub>3</sub> responses as was  
2120 seen at the Aspen FACE experiment (King et al., 2005; Karnosky et al., 2007; Kubiske et al., 2007),  
2121 attack by pests and diseases, nutrient limitation, drought stress. Nevertheless, we now include an  
2122 evaluation of the O<sub>3</sub> model against the flux network model tree ensemble (MTE) product of (Jung et  
2123 al., 2011). We compare mean GPP from 1991 to 2001 for each of the JULES scenarios and both high  
2124 and low plant O<sub>3</sub> sensitivities against Jung et al., (2011). See methods section 2.4.3, results section 3.2  
2125 with new Figure 3, and section S5 in the supplementary information with new figures S10, S11 and  
2126 S12.

2127

2128 **RC4) Is Jacobs  $g_s$  used in the ozone dry deposition parameterization that is used in the EMEP**  
2129 **model used to project the ozone concentrations? Typically stomatal conductance in the dry**  
2130 **deposition parameterizations is some form of Wesely (1989). If Wesely is used, how does the**  
2131 **magnitude of Medlyn differs from the magnitude of stomatal conductance from Wesely? If**  
2132 **Wesely is used, then CO<sub>2</sub> fertilization is not in there, nonetheless ozone damage. Another caveat**  
2133 **is that ozone damage can feedback onto ozone concentrations as demonstrated by Sadiq et al.**  
2134 **ACP 2017.**

2135  
2136  
2137 AC: Calculations of O<sub>3</sub> deposition in the EMEP model are rather detailed compared to most chemical  
2138 transport models. We make use of the stomatal conductance algorithm (now commonly referred to as  
2139 DO<sub>3</sub>SE) originally presented in Emberson et al. (2000;2001), which depends on temperature, light,  
2140 humidity and soil moisture. Calculation of non-stomatal sinks, in conjunction with an ecosystem  
2141 specific calculation of vertical O<sub>3</sub> profiles, is an important part of this calculation as discussed in

2142 Tuovinen et al. (2004;2009) or Simpson et al. (2003). The methodology and robustness of the  
2143 calculations of O<sub>3</sub> deposition and stomatal conductance have been explored in a number of  
2144 publications (Emberson et al., 2007;Tuovinen et al., 2004;Tuovinen et al., 2009;Tuovinen et al.,  
2145 2007).

2146  
2147 Of course, the *g<sub>s</sub>* values used in the EMEP model differ from those obtained using a Medlyn  
2148 formulation. Comparing EMEP's maximum *g<sub>s</sub>* values (*g<sub>max</sub>*) with the 95th-100th percentiles of *g<sub>s</sub>*  
2149 found in JULES simulations, we find very similar values for deciduous forest (EMEP 150-200,  
2150 JULES ~180, all units in mmole O<sub>3</sub>/m<sup>2</sup> (PLA)/s), and C3/C4 crops (EMEP 270-300, JULES ~260-  
2151 390), but large differences for coniferous forest (EMEP 140-200, JULES ~60-70) and shrubs (EMEP  
2152 60-200, JULES 360-390). The role of EMEP in this study is not to provide *g<sub>s</sub>*, however, but to  
2153 provide O<sub>3</sub> at the top of the vegetation canopy. The main driver of such O<sub>3</sub> levels is the regional-scale  
2154 production and transport of ozone, and the main impact of *g<sub>s</sub>* is just in affecting the vertical O<sub>3</sub>  
2155 gradients just above the plant canopy. Differences in *g<sub>s</sub>* are known to have minimal impact on  
2156 canopy-top O<sub>3</sub> for trees, mainly due to the efficient turbulent mixing above tall canopies, but also due  
2157 to non-stomatal sink processes. For shorter vegetation, substantial O<sub>3</sub> gradients, driven by deposition,  
2158 occur in the lowest 10s of metres of the atmosphere, and stomatal sinks (as given by *g<sub>s</sub>*) can have a  
2159 significant role. However, calculations of such gradients made with the EMEP model for CLRTAP  
2160 (2017) showed that such differences amounted to ca. 10% when comparing O<sub>3</sub> concentrations at 1m  
2161 height above high-*g<sub>s</sub>* crops (*g<sub>max</sub>*=450 mmole O<sub>3</sub>/m<sup>2</sup> (PLA)/s) species compared to moderate-*g<sub>s</sub>*  
2162 (*g<sub>max</sub>* 270 mmole O<sub>3</sub>/m<sup>2</sup> (PLA)/s).

2163  
2164 These inconsistencies are not ideal, but inevitable given that we link two different model systems.  
2165 There are of course many uncertainties in all estimates of deposition and stomatal ozone flux (e.g.  
2166 Tuovinen et al., 2009), and we believe that this particular uncertainty is an acceptable part of our  
2167 procedure.

2168  
2169 The referee's comments about CO<sub>2</sub> and the impacts mentioned by Sadiq are also relevant, but again  
2170 there are many uncertainties associated with such effects and assessments too.

2171  
2172 In order to keep a concise text, but mention the above points, we have added a summary of the above  
2173 points to the manuscript in the discussion section 4.3, pg. 25, lines 790 to 806.

2174  
2175  
2176 **RC5) A large part of the results hinge on the seasonality of surface ozone concentrations, and**  
2177 **how they change from PI to present. There is some discussion of this on pages 401-405 as**  
2178 **authors examine the change in seasonality from 2001 to 2050, but there is no citation of previous**  
2179 **work examining changes in ozone seasonality, or the implications of this for their conclusions.**  
2180 **Also, the authors say that tropospheric ozone is increasing (e.g., line 74), but I think this is a bit**  
2181 **misleading - due to strong changes in seasonality that are observed - please revise.**

2182  
2183 AC: We have added a paragraph to the manuscript to acknowledge and discuss the importance of the  
2184 seasonality of surface ozone concentrations, citing previous work examining these changes, and the  
2185 implications of this for our results (section 2.1.4, pg. 12, lines 420 to 442). Line 74 has been revised  
2186 (now line 75).

2187  
2188  
2189 **RC6) In general, the paper is a bit poorly organized. Many times the authors say "see details in**  
2190 **SI" when it's not clear what information is in there, and why it is relevant. Further it seems like**  
2191 **some info in the SI should really be in the actual paper. In addition, the authors neglect to**

2192 **mention many substantial caveats (such as the uncertainties around CO<sub>2</sub> fertilization w.r.t.**  
2193 **nutrient cycling, using uncoupled tropospheric chemistry & stomatal dry deposition, and**  
2194 **stomatal sluggishness) until the very end. I think the paper would be much better if much of the**  
2195 **discussion was moved to the introduction and used to frame the work, and motivate the**  
2196 **authors' objectives.**

2197  
2198 AC: We apologise for the lack of clarity when referring to the supplementary information, we have  
2199 amended this to make clear what section in the SI we refer to and why. In response to referee requests  
2200 we have revamped the introduction to clarify the specific focus of the manuscript (i.e. carbon cycle  
2201 impact of the plant physiological response to O<sub>3</sub> and CO<sub>2</sub>), and therefore make it easier to understand  
2202 what is and what is not included.

2203  
2204 We discuss the caveats of the study at length in the original manuscript. These are very important, so  
2205 we are sure to make clear that we are fully aware of the caveats. We also now include an additional  
2206 paragraph in the discussion section 4.3 on the potential implications of uncoupled tropospheric  
2207 chemistry and stomatal dry deposition for our results which was previously missing. We also  
2208 introduce the issue of sluggish stomata and CO<sub>2</sub> fertilization in the introduction to help frame the  
2209 study. However, on the whole we think that discussion of the caveats is more appropriate in the  
2210 discussion.

2211  
2212 **Minor comments**

2213 **RC1. The authors use the term "significant" a lot - but don't do any sort of statistical testing.**  
2214 **Please only use the word significant when describing results that are statistically significant.**

2215  
2216 AC: We have revised our use of significant where appropriate.

2217 **RC2. Line 78: Lightning is a source of NO<sub>x</sub>, not O<sub>3</sub> – please revise**

2218  
2219 AC: This has been amended to read "... and lightning which is a source of NO<sub>x</sub>". (line 79)

2220  
2221 **RC3. Lines 86-87: Parrish et al. 2012 is not really the appropriate citation here**

2222  
2223 AC: We have changed this reference for Vingarzan (2004). (line 88)

2224  
2225 **RC4. Lines 93-94: "Intercontinental transport" doesn't mean that background ozone has**  
2226 **increased, there has always been intercontinental transport.**

2227  
2228 AC: This sentence has been changed to: "Intercontinental transport of air pollution from regions such  
2229 as Asia that currently have poor emission controls are thought to contribute largely to rising  
2230 background O<sub>3</sub> concentrations in Europe over the last decades (Cooper et al., 2010;Verstraeten et al.,  
2231 2015)." (line 103)

2232  
2233 **RC5. Line 101: Citations for ozone impacts on crop yields and nutritional quality are needed**

2234  
2235 AC: We have added the following references: Ainsworth et al., (2010) and Avnery et al., (2011). (line  
2236 114)

2237  
2238 **RC6. Line 106: Do the authors mean indirect here?**

2239  
2240 AC: We mean direct – ozone has a direct effect on radiative forcing of the climate. The indirect effect  
2241 is ozone damage of vegetation which reduces uptake of carbon by plant photosynthesis, allowing  
2242 more CO<sub>2</sub> to remain in the atmosphere. (line 118)

2243  
2244 **RC7. Line 110: Fowler et al. 2009 isn't really the appropriate citation here - i.e., for saying that**  
2245 **dry deposition is a substantial sink of tropospheric ozone**  
2246  
2247 AC: We have added an additional reference: Fowler et al., (2001). (line 123)  
2248  
2249 **RC8. Line 152 - as the authors mention in the discussion, ozone can directly impact  $g_s$  - please**  
2250 **revise accordingly**  
2251  
2252 AC: This has been amended at line 195.  
2253  
2254 **RC9. Line 160-168: please clarify the spatial domain and the resolution of this model; also, is**  
2255 **the resolution the same as the meteorological and ozone forcing files?**  
2256  
2257 AC: We added the following sentence to clarify the resolution of the model (line 247): "This work  
2258 uses JULES version 3.3 (<http://www.jchmr.org>) at  $0.5^\circ \times 0.5^\circ$  spatial resolution and hourly model time  
2259 step, the spatial domain is shown in Fig. S5." We also explicitly state the resolution of the all the  
2260 forcing data (meteorology, CO<sub>2</sub>, ozone and land cover) to show that they are all the same  $0.5^\circ \times 0.5^\circ$   
2261 resolution.  
2262  
2263 **RC10. Lines 193-194:  $\kappa_{O_3}$  is not exactly the ratio of the resistances; it's the ratio of the**  
2264 **diffusivities**  
2265  
2266 AC: This has been changed to : " $K_{O_3}$  accounts for the different diffusivity of ozone to water vapour  
2267 and takes a value of 1.51 after Massman (1998)" (line 280).  
2268  
2269 **RC11. Lines 220-222: What is CLRTAP (2017)? It is not in the references. Why is it being**  
2270 **treated as the "truth"?**  
2271  
2272 AC: The reference for CLRTAP (2017) is now in the reference list. It is a report on ozone impacts on  
2273 vegetation, providing a synthesis of the latest peer reviewed literature, collated by a panel of experts  
2274 and so is considered the state-of the art knowledge. It provides the O<sub>3</sub> dose response functions  
2275 compiled from numerous field studies that we use to calibrate our model PFTs for sensitivity to O<sub>3</sub>.  
2276 We have expanded section 2.2 which explains this more clearly.  
2277  
2278 **RC12. Section 2.3 - please clarify that Lin et al. 2015 fit  $g_l$  parameters based on the Medlyn et**  
2279 **al. 2011 equation for stomatal conductance (except no  $g_0$  term), which is not exactly the**  
2280 **same as putting equation 7 into equation 5; it's confusing to refer to this equation as**  
2281 **Medlyn et al. (2011); also, I do not think that multiplying the  $A_{net}/(C_a - C_i)$  by  $R \cdot T$  is the**  
2282 **right way to convert from mol s<sup>-1</sup> m<sup>-2</sup> to m/s.**  
2283  
2284 AC: We clarify this in the following sentence (line 352): "The  $g_l$  parameter represents the sensitivity  
2285 of  $g_s$  to the assimilation rate, i.e. plant water use efficiency, and was derived as in Lin et al. (2015) by  
2286 fitting the Medlyn *et al.*, (2011) model to observations of  $g_s$ , photosynthesis, and VPD, with no  $g_0$   
2287 term." At line 346 we also say "In this work, we replace equation 6 with the closure described in  
2288 Medlyn et al. (2011), ...." and then refer to it from then on as the MED model instead of the Medlyn  
2289 et al (2011) model.  
2290  
2291 **RC13. Lines 252-254: Please clarify "the effect" that Hoshika et al. 2013 find; does O3 increase**  
2292 **or decrease WUE? This seems relevant to your discussion/conclusions.**  
2293

2294 AC: We clarify by adding the following (line 355): “Hoshika et al., (2013) show a significant  
2295 difference in the  $g_1$  parameter (higher in elevated  $O_3$  compared to ambient) in Siebold’s beech in June  
2296 of their experiment. However, this is only at the start of the growing season, further measurements  
2297 show no difference in this parameter between  $O_3$  treatments.”

2298  
2299 **RC14. Lines 300-301: Clarify the “disaggregation” of ozone from the daily mean to the hourly**  
2300 **time step. As ozone has a diurnal cycle, and stomatal conductance does as well, this could have a**  
2301 **substantial impact on your work, and should be discussed.**

2302  
2303 AC: We have added the following sentence to clarify the disaggregation (line 408): “The daily mean  
2304  $O_3$  forcing was disaggregated to follow a mean diurnal profile of  $O_3$ , this was generated from hourly  
2305  $O_3$  output from EMEP MSC-W for the two land cover categories across the same domain as in this  
2306 study.”

2307  
2308 **RC15. Lines 305-306: Clarify the calculation of the ozone gradient from the lowest atmosphere**  
2309 **grid box to canopy height**

2310  
2311 AC: The ozone forcing used in this study was produced by the EMEP MSC-W model, here we  
2312 provide a reference to the model documentation (Simpson et al., 2012) so readers can follow up  
2313 further details. It is beyond the scope of this study to document how EMEP MSC-W works.

2314  
2315 **RC16. Further details on crops in JULES should be included in Section 2.4.1 in addition to the**  
2316 **discussion.**

2317  
2318 AC: We have amended this to the following: “The agricultural mask means that only  $C_3/C_4$   
2319 herbaceous PFTs are allowed to grow, with no competition from other PFTs, no form of land  
2320 management is simulated.” We discuss the limitations of this in the discussion (lines 761).

2321  
2322 **RC17. Lines 282-283: Please specify the ozone sensitivity used for forests**

2323  
2324 AC: This has been removed as it is now explained in more detail in section 2.2.

2325  
2326 **RC18. Line 882: I don’t think “in prep” studies can be cited.**

2327  
2328 AC: This has been removed.

2329  
2330 **RC19. Lines 258-259: What are the two model grid points? What does wet vs. dry refer to? This**  
2331 **info is used later on in the paper (Figure 2), so it would be helpful for more information on this.**

2332  
2333 AC: More information to clarify this is provided in the SI section S3, but this was probably not clear  
2334 because we did not make it clear which section in the SI to refer to. We have rectified this, and now  
2335 state “see SI section S3 for further details” (line 364).

2336  
2337 **RC20. Please clarify in the Figure 2 caption what exactly the readers are looking at (this**  
2338 **is just one grid cell, with each sub-tile PFT gs shown?). Why just one grid-cell? Is the**  
2339 **data shown hourly? What is the time period?**

2340  
2341 AC: Shown are hourly values for the year 2000, from a single grid cell fixed to have 20% land cover  
2342 of each PFT – therefore we are comparing  $g_s$  for each PFT under the same conditions. This  
2343 information is in the SI section S3 which we hope will be clearer now as we refer to it appropriately  
2344 earlier on in the manuscript.

2345



2346 The figure caption has been amended to: “**Figure 2.** Comparison of simulated  $g_s$  with MED (y axis)  
2347 versus JAC (x axis) for all five JULES PFTs at one grid point (lat: 48.25; lon.: 5.25) shown are hourly  
2348 values for the year 2000 (see SI section S3 for further details). Shown are stomatal conductance ( $g_s$ , top  
2349 row), and the flux of  $O_3$  through the stomata (flux\_o3, bottom row).”

2350  
2351 **RC21. Lines 384-396: It’s not clear why the authors are examining different decades for their**  
2352 **analysis here. Second, it seems like the authors could pretty easily sample their model for an**  
2353 **apples-to-apples comparison with Boden et al. 2013. Third, suggesting that the O3 impact on the**  
2354 **land carbon sink is a source of carbon is not really appropriate (lines 395-396); re-phrasing**  
2355 **would allow**  
2356 **for the same take-away**

2357 AC: We analyse different decades because it shows how the  $O_3$  effect has changed through time. The  
2358 Boden et al data is available on a country by country basis without lat/lon information for the spatial  
2359 extent of coverage. Therefore it is best to stick to our domain for comparison, but clearly  
2360 acknowledge that our domain is slightly larger in extent.

2361  
2362  
2363 **RC22. Lines 401-402: Ozone precursor emission controls do not always lead to ozone reductions**  
2364 **because formation chemistry is nonlinear; please revise.**

2365 AC: We have removed this sentence.

2366  
2367  
2368 **RC23. Line 401: Large spatial variability is not apparent to me - it would be helpful if the**  
2369 **authors were more specific.**

2370 AC: To my eye the spatial variation is apparent in Fig. 4g & h. Nevertheless, we do describe this  
2371 variation in more detail in the results section.

2372  
2373  
2374 **RC24. Lines 405-408: it’s not clear what figure the authors are talking about here.**

2375 AC: This is Fig. 4g & h. This has been updated in the text.

2376  
2377  
2378 **RC25. Figure 6 - specify whether your numbers correspond to rows or columns.**

2379 AC: They refer to columns. We have amended the legend for figure 7 to make this clearer.

2380  
2381  
2382  
2383  
2384  
2385  
2386 Refs:

2387  
2388 CLRTAP: The UNECE Convention on Long-range Transboundary Air Pollution. Manual on  
2389 Methodologies and Criteria for Modelling and Mapping Critical Loads and Levels and Air Pollution  
2390 Effects, Risks and Trends: Chapter III Mapping Critical Levels for Vegetation, accessed via,  
2391 [http://icpvegetation.ceh.ac.uk/publications/documents/Chapter3-](http://icpvegetation.ceh.ac.uk/publications/documents/Chapter3-Mappingcriticallevelsforvegetation_000.pdf)  
2392 [Mappingcriticallevelsforvegetation\\_000.pdf](http://icpvegetation.ceh.ac.uk/publications/documents/Chapter3-Mappingcriticallevelsforvegetation_000.pdf), 2017.  
2393 Cooper, O. R., Parrish, D. D., Stohl, A., Trainer, M., Nedelec, P., Thouret, V., Cammas, J. P., Oltmans,  
2394 S. J., Johnson, B. J., Tarasick, D., Leblanc, T., McDermid, I. S., Jaffe, D., Gao, R., Stith, J., Ryerson, T.,  
2395 Aikin, K., Campos, T., Weinheimer, A., and Avery, M. A.: Increasing springtime ozone mixing ratios in  
2396 the free troposphere over western North America, Nature, 463, 344-348,  
2397 [http://www.nature.com/nature/journal/v463/n7279/supinfo/nature08708\\_S1.html](http://www.nature.com/nature/journal/v463/n7279/supinfo/nature08708_S1.html), 2010.

2398 Emberson, L. D., Ashmore, M. R., Cambridge, H. M., Simpson, D., and Tuovinen, J.-P.: Modelling  
2399 stomatal ozone flux across Europe, *Environmental Pollution*, 109, 403–413, 2000.

2400 Emberson, L. D., Simpson, D., Tuovinen, J.-P., Ashmore, M. R., and Cambridge, H. M.: Modelling and  
2401 mapping ozone deposition in Europe, *Water Air Soil Pollution*, 130, 577–582, 2001.

2402 Emberson, L. D., Büker, P., and Ashmore, M. R.: Assessing the risk caused by ground level ozone to  
2403 European forest trees: A case study in pine, beech and oak across different climate regions,  
2404 *Environmental Pollution*, 147, 454–466, 2007.

2405 Jung, M., Reichstein, M., Margolis, H. A., Cescatti, A., Richardson, A. D., Arain, M. A., Arneth, A.,  
2406 Bernhofer, C., Bonal, D., Chen, J., Gianelle, D., Gobron, N., Kiely, G., Kutsch, W., Lasslop, G., Law, B.  
2407 E., Lindroth, A., Merbold, L., Montagnani, L., Moors, E. J., Papale, D., Sottocornola, M., Vaccari, F.,  
2408 and Williams, C.: Global patterns of land-atmosphere fluxes of carbon dioxide, latent heat, and  
2409 sensible heat derived from eddy covariance, satellite, and meteorological observations, *Journal of*  
2410 *Geophysical Research: Biogeosciences*, 116, n/a-n/a, 10.1029/2010JG001566, 2011.

2411 Karnosky, D. F., Skelly, J. M., Percy, K. E., and Chappelka, A. H.: Perspectives regarding 50years of  
2412 research on effects of tropospheric ozone air pollution on US forests, *Environmental Pollution*, 147,  
2413 489-506, 2007.

2414 King, J. S., Kubiske, M. E., Pregitzer, K. S., Hendrey, G. R., McDonald, E. P., Giardina, C. P., Quinn, V. S.,  
2415 and Karnosky, D. F.: Tropospheric O<sub>3</sub> compromises net primary production in young stands of  
2416 trembling aspen, paper birch and sugar maple in response to elevated atmospheric CO<sub>2</sub>, *New*  
2417 *Phytologist*, 168, 623-635, 2005.

2418 Kubiske, M., Quinn, V., Marquardt, P., and Karnosky, D.: Effects of Elevated Atmospheric CO<sub>2</sub> and/or  
2419 O<sub>3</sub> on Intra-and Interspecific Competitive Ability of Aspen, *Plant biology*, 9, 342-355, 2007.

2420 Lin, Y.-S., Medlyn, B. E., Duursma, R. A., Prentice, I. C., Wang, H., Baig, S., Eamus, D., de Dios, V. R.,  
2421 Mitchell, P., and Ellsworth, D. S.: Optimal stomatal behaviour around the world, *Nature Climate*  
2422 *Change*, 5, 459-464, 2015.

2423 Massman, W. J.: A review of the molecular diffusivities of H<sub>2</sub>O, CO<sub>2</sub>, CH<sub>4</sub>, CO, O<sub>3</sub>, SO<sub>2</sub>, NH<sub>3</sub>, N<sub>2</sub>O,  
2424 NO, and NO<sub>2</sub> in air, O<sub>2</sub> and N<sub>2</sub> near STP, *Atmospheric Environment*, 32, 1111-1127,  
2425 [http://dx.doi.org/10.1016/S1352-2310\(97\)00391-9](http://dx.doi.org/10.1016/S1352-2310(97)00391-9), 1998.

2426 Medlyn, B. E., Duursma, R. A., Eamus, D., Ellsworth, D. S., Prentice, I. C., Barton, C. V., Crous, K. Y., de  
2427 Angelis, P., Freeman, M., and Wingate, L.: Reconciling the optimal and empirical approaches to  
2428 modelling stomatal conductance, *Global Change Biology*, 17, 2134-2144, 2011.

2429 Simpson, D., Tuovinen, J.-P., Emberson, L., and Ashmore, M.: Characteristics of an ozone deposition  
2430 module II: Sensitivity analysis, *Water Air Soil Pollution*, 143, 123–137, 2003.

2431 Tuovinen, J.-P., Ashmore, M., Emberson, L., and Simpson, D.: Testing and improving the EMEP ozone  
2432 deposition module, *Atmospheric Environment*, 38, 2373–2385, 2004.

2433 Tuovinen, J.-P., Simpson, D., Emberson, L., Ashmore, M., and Gerosa, G.: Robustness of modelled  
2434 ozone exposures and doses, *Environmental Pollution*, 146, 578–586, 2007.

2435 Tuovinen, J.-P., Emberson, L., and Simpson, D.: Modelling ozone fluxes to forests for risk assessment:  
2436 status and prospects, *Annals of Forest Science*, 66, 1-14, 2009.

2437 Verstraeten, W. W., Neu, J. L., Williams, J. E., Bowman, K. W., Worden, J. R., and Boersma, K. F.:  
2438 Rapid increases in tropospheric ozone production and export from China, *Nature Geoscience* 8, 690-  
2439 695, 2015.

2440